UNIVERSIDADE DE SÃO PAULO
FACULDADE DE ODONTOLOGIA DE BAURU

ISABELA TOMAZINI SABINO

Interação entre o exercício crônico e o *background* genético no metabolismo do fluoreto

BAURU
2019

ISABELA TOMAZINI SABINO

Interação entre o exercício crônico e o *background* genético no metabolismo do fluoreto

Tese apresentada à Faculdade de Odontologia de Bauru da Universidade de São Paulo para obtenção do título de Doutora em Ciências no Programa de Ciências Odontológicas Aplicadas, na área de concentração Biologia Oral.

Orientador: Prof. Dra Marilia Afonso Rabelo Buzalaf

BAURU

2019

Tomazini Sabino, Isabela
Interação entre o exercício crônico e o *background* genético no metabolismo do fluoreto / Isabela Tomazini Sabino. – Bauru, 2019.
133p. : il. ; 31cm.

Tese (Doutorado) – Faculdade de Odontologia de Bauru. Universidade de São Paulo

Orientadora: Prof. Dra. Marilia Afonso Rabelo Buzalaf

Autorizo, exclusivamente para fins acadêmicos e científicos, a reprodução total ou parcial desta tese, por processos fotocopiadores e outros meios eletrônicos.

Assinatura:

Data:

Comitê de Ética da FOB-USP
Protocolo nº: 009/2015
Data: 16/06/2015

FOLHA DE APROVAÇÃO

DEDICATÓRIA

Dedico este trabalho à minha família, meu bem mais precioso.

Aos meus pais, **Rosana** e **Marcos**, pelo exemplo de amor, esforço, doação e zelo.

Aos meus irmãos, **Erick** e **Leonardo**, por todo cuidado, paciência, cumplicidade e companheirismo.

Ao meu marido **Denilson**, que é meu companheiro, meu amigo, meu esposo e pai. Dedicado em todas as funções. É suporte e abrigo.

Aos meus filhos **Lívia** e **Angelo**. Lívia que chegou no meio dessa jornada e Angelo que aguardamos ansiosamente por seu nascimento. São eles que dão a força e a coragem necessárias para caminhar e enfrentar o conhecido e o desconhecido, o novo passo e a rotina diária. É deles que vem a vontade e persistência em tentar ser uma pessoa melhor, todos os dias, um pouco mais.

Meu imensurável amor e eterna gratidão à todos vocês!

AGRADECIMENTOS

À **Deus**, que me deu o dom da vida, e me permite contemplar Seu imenso amor em cada etapa da minha vida, em cada detalhe do dia-a-dia.

Aos meus pais **Marcos** e **Rosana**.
Muito obrigada por serem um 'transbordar" de amor. Amor que ensina valores e princípios. Amor que não mede esforços me ver feliz. Amor que dá colo. Amor suporta. Amor em forma de confiança. Amor puro. Amor sem medidas.

Aos meus irmãos **Erick** e **Leonardo**.
Irmão é sinônimo de amor multiplicado. Obrigada, queridos, por todo companheirismo, toda cumplicidade. Obrigada por estarem comigo independente da distância e circunstâncias. Amo vocês.

Ao meu marido **Denilson**.
Agradeço a Deus por sua vida, e por ter te colocado na minha. Um marido dedicado, companheiro. Um pai bondoso e amoroso. Exemplo de força, firmeza, fé e perseverança. Obrigada por não me deixar desanimar nunca, por ser meu abrigo, minha calmaria. Te amo muito!

Aos meus tios **Antonio Carlos** e **Simone** e aos meus primos **João Otávio** e **Luiz Eduardo**.
Minha gratidão e meu amor por vocês, que, em todos os momentos fazem questão de estarem presentes. Muito obrigada pela preocupação, pelos conselhos, pelo carinho, por todo amor.

Aos meus familiares, agradeço pelo carinho e apoio ao longo da vida. **Fábio**, **Elaine**, **Lavínia**, **Miguel**, **Liliana**, **Sebastião**, **Aline**, **Luciano**, **Danilo**, **Patrícia**, as pequenas **Daphne** e **Júlia**, **Shirley**, **Altamir**, **Lucas**, **Vinicius**, **Vitória**, **Sueli**, **Sônia**, **Simone**, **Silvana**, **Júnior**, **Marcio, Matheus**, **Bia**, **Silvia**, **Estevam, Giovana**.

Aos meus avós **Erci**, **Juracy** e **Antonia** (*in memorian*), que já não brilham há algum tempo na Terra, mas que deixaram as lembranças dos bons momentos vividos conosco.

Aos meus sogros **David** e **Terezinha**.
Pelo exemplo de fé e sabedoria. Por toda ajuda e todo o apoio. Por me acolherem e me tratarem como verdadeira filha. Muito obrigada.

Aos aos meus cunhados **Josimari** e **Anderson**, e meus sobrinhos **Gabriela**, **Miguel**, **Rafaela**, **Emanuel** e **o** "agregado" **Gelson**. Família linda e abençoada, obrigada pelo carinho sempre.

Aos meus compadres **Samanta** e **Eduardo**, e meu afilhado **Kaik**.
Obrigada por estarem comigo sempre, pelo carinho e compreensão. São minha família de coração.

Aos meus compadres **Elton** e **Diana.**
Sou grata a Deus por ter colocado vocês em nossas vidas. Quantas coisas já vivemos juntos, e que Deus permita muito mais. Muito obrigada pelo apoio, carinho, orações, paciência, conselhos. Nossas famílias estão crescendo juntas e como é bom tudo isso.

Aos meus compadres **Fernando** e **Tamires.**
Fer, amigo de anos, que se tornou um verdadeiro irmão para mim e meu marido. Deus permitiu nossa aproximação quando fomos ao encontro Dele. E quantas histórias desde então. Obrigada pelo carinho para com minha família, pelos conselhos, por nos presentear com a Tamires, garota de fé, conselheira, paciente e amiga. Muito obrigada, casal.

Aos compadres **Cidinha** e **Fábio.**
Muito obrigada pelas orações, carinho e confiança. Que Deus abençoe muito nossa amizade.

Às minhas amigas **Aline** e **Beatriz**.
Li e Bia, entramos praticamente juntas no Laboratório de bioquímica, nos tornamos colegas de trabalho e Deus foi nos aproximando de certa forma que hoje somos grandes amigas-comadres. Com vocês sei que posso contar em qualquer momento. Muito obrigada pelo carinho, por serem muitas vezes apenas "ouvidos e paciência" para os desabafos, por todos os conselhos ao longo desses anos. Que nossa amizade possa crescer ainda mais e que nossas famílias possam estar sempre unidas. Amo vocês.

À **Tati Martini**.
Entrou na minha vida através de sua Iniciação Científica e permanece até hoje, com amizade que vai além das bancadas de laboratório. Muito obrigada por todo carinho e apoio, Tati.

À todos os alunos/colegas/amigos do **Laboratório de Bioquímica: Tamara, Talita, Cíntia, Even, Flávia Levy, Flávia Iano, Gabi, João, Juliana**, **Natara, Thamyris, Adriana, Simone, Mariele, Carlos, Kely, Nathalia, Vinicius, Aline Braga**. Que, de alguma forma, participaram da minha jornada durante esses anos. Agradeço pela convivência, pela ajuda, por todos os momentos juntos.

À **Heloisa Barbosa.**
Obrigada, Helô, por transmitir tudo o que sabe, com amor e dedicação. Você é exemplo de força e determinação. Obrigada pelos conselhos dados, pelo apoio e por deixar nossos dias mais doces.

Às técnicas do Laboratório de Bioquímica **Thelma** e **Larissa.**
Obrigada pelos ensinamentos, pela convivência, por toda ajuda que deram durante todo o tempo que estive no laboratório.

À **Mileni**.
Por dividir este trabalho comigo, por me ajudar sempre que precisei durante todo o tempo de Bioquímica, por responder minhas mil mensagens mesmo tendo todos os seus afazeres. Muito obrigada, Mi.

À secretária **Dalva**.
Agradeço por sempre estar disposta a ajudar, dar conselhos, apoiar. Seu trabalho é essencial pra nós.

Aos docentes do Departamento de Ciências Biológicas, em especial os da Bioquímica: **Profª Carol** e **Profº Rodrigo**. Carol, é a Professora que não se cansa até que todo conteúdo fique claro pra cada aluno. Um exemplo de dedicação e amor pela profissão. Muito obrigada.
Profº Rodrigo, obrigada por sempre ser paciente e tentar ajudar da melhor forma.

À **Universidade de São Paulo – FOB.**

Minha gratidão por essa Universidade que me acolheu, por todos os funcionários que eu pude conhecer e conviver durante toda minha jornada desde a Iniciação Científica.

Agradeço à **Coordenação de Aperfeiçoamento de Pessoal de Nível Superior (CAPES)** por subsidiar este trabalho de Doutorado.

AGRADECIMENTO ESPECIAL

À Professora e Orientadora Marília Afonso Rabelo Buzalaf

São quase 10 anos desde de que cheguei na sua sala pra conversar sobre um possível estágio no LRQ. Neste momento não tem como passar um filme na cabeça. Sou imensamente grata por ter me acolhido com toda paciência e carinho. Muito obrigada por estar sempre de portas e coração abertos, disposta a me receber, me incentivar, a me "chacoalhar' quando fosse preciso. Obrigada por todos os ensinamentos. Obrigada por ser orientadora e ao mesmo tempo família. Deus te abençoe e que Nossa Senhora interceda por você em todos os seus passos.

"Aqueles que passam por nós não vão sós. Deixam um pouco de si, levam um pouco de nós".

Antoine de Saint-Exupery

“Nada é pequeno se feito com amor.”

Santa Terezinha do Menino Jesus

RESUMO

Interação entre o exercício crônico e o *background* genético no metabolismo do fluoreto

O metabolismo do fluoreto (F) é influenciado por fatores genéticos e epigenéticos, como o exercício físico. Vários estudos têm procurado desvendar a influência de fatores genéticos na suscetibilidade à fluorose dentária, utilizando linhagens de camundongos com respostas diferentes aos efeitos de F. No entanto, não existem estudos avaliando os efeitos combinados da genética e do exercício no metabolismo do F. Este estudo avaliou o efeito do exercício crônico no metabolismo do F e parâmetros relacionados à homeostase da glicose, bem como perfil proteômico do fígado e músculo gastrocnêmio, em camundongos suscetíveis (A/J; S) ou resistentes (129P3/J; R) à fluorose, em resposta à exposição ao (F). Quarenta e cinco camundongos machos de cada linhagem foram divididos em 3 grupos, de acordo com os tratamentos que receberam por 56 dias: a) água deionizada e nenhum exercício (I); b) água contendo 50ppmF (como NaF) e nenhum exercício (II); c) água contendo 50ppmF e exercício (corridas diárias em esteira, 5 dias por semana, durante 60 minutos em alta intensidade; III). A capacidade física de todos os camundongos foi medida ao longo do experimento. As concentrações plasmáticas, ósseas e renais de F foram analisadas com um eletrodo específico. Glicose e insulina plasmáticas foram analisadas pelos métodos da glicose-oxidase e ELISA, respectivamente. Análises proteômicas quantitativas, livres de marcadores, foram realizadas no fígado e músculo gastrocnêmio (n-LC-MS/MS). Os dados foram analisados por ANOVA a 2 critérios e Bonferroni ($p<0,05$). As concentrações plasmáticas e ósseas de F foram significativamente maiores nos grupos II e III em relação ao I, independentemente da linhagem. Após o exercício, os camundongos RIII apresentaram concentrações de F no osso significativamente maiores quando comparadas aos RII. As concentrações de F no rim foram significativamente maiores nos camundongos RIII em comparação aos RII e SIII. A capacidade física final foi significativamente menor nos camundongos SII em comparação aos RII. Os camundongos S, independentemente do tratamento, apresentaram níveis plasmáticos de glicose mais altos que os R (significativo para o grupo II). Os níveis

plasmáticos de insulina foram semelhantes entre os grupos. Nos grupos I e II, houve um aumento nas proteínas envolvidas no fluxo energético e nas enzimas antioxidantes nos camundongos S. No entanto, no grupo III, houve uma redução nas proteínas envolvidas na síntese proteica, metabolismo energético e desintoxicação, mas as enzimas antioxidantes ainda estavam aumentadas nos camundongos S. No músculo, os camundongos SI tiveram uma diminuição na expressão proteica em comparação com os RI. Entretanto, nas comparações SIIxRII e SIIIxRIII, houve um aumento de proteínas relacionadas ao fluxo energético e contração muscular nos camundongos S. Os resultados indicam uma complexa interação entre genética e exercício no metabolismo F. O exercício físico parece aumentar o acúmulo de F no osso de camundongos R. O estresse oxidativo em camundongos S pode ser exacerbado pelo tratamento com F. Os resultados analisados em conjunto sugerem que os indivíduos susceptíveis aos efeitos do F podem se beneficiar mais do efeito do exercício físico na homeostase da glicose do que os indivíduos resistentes, mediante exposição a este íon, o que dá respaldo à utilização do F em saúde pública.

Palavras-chave: Fluoreto. Exercício físico. *Background* genético.

ABSTRACT

Interplay between chronic exercise and genetic background on fluoride metabolism

Fluoride (F) metabolism is influenced by genetic and epigenetic factors such as exercise. Several studies have attempted to unravel the influence of genetic factors on the susceptibility to dental fluorosis, using mice strains with different responses to the effects of F. However, there are no studies evaluating the combined effects of genetics and exercise on F metabolism. This study evaluated the effect of chronic exercise on F metabolism and parameters related to glucose homeostasis, as well as liver and gastrocnemius muscle proteome, in mice susceptible (A/J; S) or resistant (129P3/J; R) to fluorosis, in response to F exposure. Forty-five male mice from each strain were divided into 3 groups according to the treatments they received for 56 days: a) deionized water and no exercise (I); b) water containing 50ppmF (as NaF) and no exercise (II); c) water containing 50ppmF and exercise (daily runs on treadmill, 5 days a week for 60 minutes at high intensity; III). The physical capacity of all mice was measured throughout the experiment. Plasma, bone and renal F concentrations were analyzed with a specific electrode. Plasma glucose and insulin were analyzed by glucose oxidase and ELISA methods, respectively. Labe-free quantitative label proteomic analyses were performed on the liver and gastrocnemius muscle (n-LC-MS/MS). Data were analyzed using 2-way ANOVA and Bonferroni´s tests ($p < 0.05$). Plasma and bone concentrations of F were significantly higher in groups II and III than I, regardless of strain. After exercise, RIII mice had significantly higher bone F concentrations compared to RII mice. Kidney F concentrations were significantly higher in RIII mice compared to RII and SIII. Final physical capacity was significantly lower in SII mice compared to RII ones. S mice, regardless of treatment, had higher plasma glucose levels than R mice (significant for group II). Plasma insulin levels were similar between the groups. In groups I and II, there was an increase in proteins involved in energy flux and antioxidant enzymes in S mice. However, in group III, there was a reduction in proteins involved in protein synthesis, energy metabolism and detoxification, but antioxidant enzymes were still increased in

S mice. In muscle, SI mice had a decrease in protein expression compared to RI mice. However, in SIIxRII and SIIIxRIII comparisons, there was an increase in proteins related to energy flux and muscle contraction in S mice. The results indicate a complex interplay between genetics and exercise in F metabolism. Exercise seems to increase F accumulation in the bone of R mice. Oxidative stress may be exacerbated by F treatment in S mice. When analyzed in conjunction, our results suggest that the individuals susceptible to the effects of F might benefit more from the effects of physical exercise on glucose homeostasis that the resistant ones, upon exposure to this ion, which gives additional support to the use of F in public health.

Keywords: Fluoride. Physical exercise. Genetic background.

SUMÁRIO

1 INTRODUÇÃO

1 INTRODUÇÃO

A importância do fluoreto (F) é bem reconhecida pela comunidade científica e extremamente importante em termos de saúde pública. Ele desempenha um papel fundamental na obtenção e manutenção da saúde bucal, devido ao seu potencial no controle da cárie dentária. Por esse motivo, o F tem sido utilizado em programas de saúde pública e também incluído em produtos odontológicos. No entanto, a "janela terapêutica" do F é bastante estreita, isto é, o espaço entre insuficiência e excesso de F é pequeno, podendo oferecer riscos ao organismo se consumido ou aplicado de forma indiscriminada ou inadequada, dentre os quais se destacam a fluorose dentária e esquelética (BUZALAF, 2018). Após sua absorção, o F é distribuído pela corrente sanguínea e armazenado em tecidos calcificados principalmente e em pequena extensão em tecidos moles, sendo sua excreção essencialmente pela via renal (BUZALAF, 2018; WHITFORD, 1996). É importante caracterizar os efeitos fisiológicos do F através de uma melhor compreensão do seu metabolismo. Tem-se sugerido qie vários fatores, incluindo nível de exposição a F, estágio de desenvolvimento esquelético, equilíbrio ácido-base, genética e exercício físico, afetam o metabolismo e a retenção de F no organismo (BUZALAF; WHITFORD, 2011). Quando ingerido em excesso, o F interfere nas principais vias metabólicas dos sistemas biológicos, funcionando como um potente inibidor de muitas enzimas, incluindo algumas da via glicolítica (ARAUJO; PEREIRA; DIONIZIO; SANCHEZ *et al.*, 2019). Além disso, efeitos tóxicos causados pela ingestão excessiva de F têm sido amplamente relatados e os mecanismos envolvidos na toxicidade têm sido investigados (BARBIER; ARREOLA-MENDOZA; DEL RAZO, 2010; PEREIRA; DIONIZIO; ARAUJO; FERNANDES *et al.*, 2018). Esses efeitos relatados demonstraram ser dependentes da dose e do tempo de exposição ao F (ARAUJO; PEREIRA; DIONIZIO; SANCHEZ *et al.*, 2019; DABROWSKA; LETKO; BALUNOWSKA, 2006; KHAN; SABINO; DE SOUZA MELO; MARTINI *et al.*, 2018; PEREIRA; DIONIZIO; ARAUJO; FERNANDES *et al.*, 2018), bem como influenciados pela bagagem genética (BUZALAF, 2018; EVERETT, 2011).

A influência do *background* genético no efeito do F tem sido bastante estudada por meio de trabalhos comparando linhagens de camundongos com

diferentes susceptibilidades aos efeitos deste íon. Dentre elas, destacam-se as linhagens A/J, susceptível (S), com início rápido e desenvolvimento mais grave de fluorose dentária, enquanto a linhagem 129P3/J é resistente (R), desenvolvendo fluorose mínima mesmo sob alta exposição a F (EVERETT, E. T.; MCHENRY, M. A. K.; REYNOLDS, N.; EGGERTSSON, H. *et al.*, 2002). Foi demonstrado que os camundongos R excretam quantidades menores de F na urina, o que leva a níveis mais altos de F circulante quando comparados aos seus homólogos S, mas mesmo assim os primeiros são notavelmente resistentes à ocorrência de fluorose dentária (CARVALHO; LEITE; YAN; EVERETT *et al.*, 2009).

Outro fator que afeta o metabolismo do F é o exercício físico, embora esse efeito ainda não seja conhecido com precisão (BUZALAF; WHITFORD, 2011). Em dois estudos realizados com roedores, o exercício leve diminuiu as concentrações plasmáticas de F (LOMBARTE; FINA; LUPO; BUZALAF *et al.*, 2013; WHITFORD, 1996). Em contrapartida, um estudo recente com camundongos A/J não encontrou efeito do exercício intensivo sobre os níveis plasmáticos de F (AMARAL; AZEVEDO; BUZALAF; FABRICIO *et al.*, 2018). Sabe-se que o exercício físico provoca alterações na expressão gênica e síntese de proteínas (BARRES; ZIERATH, 2016) que podem ser mediadas pelo conteúdo dos exossomos (LI; LIU; MA; CHEN *et al.*, 2019), melhorando a homeostase da glicose e a proteção vascular. No entanto, os efeitos de F na homeostase da glicose ainda não são precisamente conhecidos. Enquanto alguns estudos relataram efeitos benéficos do F (LIMA LEITE; GUALIUME VAZ MADUREIRA LOBO; BARBOSA DA SILVA PEREIRA; SILVA FERNANDES *et al.*, 2014; LOBO; LEITE; PEREIRA; FERNANDES *et al.*, 2015; MALVEZZI; PEREIRA; DIONIZIO; ARAUJO *et al.*, 2018), 2018], outros reportam efeitos deletérios (CHIBA; COLOMBO; SHIRAKASHI; DA SILVA *et al.*, 2012; CHIBA; COLOMBO; SHIRAKASHI; GOMES *et al.*, 2010; LOMBARTE; FINA; LUPO; BUZALAF *et al.*, 2013).

Diante do exposto, o presente estudo foi desenhado a fim de avaliar a interação entre fatores genéticos e epigenéticos (exercício crônico de alta intensidade) no metabolismo do F (artigo 1) e em parâmetros relacionados à homeostasia da glicose e perfil proteômico do fígado e músculo (artigo 2).

2 ARTIGOS

2 ARTIGOS

2.1 ARTIGO 1

Interplay between genetic and epigenetic factors (exercise) on fluoride metabolism.

Isabela T Sabino[a*], Mileni S Fernandes[a*], Mayara F Fabricio[b], Aline L Leite[a], Sandra L Amaral[b], Liane B. Azevedo[c], Ruth A. Valentine[d], Anne Maguire[d], Fatemeh V Zohoori[c], Juliana S Trevizol[a], Marília AR Buzalaf[a]

[a] Bauru School of Dentistry, University of São Paulo, Bauru, SP, Brazil, 17012-901;

[b] Department of Physical Education, Science Faculty, São Paulo State University, Bauru, São Paulo, Brazil, 17033-360;

[c] School of Health and Social Care, Teesside University, Middlesbrough, UK, TS1 3BA;

[d] Centre for Oral Health Research, School of Dental Sciences, Newcastle University, NE2 4BW, Newcastle-upon-Tyne, UK, NE2 4BW.

Running title:

Key Words: Fluoride. Metabolism. Exercise. Genetic variability.

*** Equally contributed for this study**

Corresponding author:

Professor M.A.R. Buzalaf

Department of Biological Sciences

Bauru School of Dentistry, University of São Paulo.

Al. Octavio Pinheiro Brisolla, 9-75.

17012-901, Bauru, São Paulo, Brazil.

Email: mbuzalaf@fob.usp.br

Abstract

The metabolism of fluoride (F) is influenced by genetic and epigenetic factors, among which is physical exercise. However, little is known about the effect of the latter and there are no studies evaluating the combined effect of both factors on F metabolism. The current study investigated the effect of exercise on F metabolism in mice susceptible (S; A/J) or resistant (129P3/J; R) mice. Forty-five male mice from each strain were divided into 3 groups, according with the treatments they received for 56 days: a) deionized drinking water and no exercise (I); b) drinking water containing 50ppmF (as NaF) and no exercise (II); c) drinking water containing 50ppmF and exercise (daily runs on a treadmill 5 days week for 60 minutes at high intensity; III). The physical performance of all mice was measured along the experiment and the F concentrations in plasma, bone (femur) and kidney were determined at the end of experiment. Data were analyzed by 2-way ANOVA and Bonferroni´s tests ($p<0.05$) Plasma and bone F concentrations were significantly higher for groups II and III in respect to I, regardless of the strain. Upon exercise, RIII mice had significantly higher bone F concentrations when compared RII. Kidney F concentrations were significantly higher in RIII mice compared with RII and SIII. Final physical capacity was significantly lower in SII mice compared with RII mice. Our data indicate a complex interplay between genetics and exercise on F metabolism. Exercise seems to increase F accumulation in bone of R mice, while sedentary lifestyle reduces the physical capacity in S mice exposed to F.

Introduction

Fluoride (F) is an extremely important ion in terms of public health. When used as directed or within the context of community water fluoridation programs, F is a safe and effective agent that can prevent and control dental caries. However, excessive intake of F on a chronical basis can cause dental or skeletal fluorosis, which means that exposure to F needs to be monitored (BUZALAF, 2018).

After ingestion, F is rapidly absorbed by the gastrointestinal tract and peak plasma F levels are reached within 20-60 min. The ion is avid for mineralized tissues and 99% of absorbed F is incorporated in the bone, while the portion not taken up in the organism is excreted mainly in urine. Several factors, including the stage of skeletal development, acid-base balance, genetics, altitude of residence and exercise physical have been suggested to affect F metabolism and retention in the body. These interfering factors alter the relationship between the F intake and the risk of dental and skeletal fluorosis (BUZALAF; WHITFORD, 2011). In other words, if the interplay among these factors favours the F retention in the organism, there will be an increased risk of fluorosis. Thus, it is important to have a solid knowledge on the influence of them, alone or in combination, on F metabolism, considering that F is widely employed in public health to control dental caries.

In the last years, the influence of genetics on F metabolism has gained evidence with studies conducted in mice. Everett and co-workers (EVERETT, E. T.; MCHENRY, M. A. K.; REYNOLDS, N.; EGGERTSSON, H. *et al.*, 2002) showed that A/J mice are highly susceptible to dental fluorosis, while 129P3/J mice are remarkably resistant. This observation prompted studies to evaluate the metabolism of F by these distinct mice strains. Curiously, it was shown that 129P3/J mice, despite resistant to dental fluorosis, have lower urinary F excretion and higher circulating plasma F levels (CARVALHO; LEITE; YAN; EVERETT *et al.*, 2009). These intriguing results led to molecular studies trying to unravel the mechanisms involved in the susceptibility/resistance to dental fluorosis. It was observed that A/J mice have intrinsically an increase in proteins in the liver related to energy flux and oxidative stress (KHAN; LEITE ADE; CHARONE; SABINO *et al.*, 2016), as well as higher amounts of amelogenin in the maturing enamel (EVERETT; YAN; WEAVER; LIU *et al.*, 2009), even without exposure to F, which could possibly be related to the development of dental fluorosis. It was also reported that amelogenin and type I collagen were only identified in the maturation-stage of the A/J mice but not of their

129P3/J counterparts (CHARONE; DE LIMA LEITE; PERES-BUZALAF; SILVA FERNANDES *et al.*, 2016). The possible involvement of col1a2 gene in the susceptibility to dental fluorosis is also supported by epidemiological data in areas of endemic fluorosis (HUANG; BA; CUI; CHENG *et al.*, 2008).

The effect of physical exercise on F metabolism is less studied, with only 3 studies conducted with rodents so far. It was reported that light exercise decreases plasma F concentrations of rats (LOMBARTE; FINA; LUPO; BUZALAF *et al.*, 2013; WHITFORD, 1996), but in a recent study with the susceptible A/J mice, high intensity exercise did not alter plasma F concentrations (AMARAL; AZEVEDO; BUZALAF; FABRICIO *et al.*, 2018). Considering that physical exercise provokes changes in gene expression and protein synthesis (BARRES; ZIERATH, 2016), alterations in physiological responses induced by exercise may impact the pharmacokinetics of F, which could be important in terms of the influence of this ion on tooth and bone development and the timing of F ingestion when used as a dental caries preventive therapy. Thus, the aim of the present study was to evaluate the interplay between genetics (susceptibility or resistance to the effects of F) and chronic exercise on F metabolism in mice.

Materials and methods

Animals, Treatment, and Samples Collection

The research protocol was approved by the Ethics Committee for Animal Experiments of Bauru Dental School, University of São Paulo, USP (#009-2015). Ninety 21-day-old male mice were received [n=45 from A/J strain (S) and n=45 from 129P3/J strain (R)]. The mice were kept in rooms with controlled temperature, humidity and light/dark cycles (~ 23 ± 1°C, 40-80% and 12/12 h, respectively). The mice were housed in pairs in plastic cages and had free access to water and diet with low F content (Presence, Purina, <1 ppm). Animals from both strains (S and R), at 45 days of age, where divided into 3 groups according to the treatment: a) deionized drinking water and no exercise (I); b) drinking water containing 50 ppm F (as NaF) and no exercise (II); c) drinking water containing 50 ppm F and exercise (daily runs on a treadmill 5 days week for 60 min at high intensity; III). During 4 weeks of adaptation and familiarization with the treadmill device, it was determined the volume of water consumed by the animals from both strains. For the remainder of the study the F concentrations in the water given to the animals were adjusted weekly to

equalize the F intake by the 2 strains, since it has been reported that A/J mice ingest higher volumes of water (CARVALHO; LEITE; YAN; EVERETT *et al.*, 2009). It should be noted that 2 pairs of mice from each group were housed in metabolic cages for measurement of water consumption. After the adaptation period, Group I continued to receive deionised water and the experimental Groups II and III received drinking water containing 50 ppm F, all for 8 weeks.

The exercise training regime of the groups III consisted of High Intensity Interval Training (HIIT) on a treadmill, 5 days per week, for 8 weeks. The body weight of all animals was measured weekly and water consumption per cage was recorded daily. At the end of the study, the mice were anesthetized with sodium thiopental (Thiopentax; Cristália, Itapira, Brazil). A blood sample was collected from heart into a lightly heparinized syringe for the determination of plasma F. The left femur and kidney were collected for F analysis.

Exercise protocol

The maximum capacity tests and training protocol were performed on a treadmill device (INBRAMED, Mod Era 2007, Brazil). To determine the maximum running speed, all animals were familiarized with the treadmill. The objective this adaptation was also the reduction of stress levels presented by the animals due to the task being known without the promotion of exercise training. The HIIT protocol was adapted (TOTI; BARTALUCCI; FERRUCCI; FULCERI *et al.*, 2013) and the training sessions were performed at the exact same time each weekday to avoid diurnal effects on training performance (DJAWDAN; GARLAND, 1988).

Determination of maximum running speed. To adaptation with the treadmill, sessions of 10 min at speed of 8m/min at zero incline were performed once a day for five days (BARTALUCCI; FERRUCCI; FULCERI; LAZZERI *et al.*, 2012). After this period, each mouse performed a maximum running test on the treadmill (FERREIRA; ROLIM; BARTHOLOMEU; GOBATTO *et al.*, 2007). The test began at 9 m/min at zero incline and increased by 3 m/min every 3 min thereafter until exhaustion (i.e. when the animals could no longer run). This maximum running test was repeated for each mouse in all groups after 4 weeks, to allow for any adjustment of exercise intensity and again at the end of the experimental period to measure the effect of training on maximum running speed.

Treadmill training experiment

Groups III (S; R) were submitted to a HIIT routine, 5 days per week over the 8 weeks. The HIIT sessions consisted of 5 min warm-up at 40% of each mice maximum running speed followed by sequence of nineteen short periods (1 minute each) of high intensity effort, at 80% of maximum running speed, followed by a 3-min recovery period (rest). Each training session ended when the mouse completed a distance of 1,000 meters.

Sample preparation and fluoride analysis

Blood samples were centrifuged at 1400xg for 10 min (Eppendorf 5415C) at 4°C. Plasma was separated and stored at -20°C. Kidneys were homogenized in deionized water for 2 min using a homogenizer (Marconi, Model MA 102). The femurs were cleaned of soft tissue and added at 600°C overnight in a muffle furnace (Fornitec, model HW1000; Fornitec Industria e Comercio, Santo Amaro, São Paulo, Brazil). The ashes were weighed and stored at room temperature prior to F analysis. Plasma F concentrations in kidneys and bone ash were determined after overnight hexamethyldisiloxane-facilitated diffusion (TAVES, 1968; WHITFORD, 1996) with an ion-specific electrode (Orion Research, model 9409) and a calomel electrode (Accumet, Cambridge, MA, USA; Model 13-620-79), both coupled to a potentiometer (Orion Research, Model 940A). F standards (0.005 to 0.19 µg F for plasma, 0.019 to 0.45 µg F for kidney and 1.9 to 38.0 µg F for bone) were prepared in triplicate and diffused in the same manner as the samples. In addition, non-diffused standards were prepared with exactly the same F concentrations as the diffused standards. Comparison of the mV readings demonstrated that the F in the diffused standards had been completely trapped and analyzed (recovery >95%). The mV potentials were converted to µg F using a standard curve with a correlation coefficient of r≥00.99.

Statistical Analysis

GraphPad Instat version 3.0 and GraphPad Prism software version 5.0 for Windows (GraphPad software Inc., La Jolla, USA) were used. All data showed normal distribution (Kolmogorov-Smirnov test) and equality of variance (Bartlett's test) and are presented as mean and standard deviation of means (SD). Data were analyzed by 2-way ANOVA and Tukey, Bonferroni or Sidak tests for individual comparisons. In all cases, the significance limit was set at 5%.

Results

The mean (SD) daily water consumption per mouse across the whole experimental period was 5.99±0.99, 5.92±0.96 and 4.28±0.58 g for SI, SII and SIII mice, respectively. The corresponding values for the RI, RII and RIII mice were 5.95±1.77, 6.66±1.17 and 6.46±1.19 g, respectively. There were not significant differences in the final body weight of the animals, despite exposure to F tended to reduce the final body weight in the S mice (data not shown).

Table 1 presents the mean (SD) F concentrations in plasma, bone ash (femur) and kidney for all the groups. For plasma F, the two-way ANOVA revealed a significant difference between the strains ($F=15.61$, $p=0.0002$) and among the treatments ($F=25.81$, $p<0.001$), with significant interaction between these criteria ($F=3.34$, $p=0.040$). F-exposed R mice had significantly higher plasma F concentrations than their S counterparts. When the treatments were compared, F-exposed groups had significantly higher plasma F concentrations compared with control, regardless of exercise. Regarding the femur F concentrations, a significant difference was found between the strains ($F=13.01$, $p=0.0005$) and among the treatments, ($F=75.53$, $p<0.0001$), without significant interaction between these criteria ($F=2.69$, $p=0,0744$). Similarly to which was observed for plasma, F-exposed R mice had significantly higher femur F concentrations than their S counterparts. For the comparison among the treatments, exposure to F significantly increased bone F concentrations in respect with control. Moreover, RIII mice had significantly higher bone F levels than RII ones, but the same was not observed for S mice. Kidney F concentrations were significantly different between the strains ($F=6.92$, $p=0.0111$) and among the treatments ($F=9.59$, $p=0.0003$), with interaction between these criteria ($F=6.61$, $p=0.0027$). For the comparison between the strains, RIII mice had F concentrations significantly higher than SIII ones, while for the other comparisons there were not significant differences. When the treatments were compared, the only significant difference was found for RIII mice that had significantly higher kidney F concentrations than RII and RI mice, which did not significantly differ from each other. The weight of the kidneys were evaluated and the profile obtained was similar to the one described for kidney F concentrations (Figure 1).

Results of the maximum running speed test are presented in Table 2, according to the strain, F exposure and exercise regime. The 2-way ANOVA did not find significant difference in the running speed along the treatment between the

strains (p=0.533) but it was found among the treatments (p<0.001), without significant interaction between these criteria (p=0.807). Regardless the strain, the groups that underwent HIIT had significant increases in the running speed when compared with the sedentary groups. It should be highlighted that exposure to F only did not change the mean running speed in comparison to unexposed groups. As for the final physical capacity, reported in function of the mean execution time of the last maximum test on the treadmill (Figure 2), significant differences were found between the strains (p=0.0004), as well as among the treatments (p=0.0016), without interaction between them (p=0.0228). The only difference found between the strains was between SII mice and their RII counterparts. The first had significant lower final physical capacity than the latter. After HIIT training no significant difference. Moreover, mice exposed to F and HIIT (groups III) had significantly higher final physical capacity than their sedentary counterparts (groups II), regardless of the strain.

Discussion

In the present study, we took advantage of mice with distinct susceptibilities to the effects of F (EVERETT, 2011; EVERETT, E. T.; MCHENRY, M. A. K.; REYNOLDS, N.; EGGERTSSON, H. *et al.*, 2002) to evaluate the interplay between genetics and physical exercise on F metabolism. This is the first study in which this interplay was evaluated, since previous ones assessed the effects of genetics (CARVALHO; LEITE; YAN; EVERETT *et al.*, 2009) or exercise (AMARAL; AZEVEDO; BUZALAF; FABRICIO *et al.*, 2018; LOMBARTE; FINA; LUPO; BUZALAF *et al.*, 2013) alone.

There was no significant difference in the final body weight of the animals, but the SII mice tended to have lower body weight at the end of the experiment, as reported in our previous study (AMARAL; AZEVEDO; BUZALAF; FABRICIO *et al.*, 2018; LOMBARTE; FINA; LUPO; BUZALAF *et al.*, 2013). From the toxicological point of view the lack of significant reduction in the body weight of the animals upon exposure to F reinforces the safety of the use of F in public health.

The metabolism of F is characterized by a rapid absorption, reaching peak plasma F levels around 20-60 min after ingestion of this ion. After this period, plasma F levels are reduced, which is caused mainly by two factors: urinary F excretion and F uptake in bone. F has a great affinity by hydroxyapatite and becomes rapidly taken

up by bone, which results in 99% of the F body burden associated to calcified tissues. Moreover, there is a steady-state relationship between plasma F concentrations and the F concentrations in the hydration shells of the bone crystallites (BUZALAF; WHITFORD, 2011). Considering these features of F metabolism, in the present study we evaluated plasma, bone and kidney F concentrations. R mice exposed to F have been reported to have higher plasma and femur F concentrations compared with their S counterparts (CARVALHO; LEITE; YAN; EVERETT *et al.*, 2009), which was confirmed in the present study. However, physical exercise did not impact plasma F concentrations (Table 1) but led to significantly higher femur F concentrations for the R mice only, indicating a higher retention of F in the hard tissues of these mice. This increase in femur F concentrations upon exercise has been reported previously in *Sprague dawley* rats and is associated with lower F toxicity, since F incorporation in bone reduces plasma F levels (LOMBARTE; FINA; LUPO; BUZALAF *et al.*, 2013). In addition, RIII mice had also significantly higher kidney F concentrations and kidney weight (Figure 2) upon exercise, which might possibly indicate renal alterations in these mice that need to be evaluated in further studies. It should be noted that trained S mice did not present a significant increase in femur concentrations compared to their counterparts that were only exposed to F, which is in-line with our previous study (AMARAL; AZEVEDO; BUZALAF; FABRICIO *et al.*, 2018) but is different from which was reported by Lombarte et al. (LOMBARTE; FINA; LUPO; BUZALAF *et al.*, 2013) for *Sprague dawley* rats. These results indicate a complex interplay between genetics and exercise in F metabolism, which might impact the relationship between the amount of F intake and the risk of developing dental fluorosis. In general lines, according to the protocol of the present study, plasma F levels were not affected by chronic exercise, regardless of the genetic background. However, exercise increased F taken up by bone in R mice. It is important to highlight that bone is a F reservoir, since F can be released back to the systemic circulation upon bone resorption (BUZALAF; WHITFORD, 2011) and this could impact on dental fluorosis, which should be evaluated in further studies.

Since the individual resistance to physical stress is critical to the final quality (beneficial or adverse) of the systemic effects of exercise (PETROVIC-OGGIANO; DAMJANOV; GURINOVIC; GLIBETIC, 2010), and training is important in preparing the body to adequately support physical stress, selecting a training is decisive for

producing positive effects (BARTALUCCI; FERRUCCI; FULCERI; LAZZERI *et al.*, 2012). Knowing about the importance of determining the training protocol, we conducted a pilot study (AMARAL; AZEVEDO; BUZALAF; FABRICIO *et al.*, 2018). After the determination of the appropriate training protocol, the present study was started, in which the animals were submitted to the developed HIIT protocol. The genetic factors represent a substantial portion of resistance to physical training, with a heritability estimated at around 50% (BOUCHARD; DAW; RICE; PERUSSE *et al.*, 1998). When different mice strains were analyzed, it was observed that genetic variability can substantially influence the resistance capacity; this influence is evident even when different types of motor activities are explored (COURTNEY; MASSETT, 2012; KILIKEVICIUS; VENCKUNAS; ZELNIENE; CARROLL *et al.*, 2013; KVEDARAS; MINDERIS; FOKIN; RATKEVICIUS *et al.*, 2017). In the present study, we worked with mice strains with different susceptibilities to the effects of F in the organism (EVERETT, E. T.; MCHENRY, M. A.; REYNOLDS, N.; EGGERTSSON, H. *et al.*, 2002). However, the genetic background of these strains did neither affect their final physical capacity (Figure 2) nor their change in maximum running speed along the experimental period (Table 2). Physical training can be defined as periodic repetition of exercises over time, which results in increased physical capacity (LAURSEN, 2010). This is due to metabolic and systemic adaptations, and the main adaptations induced by physical training involve the skeletal muscles. It is well established that regular exercise improves the energetic state of the muscles (DEL BALSO; CAFARELLI, 2007; LAURSEN, 2010), with consequent increase in the aerobic capacity (JONES; CARTER, 2000; LAURSEN; RHODES, 2001). In-line with this, in the present study, we observed a significant increase in the maximum running speed along the experimental period for the mice that undergone HIIT in comparison with the sedentary ones, regardless of the strain (Table 2). In addition, mice exposed to F and HIIT (groups III) had significantly higher final physical capacity than their sedentary counterparts (groups II), regardless of the strain (Figure 2), which might be explained by their higher resistance to the effects of F (CARVALHO; LEITE ADE; PERES-BUZALAF; SALVATO *et al.*, 2013; EVERETT, E. T.; MCHENRY, M. A.; REYNOLDS, N.; EGGERTSSON, H. *et al.*, 2002; KOBAYASHI; LEITE; PERES-BUZALAF; CARVALHO *et al.*, 2014; MOUSNY; BANSE; WISE; EVERETT *et al.*, 2006). However, upon exposure to F, the genetics influenced the final physical capacity, since the S sedentary mice had this parameter significantly lower that their

R counterparts (Figure 2), but this deleterious effect was counteracted by physical exercise. In other words, the sedentary lifestyle poses greater risks to physical capacity after exposure to F.

In summary, our results indicate a complex interplay between genetics and exercise on F metabolism. Exercise seems to increase F accumulation in bone of R mice, while sedentary lifestyle reduces the physical capacity in S mice exposed to F. Ultimately, our data indicate that the S mice might benefit more from physical training than the R ones. Studies with similar designs should be conducted with humans presenting different susceptibilities to the effects of F to see if they respond similarly to the interplay between genetics and physical exercise on F metabolism.

The results showed that chronic exercise has no effect on F in plasma and bone of fluorosis-susceptible mice, providing important data for developing appropriate strategies to optimize general and oral health. The profile obtained was that the sedentary lifestyle offers a greater risks to physical capacity after exposure to F and the possibly of renal alteration with the association between F exposure and physical exercise. This study may help to understand the molecular mechanisms underlying genetic susceptibility to dental fluorosis, which should be better addressed in future studies.

References

Amaral, S. L., L. B. Azevedo, M. A. R. Buzalaf, M. F. Fabricio, M. S. Fernandes, R. A. Valentine, A. Maguire and F. V. Zohoori (2018). "Effect of chronic exercise on fluoride metabolism in fluorosis-susceptible mice exposed to high fluoride." Sci Rep **8**(1): 3211.

Barres, R. and J. R. Zierath (2016). "The role of diet and exercise in the transgenerational epigenetic landscape of T2DM." Nature Reviews Endocrinology **12**(8): 441-451.

Bartalucci, A., M. Ferrucci, F. Fulceri, G. Lazzeri, P. Lenzi, L. Toti, F. R. Serpiello, A. La Torre and M. Gesi (2012). "High-intensity exercise training produces morphological and biochemical changes in adrenal gland of mice." Histol Histopathol **27**(6): 753-769.

Bouchard, C., E. W. Daw, T. Rice, L. Perusse, J. Gagnon, M. A. Province, A. S. Leon, D. C. Rao, J. S. Skinner and J. H. Wilmore (1998). "Familial resemblance for VO2max in the sedentary state: the HERITAGE family study." Med Sci Sports Exerc **30**(2): 252-258.

Buzalaf, M. A. and G. M. Whitford (2011). "Fluoride metabolism." Monogr Oral Sci **22**: 20-36.

Buzalaf, M. A. R. (2018). "Review of Fluoride Intake and Appropriateness of Current Guidelines." Adv Dent Res **29**(2): 157-166.

Carvalho, J. G., A. L. Leite, D. Yan, E. T. Everett, G. M. Whitford and M. A. Buzalaf (2009). "Influence of genetic background on fluoride metabolism in mice." J Dent Res **88**(11): 1054-1058.

Charone, S., A. De Lima Leite, C. Peres-Buzalaf, M. Silva Fernandes, L. Ferreira de Almeida, M. S. Zardin Graeff, R. Cardoso de Oliveira, A. P. Campanelli, S. Groisman, G. M. Whitford, E. T. Everett and M. A. Buzalaf (2016). "Proteomics of Secretory-Stage and Maturation-Stage Enamel of Genetically Distinct Mice." Caries Res **50**(1): 24-31.

Courtney, S. M. and M. P. Massett (2012). "Identification of exercise capacity QTL using association mapping in inbred mice." Physiol Genomics **44**(19): 948-955.

Del Balso, C. and E. Cafarelli (2007). "Adaptations in the activation of human skeletal muscle induced by short-term isometric resistance training." J Appl Physiol (1985) **103**(1): 402-411.

Djawdan, M. and T. Garland (1988). "Maximal Running Speeds of Bipedal and Quadrupedal Rodents." Journal of Mammalogy **69**(4): 765-772.

Everett, E. T. (2011). "Fluoride's Effects on the Formation of Teeth and Bones, and the Influence of Genetics." Journal of Dental Research **90**(5): 552-560.

Everett, E. T., M. A. McHenry, N. Reynolds, H. Eggertsson, J. Sullivan, C. Kantmann, E. A. Martinez-Mier, J. M. Warrick and G. K. Stookey (2002). "Dental fluorosis: variability among different inbred mouse strains." J Dent Res **81**(11): 794-798.

Everett, E. T., M. A. K. McHenry, N. Reynolds, H. Eggertsson, J. Sullivan, C. Kantmann, E. A. Martinez-Mier, J. M. Warrick and G. K. Stookey (2002). "Dental

fluorosis: Variability among different inbred mouse strains." Journal of Dental Research **81**(11): 794-798.

Everett, E. T., D. Yan, M. Weaver, L. Liu, T. Foroud and E. A. Martinez-Mier (2009). "Detection of dental fluorosis-associated quantitative trait Loci on mouse chromosomes 2 and 11." Cells Tissues Organs **189**(1-4): 212-218.

Ferreira, J. C., N. P. Rolim, J. B. Bartholomeu, C. A. Gobatto, E. Kokubun and P. C. Brum (2007). "Maximal lactate steady state in running mice: effect of exercise training." Clin Exp Pharmacol Physiol **34**(8): 760-765.

Huang, H., Y. Ba, L. Cui, X. Cheng, J. Zhu, Y. Zhang, P. Yan, C. Zhu, B. Kilfoy and Y. Zhang (2008). "COL1A2 gene polymorphisms (Pvu II and Rsa I), serum calciotropic hormone levels, and dental fluorosis." Community Dent Oral Epidemiol **36**(6): 517-522.

Jones, A. M. and H. Carter (2000). "The effect of endurance training on parameters of aerobic fitness." Sports Med **29**(6): 373-386.

Khan, Z. N., L. Leite Ade, S. Charone, I. T. Sabino, T. Martini, H. A. Pereira, R. C. Oliveira and M. A. Buzalaf (2016). "Liver proteome of mice with different genetic susceptibilities to the effects of fluoride." J Appl Oral Sci **24**(3): 250-257.

Kilikevicius, A., T. Venckunas, R. Zelniene, A. M. Carroll, S. Lionikaite, A. Ratkevicius and A. Lionikas (2013). "Divergent physiological characteristics and responses to endurance training among inbred mouse strains." Scand J Med Sci Sports **23**(5): 657-668.

Kvedaras, M., P. Minderis, A. Fokin, A. Ratkevicius, T. Venckunas and A. Lionikas (2017). "Forced Running Endurance Is Influenced by Gene(s) on Mouse Chromosome 10." Front Physiol **8**: 9.

Laursen, P. B. (2010). "Training for intense exercise performance: high-intensity or high-volume training?" Scand J Med Sci Sports **20 Suppl 2**: 1-10.

Laursen, P. B. and E. C. Rhodes (2001). "Factors affecting performance in an ultraendurance triathlon." Sports Med **31**(3): 195-209.

Lombarte, M., B. L. Fina, M. Lupo, M. A. Buzalaf and A. Rigalli (2013). "Physical exercise ameliorates the toxic effect of fluoride on the insulin-glucose system." J Endocrinol **218**(1): 99-103.

Petrovic-Oggiano, G., V. Damjanov, M. Gurinovic and M. Glibetic (2010). "[Physical activity in prevention and reduction of cardiovascular risk]." Med Pregl **63**(3-4): 200-207.

Taves, D. R. (1968). "Separation of fluoride by rapid diffusion using hexamethyldisiloxane." Talanta **15**(9): 969-974.

Toti, L., A. Bartalucci, M. Ferrucci, F. Fulceri, G. Lazzeri, P. Lenzi, P. Soldani, P. Gobbi, A. La Torre and M. Gesi (2013). "High-intensity exercise training induces morphological and biochemical changes in skeletal muscles." Biol Sport **30**(4): 301-309.

Whitford, G. M. (1996). "The metabolism and toxicity of fluoride." Monogr Oral Sci **16 Rev 2**: 1-153.

Acknowledgements

This study was supported by FAPESP (2015/12109-2 and 2016/20020-4) and Coordenação de Aperfeiçoamento de Pessoal de Nível Superior - Brasil (CAPES) - Finance Code 001.

Author Contributions

M.A.R.B., S.L.A., F.V.Z., L.B.A., A.M., R.V., M.F.F and M.S.F. designed the study. S.L.A., M.F.F. and L.B.A. developed the exercise protocol. M.S.F and M.F.F. conceived the experiments, collected the data/samples and analyzed the samples. M.S.F., A.L.L., I.T.S., J.S.T., participated in the experiments analysis M.S.F., I.T.S., S.L.A., M.F.F and M.A.R.B. drafted the article; analyzed and interpreted the results. All authors reviewed and approved the manuscript.

Additional Information
Supplementary information
Competing Interests: The authors declare no competing interests.

Table 1. Mean (SD) F concentrations of plasma (µg/mL), femur ash (mg/Kg) and kidney (µg/g) in groups SI, RI (Control), Groups SII., RII (50 ppm F, No-exercise) and groups SIII., RIII (50 ppm, Exercise) at the end of experiment. Distinct uppercase superscripts indicate significant differences between the strains. Distinct lowercase superscripts in the same row indicate significant differences among the treatments.

		Treatment		
	Strain	**Control (I)**	**50 ppm F, No Exercise (II)**	**50 ppm F, Exercise (III)**
[F] Plasma	A/J (S)	$0.014±0.004^{Aa}$	$0.053±0.030^{Bb}$	$0.044±0.015^{Bb}$
(µg/mL)	129P3/J (R)	$0.017±0.004^{Aa}$	$0.086±0.037^{Ab}$	$0.089±0.062^{Ab}$
[F] Femur	A/J (S)	$217±60^{Aa}$	$2024±736^{Bb}$	$2560±1227^{Bb}$
(mg/Kg)	129P3/J (R)	$274±173^{Aa}$	$2915±697^{Ab}$	$3709±1371^{Ac}$
[F] Kidney	A/J (S)	$0.034±0.010^{Aa}$	$0.055±0.030^{Aa}$	$0.045±0.020^{Ba}$
(µg/g)	129P3/J (R)	$0.035±0.020^{Aa}$	$0.056±0.010^{Aa}$	$0.103±0.060^{Ab}$

Table 2. Mean (SD) maximum running speed (m/min) at baseline and at the end of experiment and respective change in running speed.

Strain	**Group**	**No**	**Mean (SD) maximum running speed (m/min)**		**Change***
			Baseline	**End of experiment**	**Mean (SEM)**
A/J[A]	SI (Control)	15	19.8 (6.0)	18.0 (5.4)	-1.8 (3.0) [a]
	SII (50ppmF, no-exercise)	16	19.3 (6.6)	17.2 (5.7)	-2.0 (2.1) [a]
	SIII (50ppmF, exercise)	14	20.8 (5.5)	22.5 (4.5)	+1.7 (5.4) [b]
129P3/J[A]	RI (Control)	15	24.8 (4.0)	21.8 (4.6)	-3.0 (3.2) [a]
	RII (50ppmF, no-exercise)	15	24.2 (3.7)	22.0 (3.9)	-2.2 (3.3) [a]
	RIII (50ppmF, exercise)	15	25.0 (4.0)	26.6 (4.8)	+1.6 (4.4) [b]

* "Change = speed at the end of experiment – speed at baseline". Similar uppercase superscripts indicate lack of significant difference between the strains for the change in running speed. Distinct lowercase superscripts indicate significant differences among the treatments, for each strain. Two-way ANOVA followed by Bonferroni´s test ($p<0.05$). n=15.

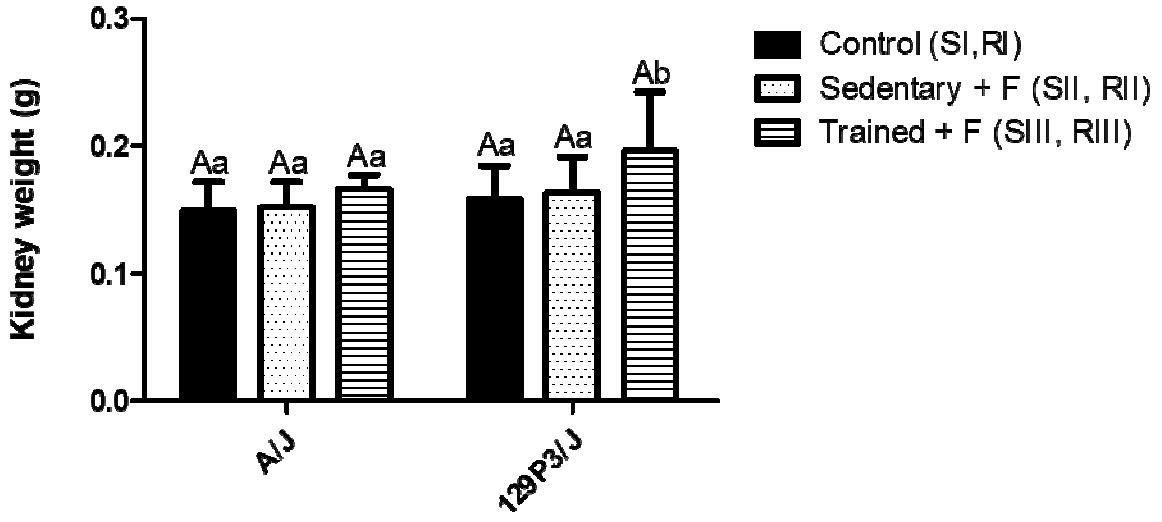

Figure 1. Mean (SD) kidney weight in all experimental groups. Similar uppercase letters denote lack of significant difference between the strains, for each type of treatment. Distinct lowercase letters indicate significant difference among the treatments, for each strain. Two-way ANOVA followed by Bonferroni test, p<0.05). n=15.

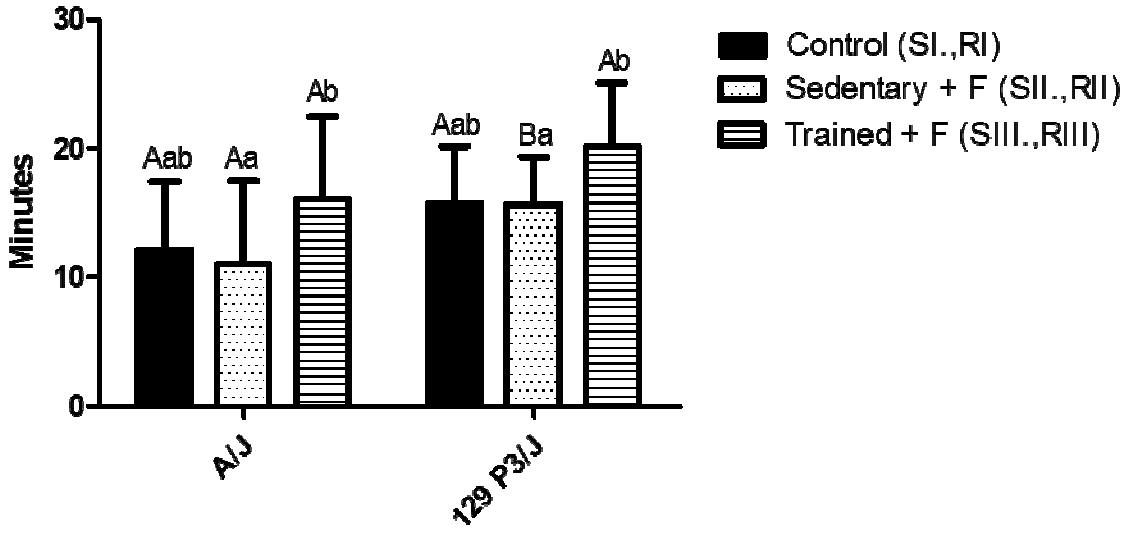

Figure 2. Average execution time of the last maximum test (final physical capacity) on the treadmill, for all experimental groups. Distinct uppercase letters indicate significant difference between the strains, for each type of treatment. Distinct lowercase letters indicate significant difference among the treatments, for each strain. P-values using two-way ANOVA followed by Bonferroni test, p<0.05. n=15.

2.2 ARTIGO 2

Article formatted according to Journal of Applied Oral Science.

Chronic exercise and genetic background affect glucose homeostasis and liver/muscle proteome in mice

Isabela T Sabino[a]
e-mail: belatomazini@gmail.com
Mileni S Fernandes[a]
e-mail: mi_biol@yahoo.com.br
Aline S Dionízio[a]
e-mail: stars_line@hotmail.com
Mayara F Fabricio[b]
e-mail: mayara.fabricio@hotmail.com
Liane B. Azevedo[c]
e-mail: L.Azevedo@tees.ac.uk
Ruth A. Valentine[d]
e-mail: Ruth.Valentine@newcastle.ac.uk
Anne Maguire[d]
e-mail: anne.maguire@newcastle.ac.uk
Fatemeh V Zohoori[c]
e-mail: V.Zohoori@tees.ac.uk
Sandra L Amaral[b]
e-mail: slamaral70@gmail.com
Marília AR Buzalaf[a]
e-mail: mbuzalaf@fob.usp.br

[a] Faculdade de Odontologia de Bauru, Universidade de São Paulo, Bauru, SP, Brasil, 17012-901;
[b] Departamento de Educação Física, Faculdade de Ciências, Universidade Estadual Paulista, Bauru, SP, Brasil, 17033-360;
[c] School of Health and Social Care, Teesside University, Middlesbrough, UK, TS1 3BA
[d] Centre for Oral Health Research, School of Dental Sciences, Newcastle University, NE2 4BW, Newcastle-upon-Tyne, UK, NE2 4BW

Keywords: Fluoride. Exercise. Genetic background.

***Corresponding Author:** Marília Afonso Rabelo Buzalaf - Department of Biological Sciences, Bauru Dental School, University of São Paulo. Al. Octávio Pinheiro Brisolla, 9-75, Bauru-SP, 17012-901 Brazil. Tel. + 55 14 32358346; E-mail: mbuzalaf@fob.usp.br

Chronic exercise and genetic background affect glucose homeostasis and liver/muscle proteome in mice

ABSTRACT

Introduction: The metabolism and retention of F seem to be influenced by genetic, as well as by interaction with the environment, such as exercise. **Objectives:** Were compared parameters related to glucose homeostasis and proteome of liver and muscle in mice susceptible (A/J) or resistant (129P3/J) to dental fluorosis in response to exposure to F, with and without exercise. **Methods:** 45 A/J (S) and 45 129P3/J (R) (n= 15 per group) male mice were divided into 6 groups, treated by 56 days: a) 0ppmF water and no exercise (SI; RI); b) 50ppmF water and no exercise (SII;RII); c) 50ppmF water and exercise (daily runs 5 days/week for 60', high intensity) (SIII;RIII). Plasma F, glycemia and insulinemia were analyzed. Proteomic analyses were conducted in the liver and gastrocnemius muscle (n-LC-MS/MS). Data were analyzed by 2-way ANOVA and Bonferroni´s tests ($p<0.05$). **Results:** The S mice, had higher plasma glucose levels than the R ones (significant for group II). Plasma insulin were similar among the groups. Liver proteome of the S and R, in groups I and II, there was an increase in proteins involved in energy flux. However, in group III, there was a reduction in proteins involved in protein synthesis, energy metabolism and detoxification, but antioxidant enzymes were still increased in the S mice. In muscle, SI x RI, SI had a decrease in protein expression. However, for the comparisons SIIxRII and SIIIxRIII, there was an increase in proteins related to energy flux and muscle contraction in the S mice. **Conclusion:** These results suggest an increased state of oxidative stress in S mice that is inherent to this strain and might be exacerbated by the treatment with F. In addition, S individuals might benefit more of the effect of physical exercise on glucose homeostasis than the R ones, upon exposure to F.

Keywords: Fluoride. Exercise. Genetic background.

INTRODUCTION

The importance of fluoride (F) is well recognized by the scientific community. This element plays a key role in achieving and maintaining oral health due to its potential to control the development of dental caries lesion. For this reason, F has been employed in public health programs and also included in dental products. However, the "therapeutic window" of F is rather narrow, i.e., the space between insufficiency and excess of F is small. Thus, it is highly desirable to know the appropriate level of exposure of the organism to F in order to minimize the risks and maximize the benefits arising from exposure to this element (BUZALAF, 2018).

Upon excessive ingestion, F interferes with the major metabolic pathways of the biological systems, functioning as a potent inhibitor of many enzymes, including some of the glycolytic pathway (ARAUJO; PEREIRA; DIONIZIO; SANCHEZ *et al.*, 2019). Only a small amount can be tolerated by any living cell and can cause several biochemical changes. Toxic effects of excessive ingestion of F have been extensively reported and the mechanisms involved in the toxicity have been investigated (BARBIER; ARREOLA-MENDOZA; DEL RAZO, 2010; PEREIRA; DIONIZIO; ARAUJO; FERNANDES *et al.*, 2018). These effects have reported to be dose and time-dependent (ARAUJO; PEREIRA; DIONIZIO; SANCHEZ *et al.*, 2019; DABROWSKA; LETKO; BALUNOWSKA, 2006; KHAN; SABINO; DE SOUZA MELO; MARTINI *et al.*, 2018; PEREIRA; DIONIZIO; ARAUJO; FERNANDES *et al.*, 2018) and influenced by the genetic background (BUZALAF, 2018; EVERETT, 2011).

The metabolism of F is influenced by genetics (CARVALHO; LEITE; YAN; EVERETT *et al.*, 2009), which makes difficul to precisely determine the “optimal” range of F intake that is able to prevent caries with minimum side-effects (BUZALAF, 2018). Mice susceptible (A/J) or resistant (129P3/J) to F have been evaluated since 2002 to better understand how the genetic background plays a role on the effects of F in the organism (EVERETT, E. T.; MCHENRY, M. A. K.; REYNOLDS, N.; EGGERTSSON, H. *et al.*, 2002). It has been shown that 129P3/J mice excrete lower amounts of F in urine, which leads to higher circulating F levels when compared to their A/J counterparts, but even so the first are remarkably resistant to the occurrence of dental fluorosis (CARVALHO; LEITE; YAN; EVERETT *et al.*, 2009). Another factor affecting F metabolism is exercise, although this effect is not precisely known so far (BUZALAF; WHITFORD, 2011). To date, only 3 studies evaluated the effects of

physical exercise on F metabolism in rodents. In two of them, light exercise decreased plasma F concentrations of rats (LOMBARTE; FINA; LUPO; BUZALAF *et al.*, 2013; WHITFORD, 1996). However, a recent study with A/J mice found no effect of intensive exercise on plasma F levels in A/J mice (AMARAL; AZEVEDO; BUZALAF; FABRICIO *et al.*, 2018). It is known that physical exercise provokes changes in gene expression and protein synthesis (BARRES; ZIERATH, 2016) that may be mediated by the content of exosomes (LI; LIU; MA; CHEN *et al.*, 2019), improving glucose homeostasis and vascular protection. On the other hand, the effects of F on glucose homeostasis are not precisely known so far. While some studies have reported beneficial effects of F (LIMA LEITE; GUALIUME VAZ MADUREIRA LOBO; BARBOSA DA SILVA PEREIRA; SILVA FERNANDES *et al.*, 2014; LOBO; LEITE; PEREIRA; FERNANDES *et al.*, 2015; MALVEZZI; PEREIRA; DIONIZIO; ARAUJO *et al.*, 2018), others have not (CHIBA; COLOMBO; SHIRAKASHI; DA SILVA *et al.*, 2012; CHIBA; COLOMBO; SHIRAKASHI; GOMES *et al.*, 2010; LOMBARTE; FINA; LUPO; BUZALAF *et al.*, 2013).

The present study was designed to shed light into the complex interplay between genetic and epigenetic (exercise) factors on the effects of F on glucose homeostasis, by assessing alterations in the proteomic profile of liver and muscle of mice with distinct susceptibilities to the effects of F.

MATERIAL AND METHODS

Animals, treatment and samples collection

This project was approved by the Animal Research Ethics Committee of Bauru School of Dentistry, University of São Paulo (FOB-USP, Proc.009/2015). Ninety 21-day-old male mice were used, being 45 of the 129P3/J strain and 45 of the A/J strain. The reason for the selection of these two strains was based on the fact that the A/J strain (S) is highly susceptible to dental fluorosis, presenting a rapid and severe development of the disease when the animal is exposed to F, while the 129P3/J strain (R) is less affected, with low severity of dental fluorosis (EVERETT, E. T.; MCHENRY, M. A.; REYNOLDS, N.; EGGERTSSON, H. *et al.*, 2002). All mice remained in metabolic cages (n = 2 per cage), in rooms with temperature, humidity and controlled light/dark cycles (~ 23 ± 1°C, 40-80% and 12/12 h, respectively). The animals had free access to a diet with a low concentration of F (Presence, Purina, <1 ppm). Animals from both strains (S and R), at 45 days of age, where divided into

groups according to the exposure to F (0 or 50 ppm) through the drinking water and physical exercise (Figure 1).

For the experimental groups SIII and RIII, physical exercise was performed 5 days a week on an appropriate treadmill for 8 weeks (TOTI; BARTALUCCI; FERRUCCI; FULCERI *et al.*, 2013). All mice were familiarized with the treadmill for 10 min/session at a speed of 8 m/min once a day for 1 week (BARTALUCCI; FERRUCCI; FULCERI; LAZZERI *et al.*, 2012). After the period of familiarization, the mice performed a maximum test to determine the maximum velocity reached in the treadmill (FERREIRA; ROLIM; BARTHOLOMEU; GOBATTO *et al.*, 2007). The test started at a speed of 6 m/min and was increased by 3 m/min every 3 min until exhaustion when the animals stopped running. This maximal test was repeated after 4 weeks (to adjust exercise intensity) and at the end of 8 weeks.

The animals of groups SIII and RIII underwent a high intensity interval training protocol (HIIT), 5 days per week for 8 weeks. The HIIT sessions were adapted (TOTI; BARTALUCCI; FERRUCCI; FULCERI *et al.*, 2013) and consisted of 5 min of heating at 40% of maximum speed and a sequence of short periods (1 min) of intense exercize at 80% of maximum running speed, followed by recovery time of 3 min. The training sessions ended when the mice completed the distance of 1000 m. All training sessions were held at the same time each day to avoid effects on training performance (DJAWDAN; GARLAND, 1988).

At the end of study (8 weeks), the animals were anaesthetized with sodium thiopental. Blood was collected and stored at −20 °C until analysis of F, glucose and insulin. Liver and gastrocnemius muscle were collected and stored at −80 °C for proteomic analysis.

Fluoride analysis in plasma

Plasma F concentrations of F in the plasma were analyzed in duplicate, as previously described (PEREIRA; LEITE ADE; CHARONE; LOBO *et al.*, 2013). Analysis was performed with the ion-specific electrode (Orion Research, Model 9409) and a miniature calomel electrode (Accumet, #13-620-79), both coupled to a potentiometer (Orion Research, Model EA 940), after hexamethyldisiloxane-facilitated diffusion (TAVES, 1968; WHITFORD, 1996). Fluoride standards (0.00475–0.95 µg F) were prepared in triplicate and diffused in the same manner as the samples.

Analysis of plasma glucose and insulin and calculation of the HOMA2-IR

Glycemia was analyzed by the glucose oxidase method, using a commercial kit (Katal Biotecnologia, São Paulo, Brazil). Insulinemia was evaluated by ELISA (Mouse Insulin kit, #80-INSMN-E01, ALPCO Diagnostics, Salem, USA). Both analyses were performed in duplicate, according to manufacturer´s instructions. HOMA2-IR (homeostasis model assessment 2 of insulin resistance) was evaluated from paired plasma glucose and insulin concentrations, using the software HOMA Calculator v.2.2 (available from http:/www.dtu.ox.ac.uk/homacalculator/download.php). The software provides calculation of HOMA2-IR index, as well as insulin sensitivity (% S) and β-cell function (%B) (LEVY; MATTHEWS; HERMANS, 1998)(Levy et al., 1998).

Liver and gastrocnemius muscle preparation for proteomic analysis

For the protein extraction from gastrocnemius muscle and liver, 50 mg of each tissue from each animal (n=6) were transferred to a microtube and 100 µL of extraction buffer containing 7 M urea, 2 M thiourea and 40 mM Dithiothreitol (DTT) were added. After 1-hour incubation at low temperature (ice), with vortexing performed every 10 min, the homogenate was centrifuged at 8,000 g for 30 min at 4°C and the supernatant was collected. After extraction, the proteins were quantified by the Bradford method (BRADFORD, 1976). For each group, twenty-five µg of liver protein from two animals were pooled, in order to obtain biological triplicates. Then, protein samples (50 µg) were transferred to a microtube and 10 µL of 50 mM ammonium bicarbonate and 25 µL of 0.2% RapiGest™ (Waters Co., Manchester, UK) were added and incubated at 37°C for 60 min. Then they were reduced and alkylated, respectively by incubating with 2.5 µL of 100 mM DTT (dithiotreitol) at 37°C for 40 min and 2.5 µL of 300 mM IAA (iodocetamide) for 30 min in the dark at room temperature. Proteolytic digestion was performed by the addition of 10 µL trypsin (100 ng; Trypsin Gold Mass Spectrometry, Promega, Madison, USA) by incubation for 14 h at 37°C. After digestion, 10 µL of 5% TFA (trifluoroacetic acid) was added, incubated for 90 min at 37°C, and then centrifuged (14,000 g for 30 min). The supernatant was collected and 5 µL ADH (1 pmol/µL) and 85 µL 3% ACN (acetonitrile) were added so that the samples were destined for nLC-ESI-MS/MS analysis.

nLC-ESI-MS/MS and bioinformatics analyses

Identification of the peptides was performed in the nanoAcquity UPLCXevo QTof MS system (Waters, Manchester, UK), as previously described (LIMA LEITE; GUALIUME VAZ MADUREIRA LOBO; BARBOSA DA SILVA PEREIRA; SILVA FERNANDES *et al.*, 2014). Differences in protein expression between the groups were obtained using the Protein Lynx Global Service (PLGS) software (Monte Carlo algorithm) and expressed as $p < 0.05$ for down-regulated proteins and $1-p > 0.95$ for up-regulated proteins. Comparisons were made between the strains, for each treatment (SI vs RI, SII vs RII and SIII vs RIII).

To understand the biological significance of the quantitative results of the proteomic analysis, the differentially altered proteins in each comparison were analyzed using bioinformatics tools, as previously reported (BAUER-MEHREN, 2013; LIMA LEITE; GUALIUME VAZ MADUREIRA LOBO; BARBOSA DA SILVA PEREIRA; SILVA FERNANDES *et al.*, 2014; MILLAN, 2013; ORCHARD, 2012). The software CYTOSCAPE® 3.0.4 (Java®) was used to build networks of molecular interaction between the identified proteins, with the aid of ClueGo and ClusterMark applications (DIONIZIO; MELO; SABINO-ARIAS; VENTURA *et al.*, 2018).

Statistical analysis

Data of F, glycemia and insulinemia concentrations were analyzed using GraphPad InStat version 3.0 for Windows and GraphPad Prism version 5.0 for Windows software (GraphPad Software Inc., La Jolla, CA, USA), using 2-way ANOVA. In all cases, the level of significance was set at 5%.

RESULTS

Only for illustration, clinical examination of the incisors of animals from SII and RII groups (exposed to 50 ppm F) showed the presence of fluorosis in both of them, but SII animals presented whiter teeth, indicating greater severity of dental fluorosis (Figure 2).

Plasma F concentrations (Table 1) were significantly higher in R mice, compared to S mice, but only for F-treated animals (groups II and III). When the treatments were compared, F concentrations did not significantly differ between

groups II and III that presented both significantly higher F concentrations than control group (I).

Regarding glucose homeostasis parameters, the S mice, regardless the treatment, had higher plasma glucose levels than the resistant ones, but the difference was only significant for F-exposed sedentary animals (group II). In-line with this, the susceptible mice, regardless the treatment, had lower %B when compared with the resistant ones, but the difference was only significant for F-exposed sedentary animals (Table 1). There were not significant differences in plasma insulin levels.

For the proteomic analysis, in the liver, when the strains were compared, an increase in protein expression was seen for the non-exercised A/J mice, being this increase greater when the animals received deionized water (Table 2). The functional classification based on GO annotation showed that the category with the highest percentage of number of genes association was Carboxylic acid metabolic process (16%) (Figure 3A). The interaction subnetworks (Figure 4) revealed that most of the proteins with changed expression interacted with Disks large homolog 4 (Q62108) and Calcium-activated potassium channel subunit alpha-1 (Q08460). SI mice (A/J) had increased expression or unique proteins mainly related to energy metabolism, involved both in glycolysis (such as Glyceraldehyde-3-phosphate dehydrogenase, Phosphoglycerate kinase, Enolase, Triosephosphate isomerase), Krebs cycle (Malate dehydrogenase and de hydratase) and oxidative phosphorylation (ATP synthase and Electron transfer flavoprotein) (Table 3). Isoforms of 3-ketoacyl-CoA thiolase _ peroxisomal and of Glutathione S-transferase, as well as Peroxiredoxin-4 (O08807) and Carbonic anhydrase 3 (P16015) were increased more than 2-fold in the A/J mice (Table S1).

Upon exposure to fluoride (comparison SII vs RII), A/J mice still had increased protein expression when compared with their 129P3/J counterparts, although in lower magnitude (Table 2). The category with the highest percentage of number of genes association was Cofactor metabolic process (25%) (Figure 3B). In the interaction subnetwork (Figure 5), proteins with increased expression in SII compared with RII or exclusively found in SII were related to energy flux [(such as Electron transfer flavoprotein subunits alpha and beta, mitochondrial, 3-ketoacyl-CoA thiolase, mitochondrial, Aspartate aminotransferase, mitochondrial, and Malate

dehydrogenase (both cytoplasmic and mitochondrial forms)] and oxidative stress (Peroxiredoxin-1 and -6, Glutathione S-transferase Mu 1 and Glutathione Peroxidase 1) (Table 3), as seen for the comparison SI *vs* RI.

Upon exercise, there was a reduction in protein expression in the A/J mice, compared with their 129P3/J counterparts (Table 2). The category with the highest percentage of number of genes association was Organic acid metabolic process (14%) (Figure 3C). In the interaction subnetworks (Figure 6A-D), proteins with most of the proteins with altered expression in SIII compared with RIII were related to energy flux (Table 3) and interacted with Protein fantom (Figure 4A), High mobility group protein HMGI-C (Figure 4B), Disks large homolog 4 (Figure 4C) and Calcium-activated potassium channel subunit alpha-1 (Figure 4D). The two latter ones were also interacting partners in the comparison between groups SI *vs* RI. Several pathways of the energy metabolism were impaired in SIII when compared with RIII. Important enzymes of aerobic (Phosphoglycerate kinases 1 and 2, as well as beta enolase) and anaerobic (L-lactate dehydrogenase B and C chains) glycolysis were absent in SIII group (Table 3). Also enzymes involved in aminoacid metabolism were reduced (Table 3), such as Fumarylacetoacetase (more than 2-fold; Table S3). Enzymes involved in oxidative phosphorylation, such as Electron transfer flavoprotein subunit beta and ATP synthase subunit alpha, mitochondrial, were reduced in the SIII group (Table 3). Chaperones, such as Heat shock protein 75 kDa, mitochondrial, were absent in SIII. There was absence of Protein/nucleic acid deglycase DJ-1 in the SIII group. Indolethylamine N-methyltransferase, was also absent in the SIII group, while 2-iminobutanoate/2-iminopropanoate deaminase, was reduced.

In the gastrocnemius muscle (Table 4), untreated A/J mice showed a decrease in protein expression when compared with their 129P3/J counterparts (comparison SI *vs* RI). The functional classification based on GO annotation showed that the category with the highest percentage of number of genes association was Purine nucleoside triphosphate metabolic process (20%) (Figure 7A). The interaction subnetworks showed several proteins involved in muscle contraction downregulated or absent in the SI group, (Table 5) such as Actin alpha, Skeletal muscle (P68134), Actin, cytoplasmic 2 (P63260), Myosin light chain 6B (Q8CI43), Myosin 7 (Q91Z83) and Myosin light chain 3 (P09542). Parvalbumin alpha (P32848), Glyceraldehyde-3-phosphate dehydrogenase (P16858) and Filamin-C

(Q8VHX6) were decreased more than 2-fold in the A/J mice (Table S4). Many altered proteins (mostly downregulated or absent in SI mice) are related to the protein synthesis (Table 5), such as Helicase ARIP4 (Q99NG0), Roquin (Q4VGL6), a post translational repressor of mRNA, Nuclear factor NF-kappa-B p105 subunit (P25799), a transcription factor, mRNA decay activator protein ZFP36L2 (P23949) that promotes poly(A) tail removal or deadenylation of mRNA thus attenuating protein synthesis, Forkhead box protein P3 (Q00JB6), a transcriptional regulator and Elongation factor 1-alpha 2 (P62631).

Upon exposure to fluoride, associated or not to exercise, an increase in protein expression was seen for the A/J mice compared to the respective 129P3/J mice groups (Table 4). For the sedentary groups that consumed fluoride (SII *vs* RII comparison), the functional classification based on GO annotation showed that the category with the highest percentage of number of genes association was Ribonucleoside triphosphate metabolic process (17%) (Figure 7B). In the interaction subnetworks, several proteins with increased expression or exclusively found in SII group interacted with Traf2 and NCK-interacting protein kinase (P83510) (Table 5). Among the interacting partners are Anaphase-promoting complex subunit 1 (P53995), related to ubiquitination, Mitogen-activated protein kinase kinase kinase kinase 4 P97820), Disks large homolog 1 (Q811D0) and Kinesin light chain 1 (O88447 (Figure 9A). Interestingly exposure to F increased more than 2-fold proteins related to muscle contraction and relaxation, as well as proteins related to energy flux (Table 5). Among the interacting partners are Anaphase-promoting complex subunit 1 (P53995), related to ubiquitination, Mitogen-activated protein kinase kinase kinase kinase 4 P97820), a serine/threonine kinase that plays a role in the response to environmental stress, Disks large homolog 1 (Q811D0) that acts in signal transduction and Kinesin light chain 1 (O88447) that is a microtubule-associated force-producing protein playing a role in organelle transport (Figure 9A). In addition, some proteins with altered expression interacted with players involved in the regulation of nuclear factor kappa-B (NF-kB), as well as Inhibitor of nuclear factor kappa-B kinase subunit alpha (Q60680), NF-kappa-B essential modulator (O88522) and E3 ubiquitin-protein ligase RNF31 (Q924T7). Among the proteins interacting with them are Inhibitor of nuclear factor kappa-B kinase subunit beta (O88351 that was exclusively found in the SII group, and Endoribonuclease ZC3H12A (Q5D1E7) (Figure 9B) that was exclusively identified in the 129P3/J

animals. Proteins related to muscle contraction and relaxation were increased more than 2-fold in the SII mice (Table 5), such as Parvalbumin alpha (P32848; more than 18-fold increase), Tropomyosin alpha-3 chain (P21107; more than 3- fold increase), Myosin-7B (A2AQP0) and Troponin I, fast skeletal muscle (P13412) and Calsequestrin-1 (O09165) (Table S5). Proteins related to energy flux were also increased more than 2-fold in the SII mice (Table 5), such as Glyceraldehyde-3-phosphate dehydrogenase testis-specific (Q64467; more than 6-fold), Fatty acid-binding protein, heart (P11404; more than 3-fold), AMP deaminase 1 (Q3V1D3) and ADP/ATP translocases (isoforms 1 and 2) (Table S5).

For the exercised mice (SIII *vs.* RIII comparison), based on GO annotation the category with the highest percentage of number of genes association was Purine ribonucleoside monophosphate metabolic process (30%; Figure 7C). The interaction subnetworks (Figure 10), as well as Table S6 showed that for the SIII group there was an increase or exclusivity in the expression of proteins related to energy flux (Krebs cycle and glycolytic pathway) (Table 5), such as Malate dehydrogenase (P08249), Glyceraldehyde-3-phosphate dehydrogenase (Q64467), L-lactate dehydrogenase chain (P00342), Triosephosphate isomerase (P17751), Phosphoglycerate kinase (P09411), Pyruvate kinase PKM (P52480) and Alpha- (P17182), Beta- (P21550) and Gamma- (P17183) enolase. Similarly to which was reported for SII mice, proteins related to muscle contraction/relaxation were also considerably increased in SIII mice (Table 5; Table S6).

DISCUSSION

Many factors have been shown to affect the metabolism of F, with potential to interfere in the retention of this ion in the organism and alter the relationship between F intake and the risk of fluorosis, as well as glucose homeostasis (BUZALAF; WHITFORD, 2011; BUZALAF, 2018). Among these factors are the genetic background that has been extensively studied using A/J and 129P3/J mice (CARVALHO; LEITE ADE; PERES-BUZALAF; SALVATO *et al.*, 2013; CARVALHO; LEITE; YAN; EVERETT *et al.*, 2009; CHARONE; DE LIMA LEITE; PERES-BUZALAF; SILVA FERNANDES *et al.*, 2016; KHAN; SABINO; DE SOUZA MELO; MARTINI *et al.*, 2018; KOBAYASHI; LEITE; PERES-BUZALAF; CARVALHO *et al.*, 2014), as well as epigenetic factors, such as physical exercise (AMARAL; AZEVEDO; BUZALAF; FABRICIO *et al.*, 2018; LOMBARTE; FINA; LUPO; BUZALAF

et al., 2013; WHITFORD, 1996). In the above-mentioned studies, the effects of genetic and epigenetic factors on F metabolism and/or glucose homeostasis were studied separately. This in the first study to evaluate the interplay between genetic and epigenetic factors on F metabolism and glucose homeostasis. For this, we included mice that have different susceptibilities to the effects of F in the organism (CARVALHO; LEITE; YAN; EVERETT *et al.*, 2009; EVERETT, 2011; EVERETT, E. T.; MCHENRY, M. A. K.; REYNOLDS, N.; EGGERTSSON, H. *et al.*, 2002) that were exposed to F only or to both F and physical exercise. R mice treated with F, regardless of exercise, had plasma F levels significantly higher than their S counterparts (Table 2). Despite the higher plasma F levels, the first had lower severity of dental fluorosis, in-line with previous studies (CARVALHO; LEITE; YAN; EVERETT *et al.*, 2009; CHARONE; DE LIMA LEITE; PERES-BUZALAF; SILVA FERNANDES *et al.*, 2016).

Regarding the parameters related to glucose homeostasis, the only differences found were for plasma glucose and %B for the different strains. R mice had plasma glucose levels significantly lower and %B significantly higher than their S counterparts (Table 2). These data indicate that glucose homeostasis is more influenced by genetic than by epigenetic factors (exercise). This might help to explain the conflicting results reported in previous studies. *Wistar* rats with streptozotocin-induced diabetes had increased insulin sensitivity when exposed to water containing 10 mg/L F (LOBO; LEITE; PEREIRA; FERNANDES *et al.*, 2015), while *Sprague dawley* rats exposed to water containing 15 mg/L F had increased insulin resistance (LOMBARTE; FINA; LUPO; BUZALAF *et al.*, 2013). Moreover, non-obese diabetic (NOD) mice exposed to water containing 10 mg/L F had reduced plasma glucose levels when compared to their non-exposed counterparts (MALVEZZI; PEREIRA; DIONIZIO; ARAUJO *et al.*, 2018). It is important to note that despite physical exercise did not have a significant impact in any of the parameters related to glucose homeostasis upon exposure to F (comparison between II and III groups), exercised mice of both strains had similar plasma glucose levels, while for the sedentary ones, plasma glucose was significantly higher for the S mice as compared to the R ones. These data are somewhat in-line with the findings by Lombarte et al. (LOMBARTE; FINA; LUPO; BUZALAF *et al.*, 2013) (2013), who reported that physical exercise improves the toxic effects of F on the glucose-insulin system. The data of the present

study indicate that S individuals might benefit more of the effect of physical exercise on glucose homeostasis than the R ones, upon exposure to F.

For the proteomic analysis in the liver, S non-exercized mice, especially when drinking deionized water, had an increase in protein expression (Table 2). This is in accordance with a recent study by our group when the liver proteome of these two mice strains was compared and might be explained by increase in Formimidoyltransferase-cyclodeaminase (Q91XD4; Table S1) (KHAN; ASSIR; SHAFIQ; CHAUDHARY *et al.*, 2016) that was exclusively identified in the S in the present study. This enzyme is involved in the synthesis of purines and pirimidines, as well as of aminoacids (UNIPROT). It should be noted that the category with the highest percentage of number of genes association was Carboxylic acid metabolic process and the proteins with increased expression and also uniquely expressed in S mice were related to different pathways of energy metabolism, such as glycolysis, Krebs cycle and oxidative phosphorylation (Tables 3 and S1). Increased energy flux leads to oxidative stress, which is in agreement with increase in antioxidant enzymes in S mice not exposed to F compared with their R counterparts. These findings were also observed in a previous study of our group (KHAN; LEITE ADE; CHARONE; SABINO *et al.*, 2016). The increase in proteins related to energy flux and antioxidant proteins in S mice might be a plausible explanation for their high susceptibility to the effects of F, since this ion is well known for its ability to induce oxidative stress (BARBIER; ARREOLA-MENDOZA; DEL RAZO, 2010; KHAN; LEITE ADE; CHARONE; SABINO *et al.*, 2016).

When exposed to F, S mice stil had increased protein expression (mainly in proteins involved in energy flux and oxidative stress) in the liver, although in lower extent when compared with their R counterparts. Interestingly, the category with the highest percentage of number of genes association was Cofactor metabolic process (Fig. 3B). This might be associated with the fact that fluorine is the most electronegative element in the periodic table and has high affinity for metal ions (BUZALAF; WHITFORD, 2011) which act as cofactors for several enzymes. It should be highlighted that Fructose-1,6-bisphosphatase 1 (Q9QXD6), which catalyzes the hydrolysis of fructose 1,6-bisphosphate to fructose 6-phosphate in the presence of divalent cations, acting as a rate-limiting enzyme in gluconeogenesis, was increased more than 2-fold in the SII group (Table S2). Fluoride is known as a potent inhibitor of glycolytic enzymes, such as enolase, hexokinase,

phosphofructokinase, pyruvate kinase, and enolase, due to its strong ability to bind metals (KASHIWAGI; SHERER; TOWNSEND; JACOBS *et al.*, 1970). Thus, impairment in glycolysis by F might activate the metabolism of other fuels, which is in-line with the increase in Aspartate aminotransferase_mitochondrial, 3-ketoacyl-CoA thiolase, mitochondrial and Fructose-1,6-bisphosphatase 1.

When the mice were exposed both to F and exercise, the profile of protein expression changed remarkably, i.e. SIII mice had a reduction in liver proteins expression when compared with RIII. Several proteins with reduced expression are involved in distinct pathways of energy metabolism, such as aerobic and anaerobic glycolysis, oxidative phosphorylation and aminoacids metabolism. Important detoxifying proteins were absent in SIII mice. Among them are protein/nucleic acid deglycase DJ-1 that deglycates cysteine, arginine and lysine residues in proteins, thus reactivating these proteins and preventing the formation of advanced glycation products (AGEs) (UNIPROT), as well as indolethylamine N-methyltransferase and 2-iminobutanoate/2-iminopropanoate deaminase, which facilitates the release of ammonia from potentially toxic reactive metabolites (enamine/imine intermediates) (UNIPROT). Interestingly, some antioxidant enzymes were increased in SIII group, compared to RIII. However, Peroxiredoxin-4 and several isoforms of Glutathione S-transferase (Mu2, Mu7, Mu5, A1, A2 and A3) were decreased more than 2-fold in the SIII group (Table S3). The presence of High mobility group protein HMGI-C (Figure 4B), a transcription regulator, among the interacting proteins, in addition to the absence of 60S acidic ribosomal protein P1, essential to the elongation step of protein synthesis and the absence of S-adenosylmethionine synthase isoform type-2, involved in the regulation of protein expression, as well as the reduction in more than 2-fold of in Elongation factor 1-alpha 2 (P62631; Table S3) might help to explain the reduced protein synthesis in SIII mice compared with RIII. Additionally, the quality control of synthesized proteins might have been impaired due to the absence of Heat shock 70 kDa protein 1-like, an essential molecular chaperone implicated in a wide variety of cellular processes, including protection of the proteome from stress, folding and transport of newly synthesized polypeptides, activation of proteolysis of misfolded proteins and the formation and dissociation of protein complexes (UNIPROT). In summary, when the liver proteome of the S and R strains is compared, in the presence of no stressor or one stressor (F only), there is an increase in protein synthesis, energy flux and antioxidant enzymes in the first.

However, in the presence of two stressors (F and exercise), there is a remarkable reduction in proteins involved in protein synthesis, energy metabolism and detoxification, but antioxidant enzymes are still increased in the S mice. These results, when analyzed in conjunction with the literature, suggest an increased state of oxidative stress in S mice that is inherent to this strain and might be exacerbated by the treatment with F, which is also known to provoke oxidative stress (KHAN; LEITE ADE; CHARONE; SABINO *et al.*, 2016; KHAN; SABINO; DE SOUZA MELO; MARTINI *et al.*, 2018).

Regarding the gastrocnemius muscle (Table 5), differently from which was observed for the liver (Table 3), untreated S mice showed a decrease in protein expression when compared with their R counterparts (comparison SI *vs.* RI), which might be due to downregulation or absence of several proteins involved in protein synthesis (Table 5). Remarkably, SI group had downregulation or absence of several proteins related to muscle contraction. Proteins such as Parvalbumin alpha (P32848), involved in relaxation after contraction, as well as Glyceraldehyde-3-phosphate dehydrogenase (P16858) and Filamin-C (Q8VHX6) that functions as large actin-cross-linking protein critical for maintaining the structural integrity of the muscle fibers, were decreased more than 2-fold in the A/J mice (Table S4). This might indicate impaired muscle contraction in the S mice, even in the absence of stressors. However, exposure to F, associated or not to exercise, provoked an increase in protein expression in the S mice compared to their respective R counterparts, similarly to what was found for the liver (Table 2). In the interaction subnetworks, several proteins with increased expression or exclusively found in SII group interacted with Traf2 and NCK-interacting protein kinase (P83510), a serine/threonine kinase that is an essential activator of the Wnt signaling pathway, playing a role in the response to environmental stress (UNIPROT). Among the interacting partners are Anaphase-promoting complex subunit 1 (P53995), related to ubiquitination, Mitogen-activated protein kinase kinase kinase kinase 4 P97820), a serine/threonine kinase that plays a role in the response to environmental stress, Disks large homolog 1 (Q811D0) that acts in signal transduction and Kinesin light chain 1 (O88447) that is a microtubule-associated force-producing protein playing a role in organelle transport (Figure 9A). Interestingly, some proteins with altered expression interacted with proteins involved in the regulation of nuclear factor kappa-B (NF-kB). Among them are inhibitor of nuclear factor kappa-B kinase subunit beta

(O88351), a serine kinase playing an essential role in the activation of the (NF-kB) signaling pathway by cellular stresses that was exclusively found in the SII group, as well as Endoribonuclease ZC3H12A (Q5D1E7) (Fig 9B). This enzyme, exclusively identified in the R mice, is an endoribonuclease that prevents NF-kB signaling pathway activation, negatively regulating macrophage-mediated inflammatory response and immune homeostasis. NF-kB, as a transcription factor, plays a crucial role in immune and inflammatory responses via the regulation of genes expression. In non-stimulated state, NF-kB exists mainly in cytoplasm, combined with the inhibitory protein B (IkBs). When activated by some stimulators, including pro-inflammatory cytokines, bacteria, lipopolysaccharide (LPS), viruses, physical or chemical stresses, the IkB proteins become phosphorylated and disconnect with NF-kB, which triggers NF-kB translocation to the molecule and binding to their cognate DNA binding sites to regulate the transcription of its downstream genes. Some of the genes are related to inflammatory responses, such as pro-inflammatory cytokines, chemokines, adhesion molecules, and inducible enzymes such as cyclooxygenase-2 (COX2) and iNOS (BALDWIN, 2001). Several studies have reported that treatment with F increases NF-kB in distinct cells, such as neurons (ZHANG; WANG; XIA; HE, 2008), renal and cardiac cells (OYAGBEMI; OMOBOWALE; ASENUGA; ADEJUMOBI *et al.*, 2017). Our results showed increased expression of proteins related to NF-kB pathway activation in the muscle of susceptible animals treated with fluoride (SII), while the resistant animals (RII) had increase in proteins that prevent NF-kB signaling pathway activation. This might be another probable mechanism that helps to explain the resistance of the 129P3/J mice to the effects of F. Proteins related to muscle contraction and relaxation were increased more than 2-fold in the SII mice, such as Parvalbumin alpha (P32848; more than 18-fold increase), Tropomyosin alpha-3 chain (P21107; more than 3-fold increase), Myosin-7B (A2AQP0) and Troponin I, fast skeletal muscle (P13412) and Calsequestrin-1 (O09165), a calcium-binding protein that acts as an internal calcium store in muscle and regulates the release of lumenal Ca^{2+} via the calcium release channel RYR1, which plays an important role in triggering muscle contraction (Table S5). In addition, proteins related to energy flux were also increased more than 2-fold in the SII mice, such as Glyceraldehyde-3-phosphate dehydrogenase testis-specific (Q64467; more than 6-fold), Fatty acid-binding protein, heart (P11404; more than 3-fold), AMP deaminase 1 (Q3V1D3) and ADP/ATP translocases (isoforms 1 and 2) (Table 12).

Curiously, some of these proteins, such as Parvalbumin alpha and Glyceraldehyde-3-phosphate dehydrogenase were reduced more than 2-fold in the untreated S mice (comparison SI vs RI; Table S4). Moreover, increase in Parvalbumin alpha was also recently described in the muscle of NOD mice treated with 50 ppm fluoride (MALVEZZI; PEREIRA; DIONIZIO; ARAUJO *et al.*, 2018). In addition, Neurofibromin (Q04690), which stimulates the GTPase activity of Ras, regulating its activity was also increased more than 2-fold in the SII mice (Table S5), which indicates involvement of MAPK/ERK signaling pathways in the muscle events. Simultaneous exposure to F and exercise caused an increased expression of proteins related to energy flux in SIII mice compared with their RIII counterparts. These findings indicate an increased oxidative metabolism in these mice, which might induce hypoxia, consistent with the increase in carbonic anhydrase 3 (P16015) that was also increased in the liver. In fact, this enzyme was consistently increased more than 2-fold in the S mice in comparison with 129P3/J counterparts, regardless of the treatment both in liver (Tables S1, S2 and S3) and gastrocnemius muscle (Tables S4, S5 and S6). This enzyme catalyzes interconversion of carbon dioxide (CO_2) and water into carbonic acid, protons (H^+) and bicarbonate (HCO_3^-), playing a crucial role in the acid-basic homeostasis of the organism. Increased carbonic anhydrase (CA) synthesis may be directly induced by a lower oxygen tension at the molecular level (MILLION; ZILLNER; BAUMANN, 1991). In addition, hypoventilation-induced reduction of tissue oxygen tension following oxidative metabolism acidifies the tissue, which induces elevated activities of enzymes and transporters involved in cellular pH regulation (JUEL; LUNDBY; SANDER; CALBET *et al.*, 2003). Accordingly, increased CA activity is associated with sleep apnea severity (WANG; ESKANDARI; ZOU; GROTE *et al.*, 2015). Increased levels of CA in S mice, regardless the treatment, indicate that these mice might have been submitted to hypoxia, probably caused by excessive oxidative metabolism. Hypoxia can alter the metabolism of F in several ways. It can reduce urinary pH, thus increasing F retention in the organism (BUZALAF; WHITFORD, 2011). However, A/J mice, despite being more susceptible to the development of dental fluorosis, were intriguingly shown to have lower circulating F levels than their 129P3/J counterparts (CARVALHO; LEITE; YAN; EVERETT *et al.*, 2009). In addition, CA is essential to maintain pH homeostasis in enamel during the maturation stage, when growth of enamel crystals results in excessive amounts of H^+ ions. In this situation, CA is required to avoid that the pH of

the developing enamel becomes too acidic (SMITH; CHONG; BARTLETT; MARGOLIS, 2005). In fact, isoforms of CA were identified exclusively in the enamel of A/J mice treated with 50 ppm fluoride, but not in 129P3/J mice (CHARONE; DE LIMA LEITE; PERES-BUZALAF; SILVA FERNANDES *et al.*, 2016), which is consistent with the increased levels of this enzyme found in the liver and muscle of A/J mice in the present study. The implications of this in the differential development of dental fluorosis in these two mice strains must be evaluated in further studies.

Acknowledgements

The authors thank FAPESP (2016/20020-4 and 2015/12109-2). This study was financed in part by the Coordenação de Aperfeiçoamento de Pessoal de Nível Superior - Brasil (CAPES) - Finance Code 001.

REFERENCES

1. Buzalaf MAR. Review of Fluoride Intake and Appropriateness of Current Guidelines. Adv Dent Res. 2018;29(2):157-66.

2. Araujo TT, Pereira HABS, Dionizio A, Sanchez CC, Carvalho TS, Fernandes MS, et al. Changes in energy metabolism induced by fluoride: insights from inside the mitochondria. Chemosphere. 2019;in press.

3. Barbier O, Arreola-Mendoza L, Del Razo LM. Molecular mechanisms of fluoride toxicity. Chem Biol Interact. 2010;188(2):319-33.

4. Pereira H, Dionizio AS, Araujo TT, Fernandes MDS, Iano FG, Buzalaf MAR. Proposed mechanism for understanding the dose- and time-dependency of the effects of fluoride in the liver. Toxicology and applied pharmacology. 2018;358:68-75.

5. Dabrowska E, Letko R, Balunowska M. Effect of sodium fluoride on the morphological picture of the rat liver exposed to NaF in drinking water. Advances in medical sciences. 2006;51 Suppl 1:91-5.

6. Khan ZN, Sabino IT, de Souza Melo CG, Martini T, da Silva Pereira HAB, Buzalaf MAR. Liver Proteome of Mice with Distinct Genetic Susceptibilities to Fluorosis Treated with Different Concentrations of F in the Drinking Water. Biol Trace Elem Res. 2018.

7. Everett ET. Fluoride's Effects on the Formation of Teeth and Bones, and the Influence of Genetics. J Dent Res. 2011;90(5):552-60.

8. Carvalho JG, Leite AL, Yan D, Everett ET, Whitford GM, Buzalaf MA. Influence of genetic background on fluoride metabolism in mice. J Dent Res. 2009;88(11):1054-8.

9. Everett ET, McHenry MAK, Reynolds N, Eggertsson H, Sullivan J, Kantmann C, et al. Dental fluorosis: Variability among different inbred mouse strains. J Dent Res. 2002;81(11):794-8.

10. Buzalaf MA, Whitford GM. Fluoride metabolism. Monogr Oral Sci. 2011;22:20-36.

11. Lombarte M, Fina BL, Lupo M, Buzalaf MA, Rigalli A. Physical exercise ameliorates the toxic effect of fluoride on the insulin-glucose system. J Endocrinol. 2013;218(1):99-103.

12. Whitford GM. The metabolism and toxicity of fluoride. Monogr Oral Sci. 1996;16 Rev 2:1-153.

13. Amaral SL, Azevedo LB, Buzalaf MAR, Fabricio MF, Fernandes MS, Valentine RA, et al. Effect of chronic exercise on fluoride metabolism in fluorosis-susceptible mice exposed to high fluoride. Scientific reports. 2018;8(1):3211.

14. Barres R, Zierath JR. The role of diet and exercise in the transgenerational epigenetic landscape of T2DM. Nat Rev Endocrinol. 2016;12(8):441-51.

15. Li GH, Liu H, Ma CL, Chen YF, Wang JJ, Yang Y. Exosomes are the novel players involved in the beneficial effects of exercise on type 2 diabetes. J Cell Physiol. 2019;234(9):14896-905.

16. Lima Leite A, Gualiume Vaz Madureira Lobo J, Barbosa da Silva Pereira HA, Silva Fernandes M, Martini T, Zucki F, et al. Proteomic analysis of gastrocnemius muscle in rats with streptozotocin-induced diabetes and chronically exposed to fluoride. PloS one. 2014;9(9):e106646.

17. Lobo JG, Leite AL, Pereira HA, Fernandes MS, Peres-Buzalaf C, Sumida DH, et al. Low-Level Fluoride Exposure Increases Insulin Sensitivity in Experimental Diabetes. J Dent Res. 2015;94(7):990-7.

18. Malvezzi M, Pereira H, Dionizio A, Araujo TT, Buzalaf NR, Sabino-Arias IT, et al. Low-level fluoride exposure reduces glycemia in NOD mice. Ecotoxicology and environmental safety. 2018;168:198-204.

19. Chiba FY, Colombo NH, Shirakashi DJ, da Silva VC, Moimaz SAS, Garbin CAS, et al. NaF treatment increases TNF-alpha and resistin concentrations and reduces insulin signal in rats. J Fluorine Chem. 2012;136:3-7.

20. Chiba FY, Colombo NH, Shirakashi DJ, Gomes WDS, Moimaz SA, Garbin CA, et al. Insulin Signal Decrease in Muscle but Not in the Liver of Castrated Male Rats from Chronic Exposure to Fluoride. Fluoride. 2010;43(1):25-30.

21. Everett ET, McHenry MA, Reynolds N, Eggertsson H, Sullivan J, Kantmann C, et al. Dental fluorosis: variability among different inbred mouse strains. J Dent Res. 2002;81(11):794-8.

22. Toti L, Bartalucci A, Ferrucci M, Fulceri F, Lazzeri G, Lenzi P, et al. High-intensity exercise training induces morphological and biochemical changes in skeletal muscles. Biology of sport. 2013;30(4):301-9.

23. Bartalucci A, Ferrucci M, Fulceri F, Lazzeri G, Lenzi P, Toti L, et al. High-intensity exercise training produces morphological and biochemical changes in adrenal gland of mice. Histology and histopathology. 2012;27(6):753-69.

24. Ferreira JC, Rolim NP, Bartholomeu JB, Gobatto CA, Kokubun E, Brum PC. Maximal lactate steady state in running mice: effect of exercise training. Clinical and experimental pharmacology & physiology. 2007;34(8):760-5.

25. Djawdan M, Garland T. Maximal Running Speeds of Bipedal and Quadrupedal Rodents. J Mammal. 1988;69(4):765-72.

26. Pereira HA, Leite Ade L, Charone S, Lobo JG, Cestari TM, Peres-Buzalaf C, et al. Proteomic analysis of liver in rats chronically exposed to fluoride. PloS one. 2013;8(9):e75343.

27. Taves DR. Separation of fluoride by rapid diffusion using hexamethyldisiloxane. Talanta. 1968;15(9):969-74.

28. Levy JC, Matthews DR, Hermans MP. Correct homeostasis model assessment (HOMA) evaluation uses the computer program. Diabetes Care. 1998;21(12):2191-2.

29. Bradford MM. A rapid and sensitive method for the quantitation of microgram quantities of protein utilizing the principle of protein-dye binding. Anal Biochem. 1976;72:248-54.

30. Bauer-Mehren A. Integration of genomic information with biological networks using Cytoscape. Methods Mol Biol. 2013;1021:37-61.

31. Millan PP. Visualization and analysis of biological networks. Methods Mol Biol. 2013;1021:63-88.

32. Orchard S. Molecular interaction databases. Proteomics. 2012;12(10):1656-62.

33. Dionizio AS, Melo CGS, Sabino-Arias IT, Ventura TMS, Leite AL, Souza SRG, et al. Chronic treatment with fluoride affects the jejunum: insights from proteomics and enteric innervation analysis. Scientific reports. 2018;8(1):3180.

34. Carvalho JG, Leite Ade L, Peres-Buzalaf C, Salvato F, Labate CA, Everett ET, et al. Renal proteome in mice with different susceptibilities to fluorosis. PloS one. 2013;8(1):e53261.

35. Charone S, De Lima Leite A, Peres-Buzalaf C, Silva Fernandes M, Ferreira de Almeida L, Zardin Graeff MS, et al. Proteomics of Secretory-Stage and Maturation-Stage Enamel of Genetically Distinct Mice. Caries research. 2016;50(1):24-31.

36. Kobayashi CA, Leite AL, Peres-Buzalaf C, Carvalho JG, Whitford GM, Everett ET, et al. Bone response to fluoride exposure is influenced by genetics. PloS one. 2014;9(12):e114343.

37. Khan ZN, Assir MZ, Shafiq M, Chaudhary AE, Jabeen A. High prevalence of preobesity and obesity among medical students of Lahore and its relation with dietary habits and physical activity. Indian journal of endocrinology and metabolism. 2016;20(2):206-10.

38. Khan ZN, Leite Ade L, Charone S, Sabino IT, Martini T, Pereira HA, et al. Liver proteome of mice with different genetic susceptibilities to the effects of fluoride. Journal of applied oral science : revista FOB. 2016;24(3):250-7.

39. Sherer TR, Suttie JW. Effect of fluoride on glycolytic and citric acid cycle metabolites in rat liver. J Nutr. 1970;100(7):749-56.

40. Baldwin AS, Jr. Series introduction: the transcription factor NF-kappaB and human disease. J Clin Invest. 2001;107(1):3-6.

41. Zhang M, Wang A, Xia T, He P. Effects of fluoride on DNA damage, S-phase cell-cycle arrest and the expression of NF-kappaB in primary cultured rat hippocampal neurons. Toxicology letters. 2008;179(1):1-5.

42. Oyagbemi AA, Omobowale TO, Asenuga ER, Adejumobi AO, Ajibade TO, Ige TM, et al. Sodium fluoride induces hypertension and cardiac complications through generation of reactive oxygen species and activation of nuclear factor kappa beta. Environ Toxicol. 2017;32(4):1089-101.

43. Million D, Zillner P, Baumann R. Oxygen pressure-dependent control of carbonic anhydrase synthesis in chick embryonic erythrocytes. Am J Physiol. 1991;261(5 Pt 2):R1188-96.

44. Juel C, Lundby C, Sander M, Calbet JA, Hall G. Human skeletal muscle and erythrocyte proteins involved in acid-base homeostasis: adaptations to chronic hypoxia. J Physiol. 2003;548(Pt 2):639-48.

45. Wang T, Eskandari D, Zou D, Grote L, Hedner J. Increased Carbonic Anhydrase Activity is Associated with Sleep Apnea Severity and Related Hypoxemia. Sleep. 2015;38(7):1067-73.

46. Smith CE, Chong DL, Bartlett JD, Margolis HC. Mineral acquisition rates in developing enamel on maxillary and mandibular incisors of rats and mice: implications to extracellular acid loading as apatite crystals mature. J Bone Miner Res. 2005;20(2):240-9.

Figures legends

Figure 1. Division of the experimental groups according to the strains (A/J - susceptible to dental fluorosis; 129P3/J - resistant to dental fluorosis) and treatments [I – water without fluoride, no exercise; II – water with 50 ppm fluoride, no exercise; III – water with 50 ppm fluoride, exercise (high intensity interval training (HIIT) protocol on a treadmill, 5 days per week for 8 weeks)].

Figure 2. Representative pictures of incisors of susceptible (S; A/J) and resistant (R, 129P3/J) mice that ingested water with 50 ppm of F for 8 weeks. Incisors of A/J mice presented a whiter color, indicating greater severity of dental fluorosis.

Figure 3. Functional distribution of proteins identified with differential expression in the liver of A/J and 129P3/J mice for each comparison. Comparisons are: A) SI (A/J, deionized water, no-exercise) *vs.* RI (129P3/J, deionized water, no-exercise); B) SII (A/J, water containing 50 ppm F, no-exercise) *vs.* RII (129P3/J, water containing 50 ppm F, no-exercise); C) SIII (A/J, water containing 50 ppm F, exercise) and RIII (129P3/J, water containing 50 ppm F, exercise). Categories of proteins based on GO annotation Biological Process. Terms significant (Kappa=0.4) and distribution according to percentage of number of genes association.

Figure 4. Subnetworks generated by ClusterMarker® for the com parison SI (A/J, deionized water, no-exercise) vs. RI (129P3/J, deionized water, no-exercise). The color of the nodes indicates the differential expression of the respective protein with its access code, available from UniProt protein database (http://www.uniprot.org/). The dark red and dark green nodes indicate proteins unique to RI and SI groups, respectively. The light red and light green nodes indicate down and upregulated proteins, respectively, in SI group in respect to RI. The gray nodes indicate the interaction proteins that are offered by CYTOSCAPE®, which were not identified in the presen t study.

Figure 5. Subnetworks generated by ClusterMarker® for the com parison SII (A/J, water containing 50 ppm F, no-exercise) vs. RII (129P3/J, water containing 50 ppm F, no-exercise). The color of the nodes indicates the differential expression of the respective protein with its access code, available from UniProt protein database (http://www.uniprot.org/). The dark red and dark green nodes indicate proteins unique to RII and SII groups, respectively. The light red and light green nodes indicate down and upregulated proteins, respectively, in SII group in respect to RII.

The gray nodes indicate the interaction proteins that are offered by CYTOSCAPE®, which were not identified in the present study.

Figure 6. Subnetworks generated by ClusterMarker® for the com parison SIII (A/J, water containing 50 ppm F, exercise) *vs.* RIII (129P3/J, water containing 50 ppm F, exercise). The color of the nodes indicates the differential expression of the respective protein with its access code, available from UniProt protein database (http://www.uniprot.org/). The dark red and dark green nodes indicate proteins unique to RIII and SIII groups, respectively. The light red and light green nodes indicate down and upregulated proteins, respectively, in SIII group in respect to RIII. The gray nodes indicate the interaction proteins that are offered by CYTOSCAPE®, which were not identified in the present study.

Figure 7. Functional distribution of proteins identified with differential expression in the gastrocnemius muscle of A/J and 129P3/J mice for each comparison. Comparisons are: A) SI (A/J, deionized water, no-exercise) *vs.* RI (129P3/J, deionized water, no-exercise); B) SII (A/J, water containing 50 ppm F, no-exercise) *vs.* RII (129P3/J, water containing 50 ppm F, no-exercise); C) SIII (A/J, water containing 50 ppm F, exercise) and RIII (129P3/J, water containing 50 ppm F, exercise). Categories of proteins based on GO annotation Biological Process. Terms significant (Kappa=0.4) and distribution according to percentage of number of genes association.

Figure 8. Subnetworks generated by ClusterMarker® for the comparison SI (A/J, deionized water, no-exercise) vs. RI (129P3/J, deionized water, no-exercise). The color of the nodes indicates the differential expression of the respective protein with its access code, available from UniProt protein database (http://www.uniprot.org/). The dark red and dark green nodes indicate proteins unique to RI and SI groups, respectively. The light red and light green nodes indicate down and upregulated proteins, respectively, in SI group in respect to RI. The gray nodes indicate the interaction proteins that are offered by CYTOSCAPE®, which were not identified in the present study.

Figure 9. Subnetworks generated by ClusterMarker® for the comparison SII (A/J, water containing 50 ppm F, no-exercise) vs. RII (129P3/J, water containing 50 ppm F, no-exercise). The color of the nodes indicates the differential expression of the respective protein with its access code, available from UniProt protein database (http://www.uniprot.org/). The dark red and dark green nodes indicate proteins unique

to RII and SII groups, respectively. The light red and light green nodes indicate down and upregulated proteins, respectively, in SII group in respect to RII. The gray nodes indicate the interaction proteins that are offered by CYTOSCAPE®, which were not identified in the present study.

Figure 10. Subnetworks generated by ClusterMarker® for the comparison SIII (A/J, water containing 50 ppm F, exercise) *vs.* RIII (129P3/J, water containing 50 ppm F, exercise). The color of the nodes indicates the differential expression of the respective protein with its access code, available from UniProt protein database (http://www.uniprot.org/). The dark red and dark green nodes indicate proteins unique to RIII and SIII groups, respectively. The light red and light green nodes indicate down and upregulated proteins, respectively, in SIII group in respect to RIII. The gray nodes indicate the interaction proteins that are offered by CYTOSCAPE®, which were not identified in the present study.

Tables Legends

Table 1. Mean (± SD) of plasma fluoride (F), glucose and insulin levels as well as HOMA2-IR (homeostasis model assessment 2 of insulin resistance) index, β-cell function (% B) and insulin sensitivity (% S) of A/J (susceptible to fluorosis; S) and 129P3/J (resistant to fluorosis; R) mice treated with water containing 50 ppm F or not (control; group I) and submitted to physical exercise (trained; group III) or not (sedentary; group II).

Table 2. Summary of the differences in expression and unique proteins found in the liver of A/J and 129P3/J mice, for each comparison.

Table 3. Summary of the main functions of proteins found in the liver in each comparison.

Table 4. Summary of the differences in expression and unique proteins found in gastrocnemius of A/J and 129P3/J mice, for each comparison.

Table 5. Summary of the main functions of proteins found in the gastrocnemius muscle in each comparison.

Supplementary tables

S1. Proteins with expression significantly altered in the liver of SI (A/J, deionized water, no-exercise) and RI (129P3/J, deionized water, no-exercise) mice.

S2. Proteins with expression significantly altered in the liver of SII (A/J, water containing 50 ppm F, no-exercise) and RII (129P3/J, water containing 50 ppm F, no-exercise) mice.

S3. Proteins with expression significantly altered in the liver of SIII (A/J, water containing 50 ppm F, exercise) and RIII (129P3/J, water containing 50 ppm F, exercise) mice.

S4. Proteins with expression significantly altered in the gastrocnemius of SI (A/J, deionized water, no-exercise) and RI (129P3/J, deionized water, no-exercise) mice.

S5. Proteins with expression significantly altered in the gastrocnemius of SII (A/J, water containing 50 ppm F, no-exercise) and RII (129P3/J, water containing 50 ppm F, no-exercise) mice.

S6. Proteins with expression significantly altered in the gastrocnemius of of SIII (A/J, water containing 50 ppm F, exercise) and RIII (129P3/J, water containing 50 ppm F, exercise) mice.

Figures

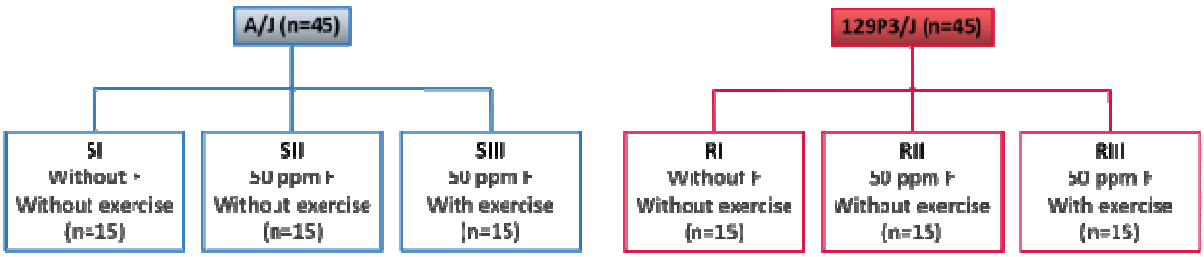

Figure 1. Division of the experimental groups according to the strains (A/J - susceptible to dental fluorosis; 129P3/J - resistant to dental fluorosis) and treatments [I – water without fluoride, no exercise; II – water with 50 ppm fluoride, no exercise; III – water with 50 ppm fluoride, exercise (high intensity interval training (HIIT) protocol on a treadmill, 5 days per week for 8 weeks)].

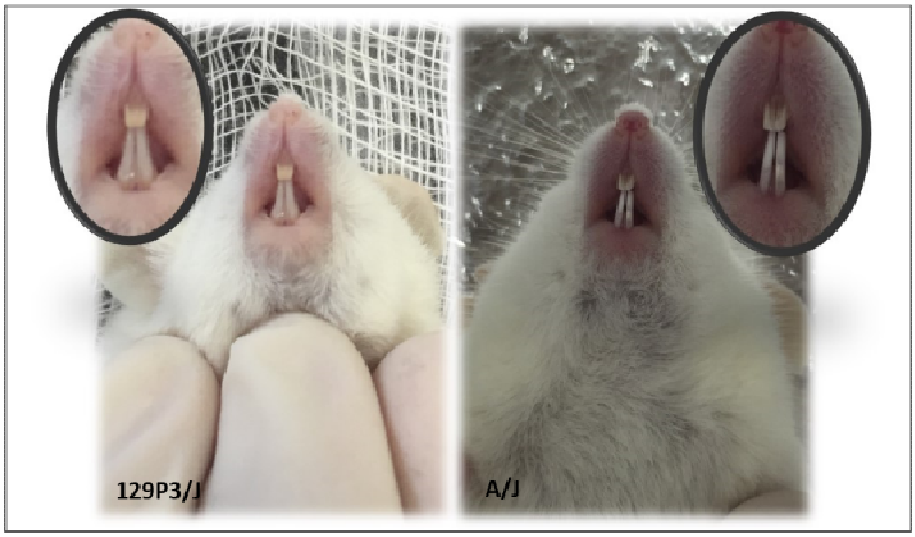

Figure 2. Representative pictures of incisors of susceptible (S; A/J) and resistant (R, 129P3/J) mice that ingested water with 50 ppm of F for 8 weeks. Incisors of A/J mice presented a whiter color, indicating greater severity of dental fluorosis.

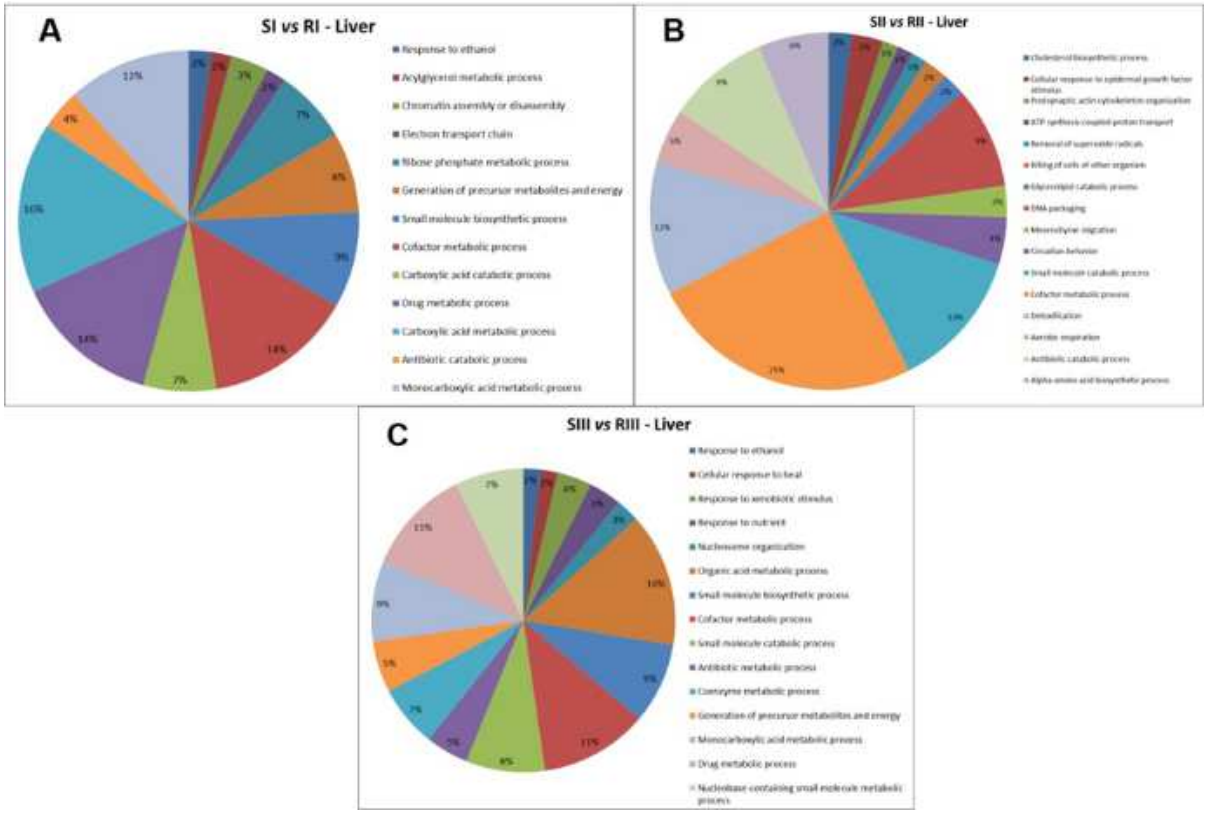

Figure 3. Functional distribution of proteins identified with differential expression in the liver of A/J and 129P3/J mice for each comparison. Comparisons are: A) SI (A/J, deionized water, no-exercise) *vs.* RI (129P3/J, deionized water, no-exercise); B) SII (A/J, water containing 50 ppm F, no-exercise) *vs.* RII (129P3/J, water containing 50 ppm F, no-exercise); C) SIII (A/J, water containing 50 ppm F, exercise) and RIII (129P3/J, water containing 50 ppm F, exercise). Categories of proteins based on GO annotation Biological Process. Terms significant (Kappa=0.4) and distribution according to percentage of number of genes association.

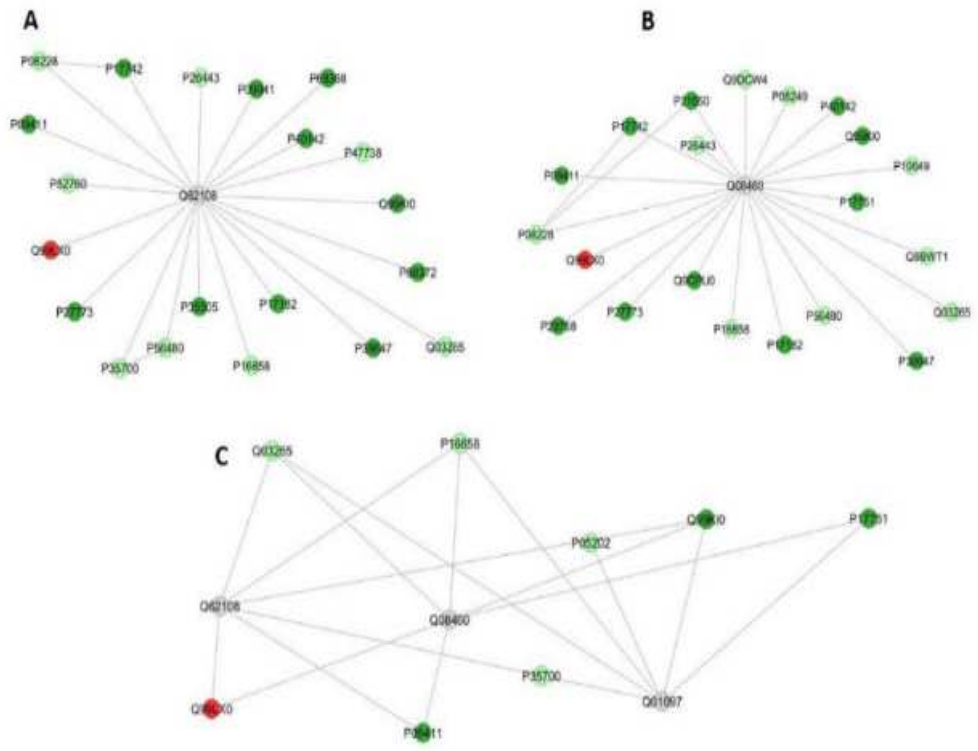

Figure 4. Subnetworks generated by ClusterMarker® for the com parison SI (A/J, deionized water, no-exercise) vs. RI (129P3/J, deionized water, no-exercise). The color of the nodes indicates the differential expression of the respective protein with its access code, available from UniProt protein database (http://www.uniprot.org/). The dark red and dark green nodes indicate proteins unique to RI and SI groups, respectively. The light red and light green nodes indicate down and upregulated proteins, respectively, in SI group in respect to RI. The gray nodes indicate the interaction proteins that are offered by CYTOSCAPE®, which were not identified in the presen t study.

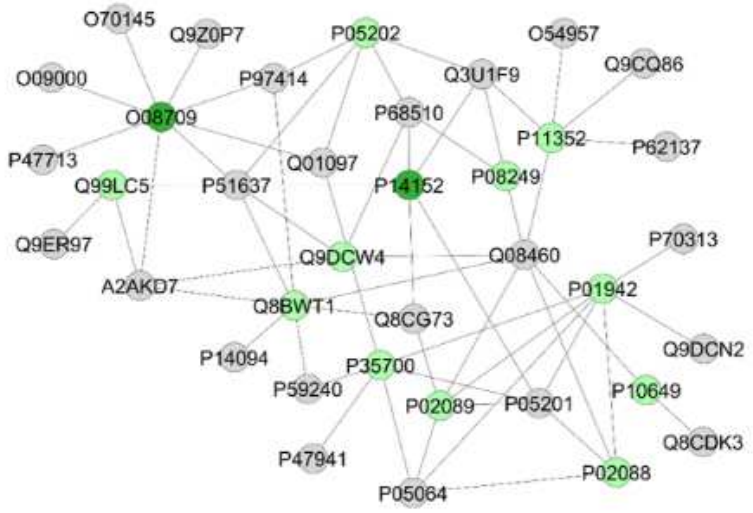

Figure 5. Subnetworks generated by ClusterMarker® for the com parison SII (A/J, water containing 50 ppm F, no-exercise) vs. RII (129P3/J, water containing 50 ppm F, no-exercise). The color of the nodes indicates the differential expression of the respective protein with its access code, available from UniProt protein database (http://www.uniprot.org/). The dark red and dark green nodes indicate proteins unique to RII and SII groups, respectively. The light red and light green nodes indicate down and upregulated proteins, respectively, in SII group in respect to RII. The gray nodes indicate the interaction proteins that are offered by CYTOSCAPE®, which were not identified in the present study.

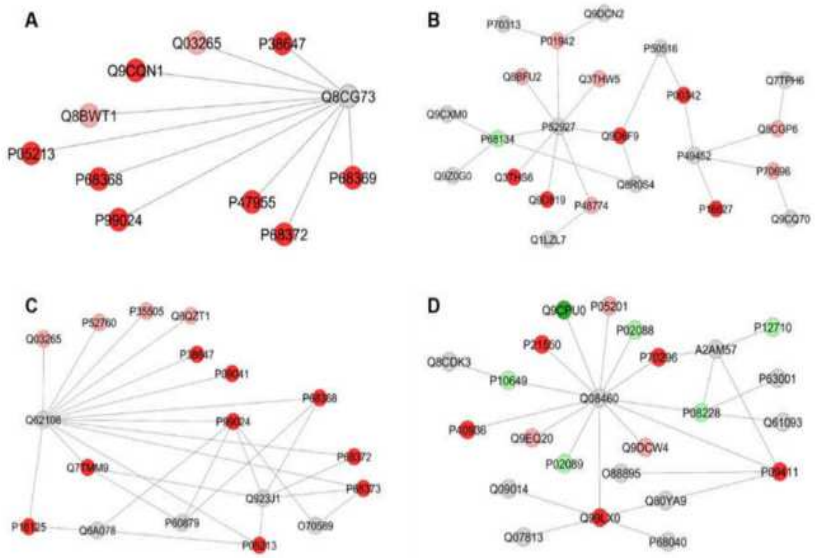

Figure 6. Subnetworks generated by ClusterMarker® for the com parison SIII (A/J, water containing 50 ppm F, exercise) *vs.* RIII (129P3/J, water containing 50 ppm F, exercise). The color of the nodes indicates the differential expression of the respective protein with its access code, available from UniProt protein database (http://www.uniprot.org/). The dark red and dark green nodes indicate proteins unique to RIII and SIII groups, respectively. The light red and light green nodes indicate down and upregulated proteins, respectively, in SIII group in respect to RIII. The gray nodes indicate the interaction proteins that are offered by CYTOSCAPE®, which were not identified in the present study.

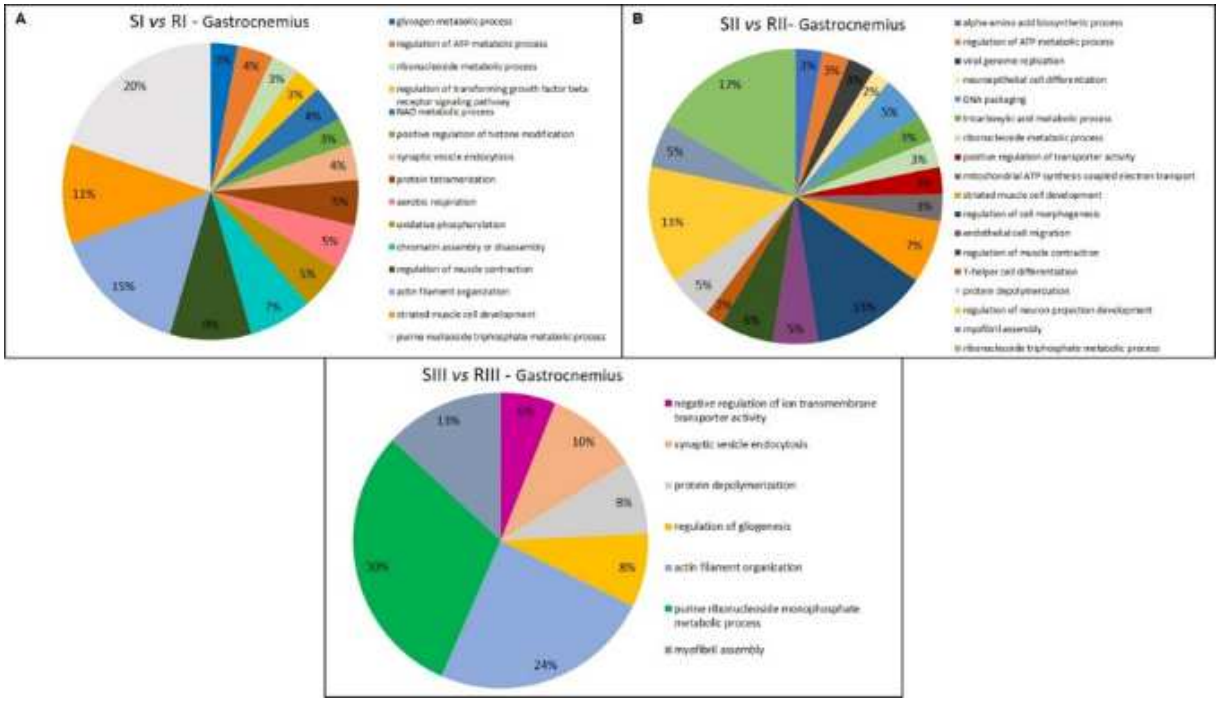

Figure 7. Functional distribution of proteins identified with differential expression in the gastrocnemius muscle of A/J and 129P3/J mice for each comparison. Comparisons are: A) SI (A/J, deionized water, no-exercise) *vs.* RI (129P3/J, deionized water, no-exercise); B) SII (A/J, water containing 50 ppm F, no-exercise) *vs.* RII (129P3/J, water containing 50 ppm F, no-exercise); C) SIII (A/J, water containing 50 ppm F, exercise) and RIII (129P3/J, water containing 50 ppm F, exercise). Categories of proteins based on GO annotation Biological Process. Terms significant (Kappa=0.4) and distribution according to percentage of number of genes association.

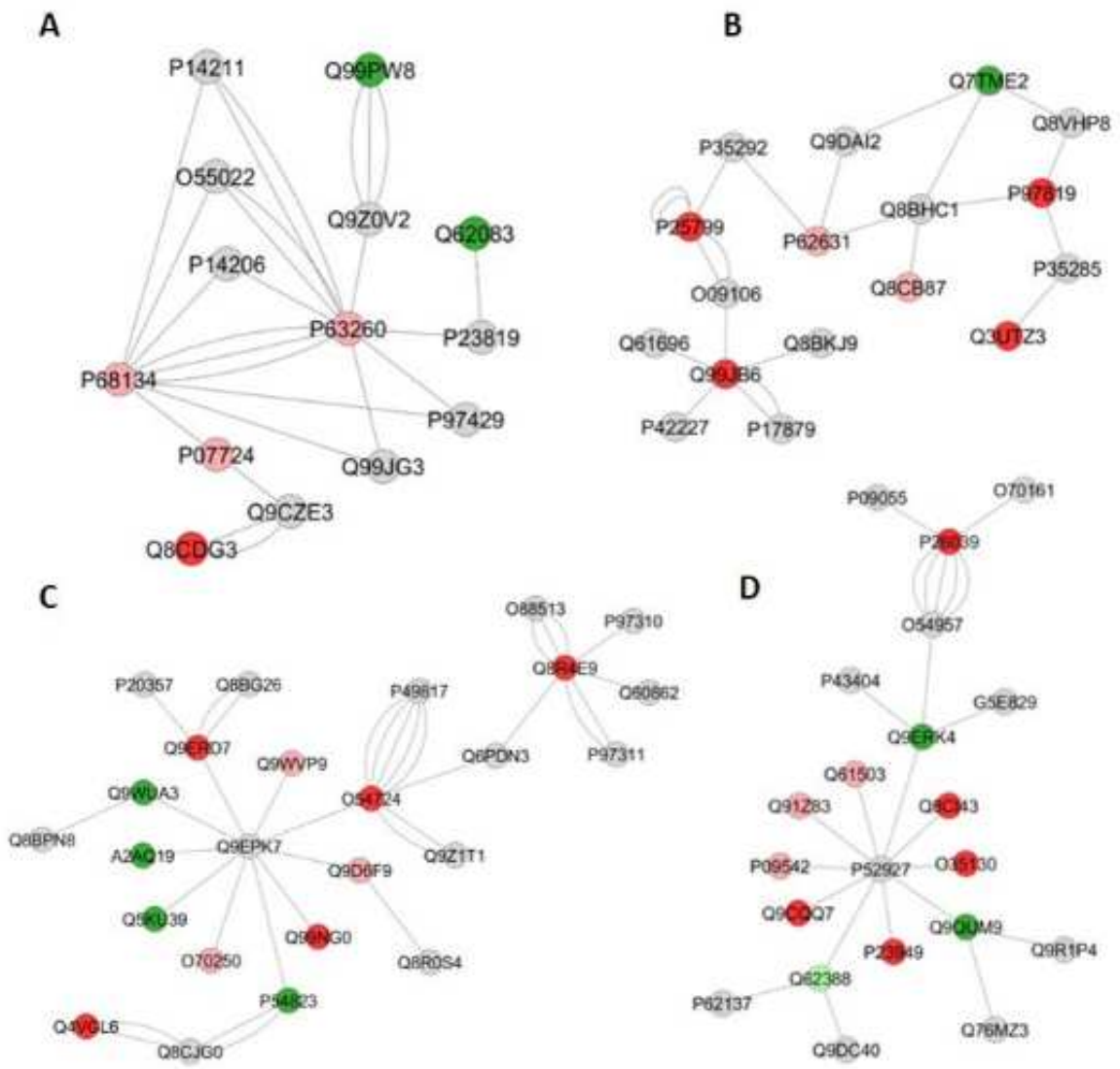

Figure 8. Subnetworks generated by ClusterMarker® for the comparison SI (A/J, deionized water, no-exercise) vs. RI (129P3/J, deionized water, no-exercise). The color of the nodes indicates the differential expression of the respective protein with its access code, available from UniProt protein database (http://www.uniprot.org/). The dark red and dark green nodes indicate proteins unique to RI and SI groups, respectively. The light red and light green nodes indicate down and upregulated proteins, respectively, in SI group in respect to RI. The gray nodes indicate the interaction proteins that are offered by CYTOSCAPE®, which were not identified in the present study.

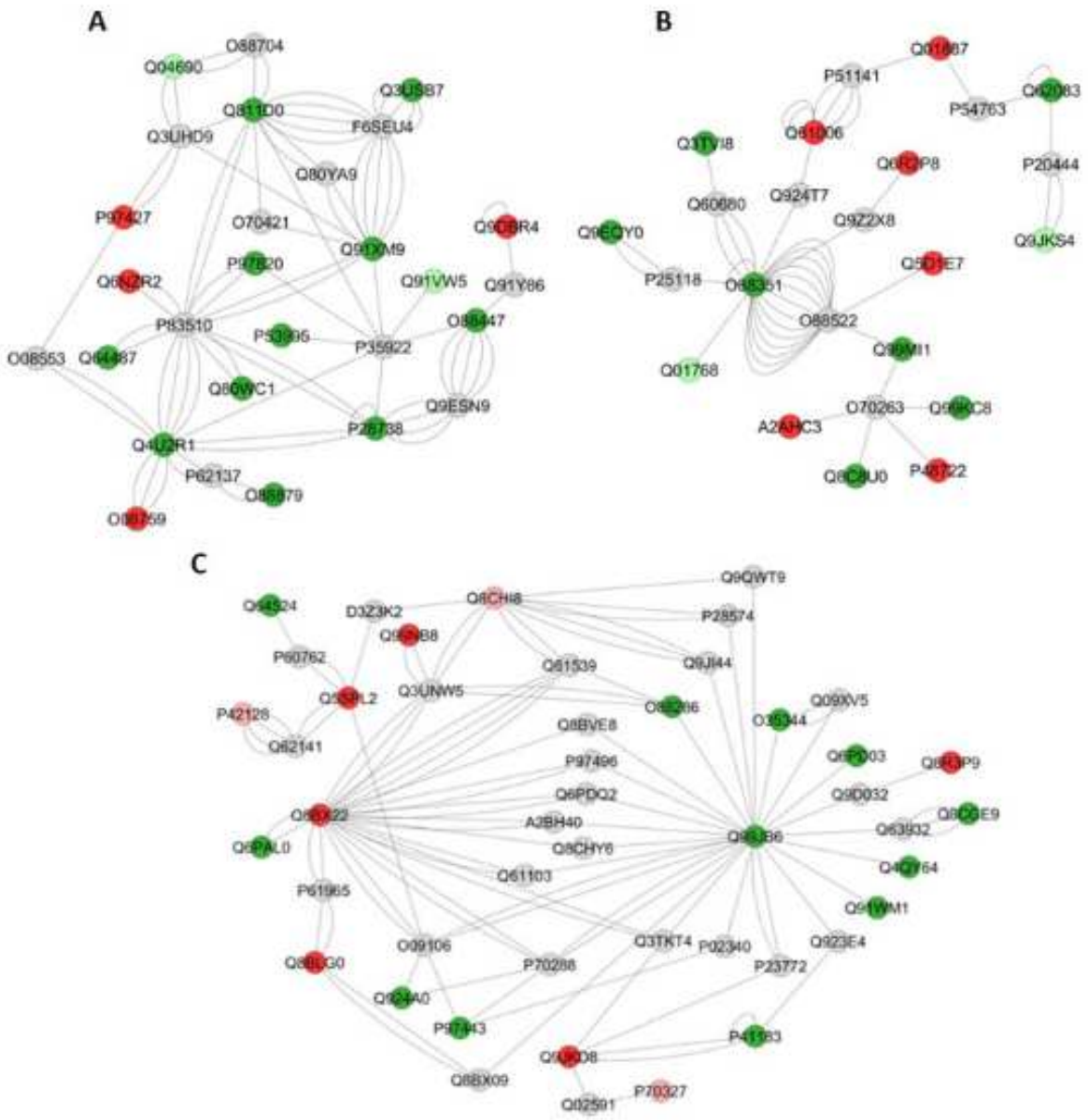

Figure 9. Subnetworks generated by ClusterMarker® for the comparison SII (A/J, water containing 50 ppm F, no-exercise) vs. RII (129P3/J, water containing 50 ppm F, no-exercise). The color of the nodes indicates the differential expression of the respective protein with its access code, available from UniProt protein database (http://www.uniprot.org/). The dark red and dark green nodes indicate proteins unique to RII and SII groups, respectively. The light red and light green nodes indicate down and upregulated proteins, respectively, in SII group in respect to RII. The gray nodes indicate the interaction proteins that are offered by CYTOSCAPE®, which were not identified in the present study.

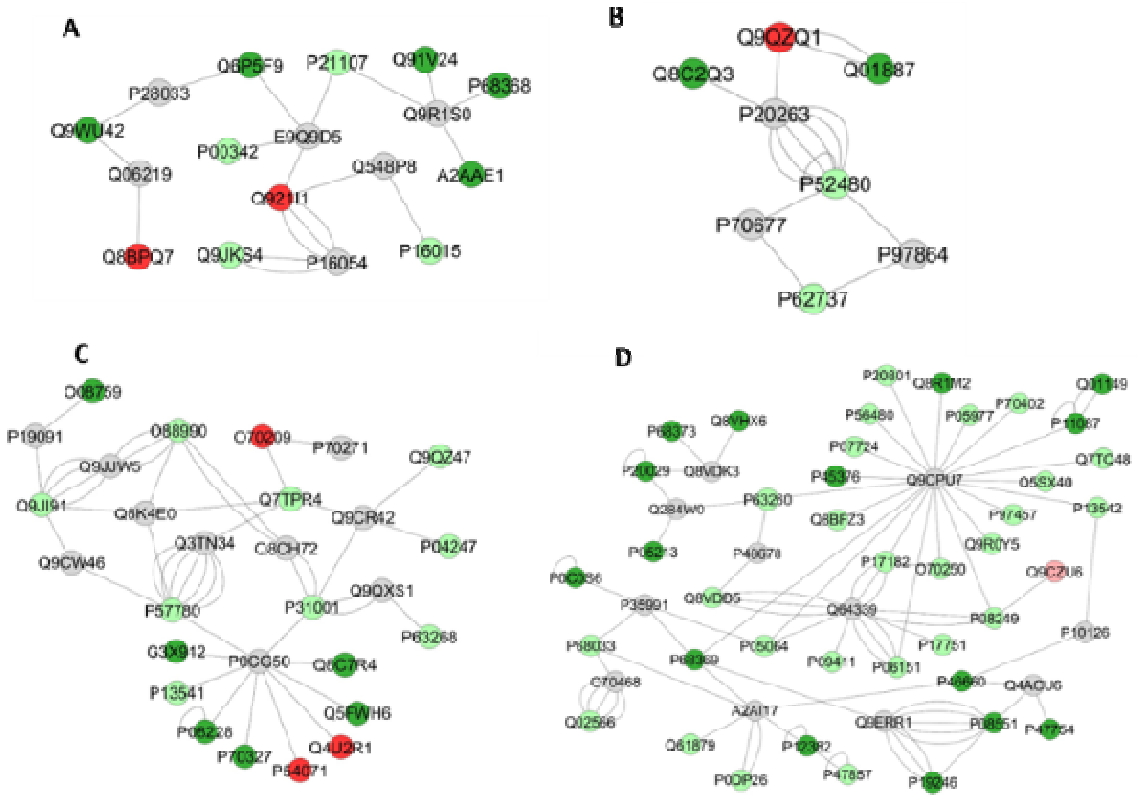

Figure 10. Subnetworks generated by ClusterMarker® for the comparison SIII (A/J, water containing 50 ppm F, exercise) *vs.* RIII (129P3/J, water containing 50 ppm F, exercise). The color of the nodes indicates the differential expression of the respective protein with its access code, available from UniProt protein database (http://www.uniprot.org/). The dark red and dark green nodes indicate proteins unique to RIII and SIII groups, respectively. The light red and light green nodes indicate down and upregulated proteins, respectively, in SIII group in respect to RIII. The gray nodes indicate the interaction proteins that are offered by CYTOSCAPE®, which were not identified in the present study.

Table 1. Mean (± SD) of plasma fluoride (F), glucose and insulin levels as well as HOMA2-IR (homeostasis model assessment 2 of insulin resistance) index, β-cell function (% B) and insulin sensitivity (% S) of A/J (susceptible to fluorosis; S) and 129P3/J (resistant to fluorosis; R) mice treated with water containing 50 ppm F or not (control; group I) and submitted to physical exercise (trained; group III) or not (sedentary; group II).

	TREATMENTS		
	CONTROL (I)	**SEDENTARY + F (II)**	**TRAINED + F (III)**
[F] plasma (µg/mL)			
A/J (S)	0.014±0.004^{Aa}	0.053±0.030^{Bb}	0.044±0.015^{Bb}
129P3/J (R)	0.017±0.004^{Aa}	0.086±0.037^{Ab}	0.089±0.062^{Ab}
Glucose (mg/dL)			
A/J (S)	176.7±28.6^{A}	174.2±20.3^{A}	168.1±32.3^{A}
129P3/J (R)	148.9±28.3^{A}	135.3±32.2^{B*}	145.5±24.2^{A}
Insulin (pmol/L)			
A/J (S)	65.8±9.5	59.7±6.7	65.8±9.8
129P3/J (R)	58.7±7.9	64.4±12.5	60.9±8.0
HOMA2-IR Index			
A/J (S)	1.41±0.22	1.28±0.16	1.30±0.25
129P3/J (R)	1.22±0.21	1.30±0.27	1.25±0.14
%B			
A/J (S)	32.7±15.0^{A}	29.4±6.8^{A}	33.2±10.3^{A}
129P3/J (R)	41.3±15.3^{A}	55.5±25.9^{B**}	48.2±28.5^{A}
%S			
A/J (S)	72.3±9.9	79.3±9.3	79.4±14.1
129P3/J (R)	84.2±14.1	79.8±16.2	80.7±9.7

For each variable, distinct uppercase letters in the same columns indicate significant differences between the strains and different lowercase letters in the same lines indicate significant difference among the treatments (2-way ANOVA and Bonferroni test for plasma). * and ** indicate Sidak and Tukey post-hoc tests, respectively. $p < 0.05$. n = 15. Physical exercise comprised a high intensity interval training (HIIT) protocol on a treadmill, 5 days per week for 8 weeks.

Table 2. Summary of the differences in expression and unique proteins found in the liver of A/J and 129P3/J mice, for each comparison

Comparison	Total number of proteins up or down-regulated*	Total number of unique proteins in each group
SI *vs* RI (Table 1)	83 up, 7 down	99 SI, 7 RI
SII *vs* RII (Table 2)	52 up, 1 down	32 SII, 8 RII
SIII *vs* RIII (Table 3)	26 up, 96 down	1 SIII, 90 RIII

* Up or down-regulation refers to the first term of each comparison.
SI – A/J mice, deionized water, no-exercise; SII – A/J mice, water containing 50 ppm F, no-exercise; SIII – A/J mice, water containing 50 ppm F, exercise; RI – 129P3/J mice, deionized water, no-exercise; RII – 129P3/J mice, water containing 50 ppm F, no-exercise; RIII – 129P3/J mice, water containing 50 ppm F, exercise.

Table 3. Summary of the main functions of proteins found in the liver in each comparison.

SI *vs* RI	SII *vs* RII	SIII *vs* RIII
SI - ↑ protein synthesis, energy flux and antioxidant enzymes.	SII - ↑ protein synthesis, energy flux and antioxidant enzymes.	SIII - ↓ protein synthesis, energy metabolism and detoxification; ↑ antioxidant enzymes.

Table 4. Summary of the differences in expression and unique proteins found in gastrocnemius of A/J and 129P3/J mice, for each comparison

Comparison	Total number of proteins up or down-regulated*	Total number of unique proteins in each group
SI *vs* RI (Table 11)	5 up, 111 down	135 SI, 180 RI
SII *vs* RII (Table 12)	99 up, 8 down	187 SII, 138 RII
SIII *vs* RIII (Table 13)	85 up, 6 down	131 SIII, 99 RIII

* Up or down-regulation refers to the first term of each comparison. SI – A/J mice, deionized water, no-exercise; SII – A/J mice, water containing 50 ppm F , no-exercise; SIII – A/J mice, water containing 50 ppm F, exercise; RI – 129P3/J mice, deionized water, no -exercise; RII – 129P3/J mice, water containing 50 ppm F, no-exercise; RIII – 129P3/J mice, water containi ng 50 ppm F, exercise.

Table 5. Summary of the main functions of proteins found in the gastrocnemius muscle in each comparison.

SI *vs* RI	SII *vs* RII	SIII *vs* RIII
SI - ↓ or absence proteins involved in muscle contraction and proteins related to the protein synthesis.	SII - ↑ proteins related to muscle contraction /relaxation, and proteins related to energy flux.	SIII - ↑ or exclusivity proteins related to energy flux; ↑ proteins related to muscle contraction/relaxation.

S1. Proteins with expression significantly altered in the liver of SI (A/J, deionized water, no-exercise) and RI (129P3/J, deionized water, no-exercise) mice.

[a]Acession number	Protein name	PLGS Score	[b]*Ratio* SI:RI
Q8VCH0	3-ketoacyl-CoA thiolase B_ peroxisomal	68	4.31
P10648	Glutathione S-transferase A2	527	2.92
O08807	Peroxiredoxin-4	70	2.86
Q921H8	3-ketoacyl-CoA thiolase A_ peroxisomal	111	2.77
P30115	Glutathione S-transferase A3	527	2.72
P13745	Glutathione S-transferase A1	527	2.69
Q6P8Q0	Glutathione S-transferase	527	2.69
P62631	Elongation factor 1-alpha 2	56	2.64
P49429	4-hydroxyphenylpyruvate dioxygenase	205	2.59
P16015	Carbonic anhydrase 3	558	2.32
P24472	Glutathione S-transferase A4	30	2.16
P0C0S6	Histone H2A.Z	246	2.12
C0HKE2	Histone H2A type 1-C	246	2.10
C0HKE9	Histone H2A type 1-P	246	2.10
C0HKE3	Histone H2A type 1-D	246	2.08
C0HKE5	Histone H2A type 1-G	246	2.08
Q64523	Histone H2A type 2-C	246	2.08
Q8BFU2	Histone H2A type 3	246	2.08
Q8R1M2	Histone H2A.J	246	2.08
Q3THW5	Histone H2A.V	246	2.08
C0HKE1	Histone H2A type 1-B	246	2.05
C0HKE4	Histone H2A type 1-E	246	2.05
C0HKE6	Histone H2A type 1-I	246	2.05
C0HKE8	Histone H2A type 1-O	246	2.05
Q6GSS7	Histone H2A type 2-A	246	2.05
Q64522	Histone H2A type 2-B	246	2.05
P62806	Histone H4	265	2.05
Q8CGP5	Histone H2A type 1-F	246	2.03
Q8CGP7	Histone H2A type 1-K	246	2.03
C0HKE7	Histone H2A type 1-N	246	2.03
P27661	Histone H2AX	246	2.03
Q8CGP6	Histone H2A type 1-H	246	2.01
P11352	Glutathione peroxidase 1	441	1.90
Q9JHW9	Aldehyde dehydrogenase family 1 member A3	46	1.70
P50247	Adenosylhomocysteinase	327	1.68
Q9CZS1	Aldehyde dehydrogenase X_ mitochondrial	46	1.68
Q9QXD6	Fructose-1_6-bisphosphatase 1	261	1.65
Q62148	Retinal dehydrogenase 2	46	1.65
O35945	Aldehyde dehydrogenase_ cytosolic 1	241	1.63
P24549	Retinal dehydrogenase 1	317	1.63

P47738	Aldehyde dehydrogenase_ mitochondrial	237	1.62
Q99LC5	Electron transfer flavoprotein subunit alpha_ mitochondrial	114	1.62
P24270	Catalase	342	1.58
P35700	Peroxiredoxin-1	284	1.58
Q9DCW4	Electron transfer flavoprotein subunit beta	236	1.55
P14152	Malate dehydrogenase_ cytoplasmic	230	1.54
P08228	Superoxide dismutase [Cu-Zn]	123	1.52
P54869	Hydroxymethylglutaryl-CoA synthase_ mitochondrial	185	1.49
Q64433	10 kDa heat shock protein_ mitochondrial	333	1.43
P05202	Aspartate aminotransferase_ mitochondrial	179	1.42
Q64374	Regucalcin	353	1.42
P26443	Glutamate dehydrogenase 1_ mitochondrial	154	1.36
P11725	Ornithine carbamoyltransferase_ mitochondrial	183	1.36
P52760	2-iminobutanoate/2-iminopropanoate deaminase	221	1.35
P12710	Fatty acid-binding protein_ liver	2940	1.35
P15626	Glutathione S-transferase Mu 2	582	1.35
Q61176	Arginase-1	956	1.34
Q8R5I6	Glutathione S-transferase mu 4	582	1.34
Q80W21	Glutathione S-transferase Mu 7	582	1.34
Q03265	ATP synthase subunit alpha_ mitochondrial	293	1.32
F6Y363	Uncharacterized protein	582	1.32
P16460	Argininosuccinate synthase	570	1.31
Q8BFZ3	Beta-actin-like protein 2	386	1.31
P08249	Malate dehydrogenase_ mitochondrial	286	1.31
P56480	ATP synthase subunit beta_ mitochondrial	352	1.30
Q8BWT1	3-ketoacyl-CoA thiolase_ mitochondrial	301	1.28
P10126	Elongation factor 1-alpha 1	238	1.28
P70694	Estradiol 17 beta-dehydrogenase 5	411	1.28
P48774	Glutathione S-transferase Mu 5	87	1.28
Q9QXF8	Glycine N-methyltransferase	274	1.28
P63260	Actin_ cytoplasmic 2	1328	1.26
Q91Y97	Fructose-bisphosphate aldolase B	301	1.23
P68033	Actin_ alpha cardiac muscle 1	1147	1.22
P68134	Actin_ alpha skeletal muscle	1147	1.22
P62737	Actin_ aortic smooth muscle	1147	1.22
P60710	Actin_ cytoplasmic 1	1328	1.22
P63268	Actin_ gamma-enteric smooth muscle	1147	1.22
P10649	Glutathione S-transferase Mu 1	368	1.19
P16858	Glyceraldehyde-3-phosphate dehydrogenase	493	1.17
O35490	Betaine--homocysteine S-methyltransferase 1	1350	1.15
P25688	Uricase	589	1.13
Q8C196	Carbamoyl-phosphate synthase [ammonia]_ mitochondrial	1600	1.12

P02089	Hemoglobin subunit beta-2	3090	1.06
P02088	Hemoglobin subunit beta-1	4320	0.90
P19157	Glutathione S-transferase P 1	396	0.89
Q91VB8	Alpha globin 1	2856	0.89
P01942	Hemoglobin subunit alpha	2604	0.89
P02104	Hemoglobin subunit epsilon-Y2	2045	0.89
P46425	Glutathione S-transferase P 2	101	0.79
V9GXQ2	Uncharacterized protein	183	0.66
Q9CQ62	2_4-dienoyl-CoA reductase_ mitochondrial	214	SI*
Q78JT3	3-hydroxyanthranilate 3_4-dioxygenase	651	SI
P47955	60S acidic ribosomal protein P1	824	SI
Q99KI0	Aconitate hydratase_ mitochondrial	83	SI
P31786	Acyl-CoA-binding protein	2938	SI
Q91VA0	Acyl-coenzyme A synthetase ACSM1_ mitochondrial	232	SI
Q64437	Alcohol dehydrogenase class 4 mu/sigma chain	197	SI
P28474	Alcohol dehydrogenase class-3	1575	SI
Q8BH00	Aldehyde dehydrogenase family 8 member A1	166	SI
Q9DBF1	Alpha-aminoadipic semialdehyde dehydrogenase	271	SI
P00687	Alpha-amylase 1	25	SI
P17182	Alpha-enolase	954	SI
P05201	Aspartate aminotransferase_ cytoplasmic	461	SI
P21550	Beta-enolase	219	SI
P34914	Bifunctional epoxide hydrolase 2	835	SI
Q8VCT4	Carboxylesterase 1D	216	SI
Q91WU0	Carboxylesterase 1F	188	SI
Q63880	Carboxylesterase 3A	235	SI
Q99KF0	Caspase recruitment domain-containing protein 14	28	SI
P56395	Cytochrome b5	772	SI
Q9CZ13	Cytochrome b-c1 complex subunit 1_ mitochondrial	214	SI
P19783	Cytochrome c oxidase subunit 4 isoform 1_ mitochondrial	518	SI
P12787	Cytochrome c oxidase subunit 5A_ mitochondrial	561	SI
Q64458	Cytochrome P450 2C29	222	SI
P28271	Cytoplasmic aconitate hydratase	84	SI
O35215	D-dopachrome decarboxylase	3765	SI
Q8CHT0	Delta-1-pyrroline-5-carboxylate dehydrogenase_ mitochondrial	463	SI
Q3U319	E3 ubiquitin-protein ligase BRE1B	26	SI
Q8BL66	Early endosome antigen 1	17	SI
P42125	Enoyl-CoA delta isomerase 1_ mitochondrial	283	SI
P19096	Fatty acid synthase	36	SI
Q91XD4	Formimidoyltransferase-cyclodeaminase	247	SI

P35505	Fumarylacetoacetase	980	SI
Q64467	Glyceraldehyde-3-phosphate dehydrogenase_ testis-specific	109	SI
Q8CBB6	Histone H2B	3067	SI
P70696	Histone H2B type 1-A	1718	SI
Q64475	Histone H2B type 1-B	3067	SI
Q6ZWY9	Histone H2B type 1-C/E/G	3067	SI
P10853	Histone H2B type 1-F/J/L	3067	SI
Q64478	Histone H2B type 1-H	3067	SI
Q8CGP1	Histone H2B type 1-K	3067	SI
P10854	Histone H2B type 1-M	3067	SI
Q8CGP2	Histone H2B type 1-P	3067	SI
Q64525	Histone H2B type 2-B	3067	SI
Q64524	Histone H2B type 2-E	2684	SI
Q9D2U9	Histone H2B type 3-A	2684	SI
Q8CGP0	Histone H2B type 3-B	2684	SI
O88844	Isocitrate dehydrogenase [NADP] cytoplasmic	250	SI
P54071	Isocitrate dehydrogenase [NADP]_ mitochondrial	174	SI
Q9CPU0	Lactoylglutathione lyase	944	SI
P41216	Long-chain-fatty-acid--CoA ligase 1	572	SI
P11588	Major urinary protein 1	389	SI
P04938	Major urinary protein 11	389	SI
P11589	Major urinary protein 2	389	SI
P11591	Major urinary protein 5	98	SI
P02762	Major urinary protein 6	389	SI
Q9JM52	Misshapen-like kinase 1	86	SI
Q8K009	Mitochondrial 10-formyltetrahydrofolate dehydrogenase	199	SI
P97820	Mitogen-activated protein kinase kinase kinase kinase 4	96	SI
Q8BZW8	NHL repeat-containing protein 2	37	SI
P32020	Non-specific lipid-transfer protein	253	SI
F6ZDS4	Nucleoprotein TPR	23	SI
P29758	Ornithine aminotransferase_ mitochondrial	318	SI
P17742	Peptidyl-prolyl cis-trans isomerase A	420	SI
O08709	Peroxiredoxin-6	457	SI
Q9DBM2	Peroxisomal bifunctional enzyme	101	SI
P09411	Phosphoglycerate kinase 1	136	SI
P09041	Phosphoglycerate kinase 2	78	SI
Q8VCR7	Protein ABHD14B	588	SI
P27773	Protein disulfide-isomerase A3	209	SI
P09103	Protein disulfide-isomerase	222	SI
O88451	Retinol dehydrogenase 7	110	SI
P17563	Selenium-binding protein 1	946	SI
Q63836	Selenium-binding protein 2	940	SI
Q07417	Short-chain specific acyl-CoA	246	SI

	dehydrogenase_ mitochondrial		
Q64442	Sorbitol dehydrogenase	347	SI
P38647	Stress-70 protein_ mitochondrial	80	SI
P52196	Thiosulfate sulfurtransferase	231	SI
B9EKN8	TRAF2 and NCK interacting kinase	86	SI
P83510	Traf2 and NCK-interacting protein kinase	86	SI
Q01853	Transitional endoplasmic reticulum ATPase	45	SI
P40142	Transketolase	76	SI
Q8BMS1	Trifunctional enzyme subunit alpha_ mitochondrial	107	SI
Q8VC30	Triokinase/FMN cyclase	209	SI
P17751	Triosephosphate isomerase	1172	SI
P68369	Tubulin alpha-1A chain	299	SI
P05213	Tubulin alpha-1B chain	299	SI
P68373	Tubulin alpha-1C chain	299	SI
P05214	Tubulin alpha-3 chain	247	SI
P68368	Tubulin alpha-4A chain	247	SI
Q9JJZ2	Tubulin alpha-8 chain	247	SI
Q9ERD7	Tubulin beta-3 chain	47	SI
Q9D6F9	Tubulin beta-4A chain	152	SI
P68372	Tubulin beta-4B chain	144	SI
P99024	Tubulin beta-5 chain	47	SI
E9Q3T0	Uncharacterized protein	685	SI
Q8VC12	Urocanate hydratase	38	SI
Q8R164	Valacyclovir hydrolase	179	SI
Q80VW5	Whirlin	22	SI
P05977	Myosin light chain 1/3_ skeletal muscle isoform	452	RI
Q5SX40	Myosin-1	96	RI
Q5SX39	Myosin-4	105	RI
Q02566	Myosin-6	63	RI
Q91Z83	Myosin-7	63	RI
P13542	Myosin-8	96	RI
Q99LX0	Protein DJ-1	172	RI

[a]Identification is based on proteins ID from UniProt protein database, reviewed only (http://www.uniprot.org/).
[b]Proteins with expression significantly altered are organized according to the ratio.
*Indicates unique proteins in alphabetical order.

S2. Proteins with expression significantly altered in the liver of SII (A/J, water containing 50 ppm F, no-exercise) and RII (129P3/J, water containing 50 ppm F, no-exercise) mice.

[a]Acession number	Protein name	PLGS Score	[b]*Ratio* SII:RII
V9GXA7	Uncharacterized protein	74	3.35
V9GXQ2	Uncharacterized protein	35	2.89
P16015	Carbonic anhydrase 3	402	2.64
Q9QXD6	Fructose-1_6-bisphosphatase 1	236	2.03
P16460	Argininosuccinate synthase	195	1.97
P02088	Hemoglobin subunit beta-1	3980	1.97
P02104	Hemoglobin subunit epsilon-Y2	1376	1.95
Q91VB8	Alpha globin 1	4327	1.84
P16858	Glyceraldehyde-3-phosphate dehydrogenase	641	1.79
P02089	Hemoglobin subunit beta-2	2526	1.77
B2RQC6	CAD protein	8	1.68
P50247	Adenosylhomocysteinase	270	1.60
P24549	Retinal dehydrogenase 1	175	1.58
P11352	Glutathione peroxidase 1	626	1.57
P07724	Serum albumin	245	1.55
O35945	Aldehyde dehydrogenase_ cytosolic 1	143	1.52
P00329	Alcohol dehydrogenase 1	180	1.51
P08249	Malate dehydrogenase_ mitochondrial	140	1.48
P24270	Catalase	351	1.46
Q99LC5	Electron transfer flavoprotein subunit alpha_ mitochondrial	111	1.46
P01942	Hemoglobin subunit alpha	4327	1.46
P10126	Elongation factor 1-alpha 1	475	1.40
Q9JHW9	Aldehyde dehydrogenase family 1 member A3	37	1.36
P35700	Peroxiredoxin-1	153	1.35
Q62148	Retinal dehydrogenase 2	37	1.35
P70694	Estradiol 17 beta-dehydrogenase 5	137	1.34
P12710	Fatty acid-binding protein_ liver	3193	1.34
P54869	Hydroxymethylglutaryl-CoA synthase_ mitochondrial	165	1.32
P05202	Aspartate aminotransferase_ mitochondrial	237	1.30
Q8BWT1	3-ketoacyl-CoA thiolase_ mitochondrial	319	1.28
P63268	Actin_ gamma-enteric smooth muscle	1730	1.26
P47738	Aldehyde dehydrogenase_ mitochondrial	226	1.26
Q9DCW4	Electron transfer flavoprotein subunit beta	349	1.26
P68033	Actin_ alpha cardiac muscle 1	1730	1.25
P62737	Actin_ aortic smooth muscle	1730	1.25
Q8C196	Carbamoyl-phosphate synthase [ammonia]_ mitochondrial	1655	1.25
P68134	Actin_ alpha skeletal muscle	1730	1.23
P56480	ATP synthase subunit beta_ mitochondrial	390	1.23

P11725	Ornithine carbamoyltransferase_ mitochondrial	206	1.23
Q64374	Regucalcin	361	1.23
Q03265	ATP synthase subunit alpha_ mitochondrial	299	1.21
P25688	Uricase	526	1.21
P60710	Actin_ cytoplasmic 1	2007	1.19
O35490	Betaine--homocysteine S-methyltransferase 1	876	1.19
P26443	Glutamate dehydrogenase 1_ mitochondrial	330	1.19
P10649	Glutathione S-transferase Mu 1	790	1.19
P63260	Actin_ cytoplasmic 2	2007	1.16
Q91Y97	Fructose-bisphosphate aldolase B	277	1.16
Q8BFZ3	Beta-actin-like protein 2	428	1.16
Q91WS4	S-methylmethionine--homocysteine S-methyltransferase BHMT2	485	1.14
P19157	Glutathione S-transferase P 1	1249	1.13
Q9QXF8	Glycine N-methyltransferase	467	1.12
P46425	Glutathione S-transferase P 2	491	0.61
P49429	4-hydroxyphenylpyruvate dioxygenase	220	SII*
P31786	Acyl-CoA-binding protein	592	SII
Q8VCT4	Carboxylesterase 1D	84	SII
O35215	D-dopachrome decarboxylase	206	SII
P62631	Elongation factor 1-alpha 2	34	SII
P13745	Glutathione S-transferase A1	355	SII
P10648	Glutathione S-transferase A2	331	SII
P30115	Glutathione S-transferase A3	355	SII
P24472	Glutathione S-transferase A4	25	SII
P15626	Glutathione S-transferase Mu 2	408	SII
P48774	Glutathione S-transferase Mu 5	212	SII
Q80W21	Glutathione S-transferase Mu 7	416	SII
Q64467	Glyceraldehyde-3-phosphate dehydrogenase_ testis-specific	4	SII
Q8CBB6	Histone H2B	590	SII
P70696	Histone H2B type 1-A	391	SII
Q64475	Histone H2B type 1-B	590	SII
Q6ZWY9	Histone H2B type 1-C/E/G	590	SII
P10853	Histone H2B type 1-F/J/L	590	SII
Q64478	Histone H2B type 1-H	590	SII
Q8CGP1	Histone H2B type 1-K	590	SII
P10854	Histone H2B type 1-M	590	SII
Q8CGP2	Histone H2B type 1-P	590	SII
Q64525	Histone H2B type 2-B	590	SII
Q64524	Histone H2B type 2-E	590	SII
Q9D2U9	Histone H2B type 3-A	590	SII
Q8CGP0	Histone H2B type 3-B	590	SII
P62806	Histone H4	161	SII
P06151	L-lactate dehydrogenase A chain	116	SII
P14152	Malate dehydrogenase_ cytoplasmic	376	SII

O08807	Peroxiredoxin-4	119	SII
O08709	Peroxiredoxin-6	36	SII
F6Y363	Uncharacterized protein	408	SII
P11588	Major urinary protein 1	849	RII
P04938	Major urinary protein 11	849	RII
B5X0G2	Major urinary protein 17	849	RII
A2BIM8	Major urinary protein 18	849	RII
P11589	Major urinary protein 2	849	RII
P11591	Major urinary protein 5	811	RII
P02762	Major urinary protein 6	849	RII
P32020	Non-specific lipid-transfer protein	82	RII

[a]Identification is based on proteins ID from UniProt protein database, reviewed only (http://www.uniprot.org/)
[b]Proteins with expression significantly altered are organized according to the ratio.
*Indicates unique proteins in alphabetical order.

S3. Proteins with expression significantly altered in the liver of SIII (A/J, water containing 50 ppm F, exercise) and RIII (129P3/J, water containing 50 ppm F, exercise) mice.

[a]Acession number	Protein name	PLGS Score	[b]*Ratio* SIII:RIII
P16015	Carbonic anhydrase 3	3069	2.94
P12710	Fatty acid-binding protein_ liver	21785	2.05
Q61176	Arginase-1	4188	1.82
O35945	Aldehyde dehydrogenase_ cytosolic 1	1018	1.79
Q8C196	Carbamoyl-phosphate synthase [ammonia]_ mitochondrial	8837	1.77
P02088	Hemoglobin subunit beta-1	27458	1.67
P54869	Hydroxymethylglutaryl-CoA synthase_ mitochondrial	1254	1.67
O35490	Betaine--homocysteine S-methyltransferase 1	5948	1.63
P24549	Retinal dehydrogenase 1	1374	1.63
P16858	Glyceraldehyde-3-phosphate dehydrogenase	2946	1.62
Q9CZS1	Aldehyde dehydrogenase X_ mitochondrial	89	1.58
P02104	Hemoglobin subunit epsilon-Y2	1854	1.57
Q9JHW9	Aldehyde dehydrogenase family 1 member A3	89	1.55
Q62148	Retinal dehydrogenase 2	89	1.49
Q91Y97	Fructose-bisphosphate aldolase B	3833	1.38
O35215	D-dopachrome decarboxylase	1061	1.32
P10649	Glutathione S-transferase Mu 1	12177	1.28
P11725	Ornithine carbamoyltransferase_ mitochondrial	1289	1.28
P08228	Superoxide dismutase [Cu-Zn]	1918	1.28
P26443	Glutamate dehydrogenase 1_ mitochondrial	1955	1.27

P02089	Hemoglobin subunit beta-2	9125	1.21
Q91WS4	S-methylmethionine--homocysteine S-methyltransferase BHMT2	1884	1.13
P68134	Actin_ alpha skeletal muscle	8945	1.12
P68033	Actin_ alpha cardiac muscle 1	8949	1.09
P62737	Actin_ aortic smooth muscle	8945	1.09
P63268	Actin_ gamma-enteric smooth muscle	8945	1.09
P01942	Hemoglobin subunit alpha	11151	0.95
P60710	Actin_ cytoplasmic 1	10876	0.94
Q8BFZ3	Beta-actin-like protein 2	2497	0.80
P52760	2-iminobutanoate/2-iminopropanoate deaminase	799	0.79
Q05920	Pyruvate carboxylase_ mitochondrial	128	0.77
P05202	Aspartate aminotransferase_ mitochondrial	1309	0.76
Q91XD4	Formimidoyltransferase-cyclodeaminase	494	0.75
P63038	60 kDa heat shock protein_ mitochondrial	306	0.73
Q99LB7	Sarcosine dehydrogenase_ mitochondrial	285	0.71
P99029	Peroxiredoxin-5_ mitochondrial	548	0.70
Q8VCN5	Cystathionine gamma-lyase	507	0.69
Q99LC5	Electron transfer flavoprotein subunit alpha_ mitochondrial	466	0.68
Q9DCW4	Electron transfer flavoprotein subunit beta	3282	0.68
P25688	Uricase	3095	0.68
P08249	Malate dehydrogenase_ mitochondrial	1105	0.67
Q8VCT4	Carboxylesterase 1D	240	0.66
P07724	Serum albumin	1088	0.65
Q8CGP5	Histone H2A type 1-F	921	0.64
Q64433	10 kDa heat shock protein_ mitochondrial	1588	0.64
P12787	Cytochrome c oxidase subunit 5A_ mitochondrial	648	0.64
Q9CQ62	2_4-dienoyl-CoA reductase_ mitochondrial	68	0.63
A0A0N4SVE0	Uncharacterized protein	2588	0.63
P11679	Keratin_ type II cytoskeletal 8	207	0.63
Q64522	Histone H2A type 2-B	921	0.62
Q03265	ATP synthase subunit alpha_ mitochondrial	1776	0.62
B2RQC6	CAD protein	58	0.62
Q8R1M2	Histone H2A.J	921	0.61
P14152	Malate dehydrogenase_ cytoplasmic	1349	0.61
P31786	Acyl-CoA-binding protein	1514	0.61
P00329	Alcohol dehydrogenase 1	1008	0.61
Q64523	Histone H2A type 2-C	921	0.61
P0C0S6	Histone H2A.Z	921	0.61
P27661	Histone H2AX	921	0.61
O09173	Homogentisate 1_2-dioxygenase	232	0.61
C0HKE3	Histone H2A type 1-D	921	0.60
C0HKE6	Histone H2A type 1-I	921	0.60

Q6GSS7	Histone H2A type 2-A	921	0.60
Q3THW5	Histone H2A.V	921	0.60
Q8K009	Mitochondrial 10-formyltetrahydrofolate dehydrogenase	133	0.60
C0HKE8	Histone H2A type 1-O	921	0.59
P20029	78 kDa glucose-regulated protein	633	0.59
P56480	ATP synthase subunit beta_ mitochondrial	2012	0.59
Q9QXD6	Fructose-1_6-bisphosphatase 1	1052	0.59
C0HKE1	Histone H2A type 1-B	921	0.59
C0HKE2	Histone H2A type 1-C	921	0.59
C0HKE5	Histone H2A type 1-G	921	0.59
Q8CGP6	Histone H2A type 1-H	921	0.59
Q8CGP7	Histone H2A type 1-K	921	0.59
C0HKE9	Histone H2A type 1-P	921	0.59
P62806	Histone H4	801	0.59
V9GXA7	Uncharacterized protein	771	0.59
Q78JT3	3-hydroxyanthranilate 3_4-dioxygenase	493	0.59
P47738	Aldehyde dehydrogenase_ mitochondrial	1659	0.59
Q8BFU2	Histone H2A type 3	921	0.58
C0HKE4	Histone H2A type 1-E	921	0.58
C0HKE7	Histone H2A type 1-N	921	0.58
Q8BWT1	3-ketoacyl-CoA thiolase_ mitochondrial	1849	0.58
Q9EQ20	Methylmalonate-semialdehyde dehydrogenase [acylating]_ mitochondrial	271	0.57
P05201	Aspartate aminotransferase_ cytoplasmic	382	0.56
Q8R0Y6	Cytosolic 10-formyltetrahydrofolate dehydrogenase	3301	0.56
Q64475	Histone H2B type 1-B	1475	0.56
P10853	Histone H2B type 1-F/J/L	1475	0.56
Q64478	Histone H2B type 1-H	1475	0.56
Q8CGP1	Histone H2B type 1-K	1475	0.56
Q8CGP2	Histone H2B type 1-P	1475	0.56
Q64525	Histone H2B type 2-B	1475	0.56
Q9D2U9	Histone H2B type 3-A	1155	0.56
P24270	Catalase	3316	0.55
P11352	Glutathione peroxidase 1	2205	0.55
Q6ZWY9	Histone H2B type 1-C/E/G	1475	0.55
P10854	Histone H2B type 1-M	1475	0.55
Q64524	Histone H2B type 2-E	1155	0.55
Q8CGP0	Histone H2B type 3-B	1155	0.55
P49429	4-hydroxyphenylpyruvate dioxygenase	1665	0.55
P35700	Peroxiredoxin-1	2693	0.55
P70696	Histone H2B type 1-A	587	0.54
Q01768	Nucleoside diphosphate kinase B	584	0.53
Q91X83	S-adenosylmethionine synthase isoform type-1	1571	0.53

P70694	Estradiol 17 beta-dehydrogenase 5	2293	0.52
P19157	Glutathione S-transferase P 1	5065	0.52
P56395	Cytochrome b5	998	0.51
P32020	Non-specific lipid-transfer protein	522	0.47
P35505	Fumarylacetoacetase	812	0.46
P50247	Adenosylhomocysteinase	5869	0.46
Q8QZT1	Acetyl-CoA acetyltransferase_ mitochondrial	959	0.45
P16460	Argininosuccinate synthase	2388	0.44
P62631	Elongation factor 1-alpha 2	427	0.43
O08807	Peroxiredoxin-4	518	0.42
F6Y363	Uncharacterized protein	3705	0.41
P15626	Glutathione S-transferase Mu 2	3705	0.41
Q80W21	Glutathione S-transferase Mu 7	3705	0.41
Q9QXF8	Glycine N-methyltransferase	3693	0.41
P48774	Glutathione S-transferase Mu 5	163	0.40
P13745	Glutathione S-transferase A1	2794	0.37
P10648	Glutathione S-transferase A2	2747	0.37
P30115	Glutathione S-transferase A3	3206	0.37
Q9CPU0	Lactoylglutathione lyase	407	SIII*
Q921H8	3-ketoacyl-CoA thiolase A_ peroxisomal	613	RIII
Q8VCH0	3-ketoacyl-CoA thiolase B_ peroxisomal	613	RIII
P14206	40S ribosomal protein SA	192	RIII
P47955	60S acidic ribosomal protein P1	1191	RIII
Q91WG0	Acylcarnitine hydrolase	17	RIII
Q91VA0	Acyl-coenzyme A synthetase ACSM1_ mitochondrial	64	RIII
Q8QZR5	Alanine aminotransferase 1	102	RIII
P28474	Alcohol dehydrogenase class-3	1777	RIII
Q8BH00	Aldehyde dehydrogenase family 8 member A1	77	RIII
Q9DBF1	Alpha-aminoadipic semialdehyde dehydrogenase	423	RIII
P17182	Alpha-enolase	769	RIII
P21550	Beta-enolase	71	RIII
P34914	Bifunctional epoxide hydrolase 2	438	RIII
Q8VCU1	Carboxylesterase 3B	89	RIII
P19783	Cytochrome c oxidase subunit 4 isoform 1_ mitochondrial	245	RIII
Q8CHT0	Delta-1-pyrroline-5-carboxylate dehydrogenase_ mitochondrial	328	RIII
Q8BVI4	Dihydropteridine reductase	368	RIII
Q9DBT9	Dimethylglycine dehydrogenase_ mitochondrial	50	RIII
Q8BH95	Enoyl-CoA hydratase_ mitochondrial	105	RIII
P19096	Fatty acid synthase	25	RIII
P15105	Glutamine synthetase	391	RIII
P24472	Glutathione S-transferase A4	35	RIII
Q64467	Glyceraldehyde-3-phosphate dehydrogenase_	45	RIII

	testis-specific		
Q61696	Heat shock 70 kDa protein 1A	157	RIII
P17879	Heat shock 70 kDa protein 1B	157	RIII
P16627	Heat shock 70 kDa protein 1-like	157	RIII
P63017	Heat shock cognate 71 kDa protein	741	RIII
Q9CQN1	Heat shock protein 75 kDa_ mitochondrial	187	RIII
P07901	Heat shock protein HSP 90-alpha	218	RIII
P11499	Heat shock protein HSP 90-beta	510	RIII
P17156	Heat shock-related 70 kDa protein 2	250	RIII
P40936	Indolethylamine N-methyltransferase	267	RIII
Q9D819	Inorganic pyrophosphatase	254	RIII
O88844	Isocitrate dehydrogenase [NADP] cytoplasmic	99	RIII
P05784	Keratin_ type I cytoskeletal 18	115	RIII
Q99M73	Keratin_ type II cuticular Hb4	7	RIII
P06151	L-lactate dehydrogenase A chain	518	RIII
P16125	L-lactate dehydrogenase B chain	293	RIII
P00342	L-lactate dehydrogenase C chain	293	RIII
P41216	Long-chain-fatty-acid--CoA ligase 1	375	RIII
P11588	Major urinary protein 1	1114	RIII
P04938	Major urinary protein 11	1114	RIII
B5X0G2	Major urinary protein 17	1114	RIII
A2BIM8	Major urinary protein 18	1114	RIII
P11589	Major urinary protein 2	1114	RIII
P11591	Major urinary protein 5	1114	RIII
P02762	Major urinary protein 6	1114	RIII
Q8R4H7	N-acetylglutamate synthase_ mitochondrial	207	RIII
P17742	Peptidyl-prolyl cis-trans isomerase A	967	RIII
P24369	Peptidyl-prolyl cis-trans isomerase B	111	RIII
O08709	Peroxiredoxin-6	710	RIII
P51660	Peroxisomal multifunctional enzyme type 2	130	RIII
P70296	Phosphatidylethanolamine-binding protein 1	506	RIII
P09411	Phosphoglycerate kinase 1	124	RIII
P09041	Phosphoglycerate kinase 2	82	RIII
Q8VCR7	Protein ABHD14B	353	RIII
P09103	Protein disulfide-isomerase	144	RIII
P27773	Protein disulfide-isomerase A3	90	RIII
Q99LX0	Protein DJ-1	506	RIII
Q8C627	Protein FAM221B	103	RIII
O55125	Protein NipSnap homolog 1	560	RIII
Q2PZL6	Protocadherin Fat 4	15	RIII
Q8QZR3	Pyrethroid hydrolase Ces2a	104	RIII
Q3THS6	S-adenosylmethionine synthase isoform type-2	309	RIII
Q99J08	SEC14-like protein 2	260	RIII
P17563	Selenium-binding protein 1	442	RIII
Q63836	Selenium-binding protein 2	423	RIII
Q9R0P3	S-formylglutathione hydrolase	331	RIII

Q64442	Sorbitol dehydrogenase	646	RIII
P38647	Stress-70 protein_ mitochondrial	129	RIII
Q8R086	Sulfite oxidase_ mitochondrial	54	RIII
Q01853	Transitional endoplasmic reticulum ATPase	134	RIII
Q8BMS1	Trifunctional enzyme subunit alpha_ mitochondrial	290	RIII
Q99JY0	Trifunctional enzyme subunit beta_ mitochondrial	80	RIII
P17751	Triosephosphate isomerase	1762	RIII
Q9R1R2	Tripartite motif-containing protein 3	153	RIII
Q3UX10	Tubulin alpha chain-like 3	10	RIII
P68369	Tubulin alpha-1A chain	377	RIII
P05213	Tubulin alpha-1B chain	381	RIII
P68373	Tubulin alpha-1C chain	377	RIII
P05214	Tubulin alpha-3 chain	236	RIII
P68368	Tubulin alpha-4A chain	241	RIII
Q9JJZ2	Tubulin alpha-8 chain	236	RIII
Q7TMM9	Tubulin beta-2A chain	333	RIII
Q9CWF2	Tubulin beta-2B chain	314	RIII
Q9ERD7	Tubulin beta-3 chain	230	RIII
Q9D6F9	Tubulin beta-4A chain	447	RIII
P68372	Tubulin beta-4B chain	470	RIII
P99024	Tubulin beta-5 chain	470	RIII
E9Q3T0	Uncharacterized protein	560	RIII

[a]Identification is based on proteins ID from UniProt protein database, reviewed only (http://www.uniprot.org/).
[b]Proteins with expression significantly altered are organized according to the ratio.
*Indicates unique proteins in alphabetical order.

S4. Proteins with expression significantly altered in the gastrocnemius of SI (A/J, deionized water, no-exercise) and RI (129P3/J, deionized water, no-exercise) mice.

[a]Acession number	Protein name	PLGS Score	[b]*Ratio* SI:RI
Q62388	Serine-protein kinase ATM	92	2.18
Q7TMW6	Cytosolic Fe-S cluster assembly factor	97	2.10
Q60974	Nuclear receptor corepressor 1	110	1.58
Q08481	Platelet endothelial cell adhesion molecule	68	1.57
Q8R429	Sarcoplasmic/endoplasmic reticulum calcium ATPase 1	1310	1.07
Q9WUB3	Glycogen phosphorylase_ muscle form	4719	0.98
P58771	Tropomyosin alpha-1 chain	10907	0.90
P52480	Pyruvate kinase	9371	0.84
P21107	Tropomyosin alpha-3 chain	526	0.81
P07310	Creatine kinase M-type	20796	0.80
Q3TJD7	PDZ and LIM domain protein 7	1073	0.80

P13412	Troponin I_ fast skeletal muscle	1865	0.80
Q7TQ48	Sarcalumenin	57	0.79
P05202	Aspartate aminotransferase_ mitochondrial	238	0.79
P97457	Myosin regulatory light chain 2_ skeletal muscle isoform	7565	0.77
Q99KI0	Aconitate hydratase_ mitochondrial	170	0.76
P47857	ATP-dependent 6-phosphofructokinase_ muscle type	551	0.76
A2AQP0	Myosin-7B	1899	0.76
Q8VDD5	Myosin-9	314	0.76
Q9R0Y5	Adenylate kinase isoenzyme 1	6335	0.76
Q62234	Myomesin-1	185	0.76
Q6URW6	Myosin-14	309	0.76
Q9QZ47	Troponin T_ fast skeletal muscle	1883	0.76
O09165	Calsequestrin-1	1739	0.75
O08638	Myosin-11	319	0.75
P60710	Actin_ cytoplasmic 1	78650	0.74
P63260	Actin_ cytoplasmic 2	78650	0.74
Q61879	Myosin-10	309	0.74
Q5XKE0	Myosin-binding protein C_ fast-type	2080	0.74
Q5SX39	Myosin-4	19417	0.73
Q03265	ATP synthase subunit alpha_ mitochondrial	667	0.73
P31001	Desmin	117	0.73
P14152	Malate dehydrogenase_ cytoplasmic	409	0.73
P08249	Malate dehydrogenase_ mitochondrial O	1446	0.73
Q9D0F9	Phosphoglucomutase-1	201	0.73
P58774	Tropomyosin beta chain	7827	0.72
Q02566	Myosin-6	5984	0.71
P13542	Myosin-8	11378	0.71
P15532	Nucleoside diphosphate kinase A	281	0.71
P57780	Alpha-actinin-4	178	0.70
Q5SX40	Myosin-1	14904	0.70
Q91Z83	Myosin-7	7429	0.70
P07724	Serum albumin	1403	0.70
P17182	Alpha-enolase	4627	0.69
Q9JKS4	LIM domain-binding protein 3	850	0.69
Q60605	Myosin light polypeptide 6	4175	0.69
P09041	Phosphoglycerate kinase 2	639	0.69
P09542	Myosin light chain 3	9702	0.68
Q64518	Sarcoplasmic/endoplasmic reticulum calcium ATPase 3	130	0.68
P13541	Myosin-3	4714	0.68
P05201	Aspartate aminotransferase_ cytoplasmic	85	0.67
P16015	Carbonic anhydrase 3	2095	0.67
P06151	L-lactate dehydrogenase A chain	2596	0.67
P20801	Troponin C_ skeletal muscle	1409	0.67
Q6P8J7	Creatine kinase S-type_ mitochondrial	389	0.66

P09411	Phosphoglycerate kinase 1	686	0.66
O88990	Alpha-actinin-3	2430	0.65
P00342	L-lactate dehydrogenase C chain	1187	0.65
Q9JI91	Alpha-actinin-2	1054	0.63
Q7TPR4	Alpha-actinin-1	193	0.63
P56480	ATP synthase subunit beta_ mitochondrial	1129	0.63
P0DP26	Calmodulin-1	502	0.63
O70250	Phosphoglycerate mutase 2	1961	0.63
P0DP28	Calmodulin-3	502	0.62
P21550	Beta-enolase	9402	0.61
P0DP27	Calmodulin-2	502	0.61
P17183	Gamma-enolase	444	0.61
P05064	Fructose-bisphosphate aldolase A	18392	0.61
P17751	Triosephosphate isomerase	6732	0.61
P16125	L-lactate dehydrogenase B chain	353	0.60
Q64478	Histone H2B type 1-H	890	0.59
P68134	Actin_ alpha skeletal muscle	111877	0.59
P10126	Elongation factor 1-alpha 1	108	0.59
P04247	Myoglobin	304	0.59
Q8BFZ3	Beta-actin-like protein 2	26045	0.58
Q64475	Histone H2B type 1-B	890	0.58
P10853	Histone H2B type 1-F/J/L	890	0.58
Q64525	Histone H2B type 2-B	890	0.58
Q9QXS1	Plectin	100	0.58
Q6ZWY9	Histone H2B type 1-C/E/G	890	0.58
Q8CGP1	Histone H2B type 1-K	890	0.58
P68033	Actin_ alpha cardiac muscle 1	106303	0.57
P05063	Fructose-bisphosphate aldolase C	1869	0.57
P70696	Histone H2B type 1-A	708	0.57
Q9D2U9	Histone H2B type 3-A	890	0.57
Q8CGP0	Histone H2B type 3-B	890	0.57
Q9JK37	Myozenin-1	466	0.57
P63268	Actin_ gamma-enteric smooth muscle	102366	0.57
P62631	Elongation factor 1-alpha 2	417	0.57
Q8CGP2	Histone H2B type 1-P	890	0.57
P62737	Actin_ aortic smooth muscle	102579	0.56
Q64524	Histone H2B type 2-E	890	0.55
P09541	Myosin light chain 4	6543	0.55
P10854	Histone H2B type 1-M	890	0.54
Q9JIF9	Myotilin	216	0.52
Q9D051	Pyruvate dehydrogenase E1 component subunit beta_ mitochondrial	88	0.51
Q3UU96	Serine/threonine-protein kinase MRCK alpha	128	0.50
P05977	Myosin light chain 1/3 skeletal muscle isoform	33434	0.50
P16858	Glyceraldehyde-3-phosphate dehydrogenase	25084	0.48
P01942	Hemoglobin subunit alpha	10325	0.45

P02104	Hemoglobin subunit epsilon-Y2	2425	0.44
Q99PT9	Kinesin-like protein KIF19	181	0.41
P02088	Hemoglobin subunit beta-1	3958	0.41
Q8CB87	Ras-related protein Rab-44	115	0.37
P99024	Tubulin beta-5 chain	222	0.34
Q9D6F9	Tubulin beta-4A chain	1641	0.32
Q9WVP9	Interferon-induced GTP-binding protein Mx2	298	0.32
P68372	Tubulin beta-4B chain	161	0.31
Q7TMM9	Tubulin beta-2A chain	222	0.31
Q9CWF2	Tubulin beta-2B chain	222	0.31
Q3U435	Matrix metalloproteinase-25	93	0.30
P09922	Interferon-induced GTP-binding protein Mx1	327	0.30
Q61503	5'-nucleotidase	105	0.29
P32848	Parvalbumin alpha	7739	0.28
Q8VHX6	Filamin-C	118	0.23
Q3UVV9	von Willebrand factor A domain-containing protein 3A	118	0.12
Q8VI93	2'-5'-oligoadenylate synthase 3	51	SI*
P20029	78 kDa glucose-regulated protein	46	SI
Q5SWU9	Acetyl-CoA carboxylase 1	123	SI
Q9QY83	Actin-like protein 7B	95	SI
P03958	Adenosine deaminase	71	SI
Q8C0T9	Adenylate cyclase type 10	30	SI
P46660	Alpha-internexin	72	SI
G3UZ78	Androglobin	97	SI
Q9WV74	Ankyrin repeat and SOCS box protein 1	243	SI
O88512	AP-1 complex subunit gamma-like 2	58	SI
P12382	ATP-dependent 6-phosphofructokinase liver type	77	SI
Q9WUA3	ATP-dependent 6-phosphofructokinase_ platelet type	85	SI
Q8C0J2	Autophagy-related protein 16-1	46	SI
O70318	Band 4.1-like protein 2	31	SI
P21855	B-cell differentiation antigen CD72	88	SI
Q91Z96	BMP-2-inducible protein kinase	100	SI
Q8VHF2	Cadherin-related family member 5	31	SI
Q80V31	Centrosomal protein of 104 kDa	237	SI
Q8C6E0	Cilia- and flagella-associated protein 36	171	SI
Q9D180	Cilia- and flagella-associated protein 57	51	SI
E9Q1U1	Coiled-coil domain-containing protein 171	74	SI
P11087	Collagen alpha-1(I) chain	70	SI
P02463	Collagen alpha-1(IV) chain	96	SI
Q07643	Collagen alpha-2(IX) chain	63	SI
Q04447	Creatine kinase B-type	52	SI
O88874	Cyclin-K	91	SI
P00405	Cytochrome c oxidase subunit 2	97	SI

P43023	Cytochrome c oxidase subunit 6A2_ mitochondrial	1471	SI
Q8R1A4	Dedicator of cytokinesis protein 7	109	SI
A2RSQ0	DENN domain-containing protein 5B	79	SI
O08749	Dihydrolipoyl dehydrogenase_ mitochondrial	81	SI
Q9EQF6	Dihydropyrimidinase-related protein 5	120	SI
Q9DA79	Dipeptidase 3	80	SI
Q811D0	Disks large homolog 1	63	SI
P22682	E3 ubiquitin-protein ligase CBL	60	SI
Q4U2R1	E3 ubiquitin-protein ligase HERC2	226	SI
Q8R0K2	E3 ubiquitin-protein ligase TRIM31	58	SI
Q99MI1	ELKS/Rab6-interacting/CAST family member 1	65	SI
Q62420	Endophilin-A1	71	SI
Q62419	Endophilin-A2	71	SI
P48299	Endothelin-3	139	SI
Q9ERK4	Exportin-2	93	SI
Q5RJI4	Extracellular tyrosine-protein kinase PKDCC	290	SI
A3KGK3	Fer-1-like protein 4	107	SI
Q9JJN1	Fibroblast growth factor 21	137	SI
Q8BY35	FYVE_RhoGEF and PH domain-containing protein 2	55	SI
Q9DBA9	General transcription factor IIH subunit 1	82	SI
Q00612	Glucose-6-phosphate 1-dehydrogenase X	95	SI
Q9WU65	Glycerol kinase 2	53	SI
Q9JLM9	Growth factor receptor-bound protein 14	120	SI
Q9ERL9	Guanylate cyclase soluble subunit alpha-3	67	SI
P79457	Histone demethylase UTY	42	SI
Q9Z148	Histone-lysine N-methyltransferase EHMT2	84	SI
Q63ZW7	InaD-like protein	41	SI
Q8CIM8	Integrator complex subunit 4	86	SI
A2ARA8	Integrin alpha-8	46	SI
Q80U22	Iporin	131	SI
Q69ZK5	Kelch-like protein 14	91	SI
Q9D312	Keratin_ type I cytoskeletal 20	60	SI
L0N7N1	Kinesin-like protein KIF14	105	SI
Q99PW8	Kinesin-like protein KIF17	51	SI
Q80WE4	Kinesin-like protein KIF20B	49	SI
E9Q5G3	Kinesin-like protein KIF23	47	SI
Q9D3W5	Leucine-rich repeat-containing protein 71	122	SI
Q8CBY3	Leukocyte receptor cluster member 8 homolog	69	SI
Q148V7	LisH domain and HEAT repeat-containing protein KIAA1468	103	SI
Q61790	Lymphocyte activation gene 3 protein	90	SI
Q8CDB0	MAP kinase-interacting serine/threonine-protein kinase 2	147	SI
Q8VCD5	Mediator of RNA polymerase II transcription	68	SI

	subunit 17		
O35954	Membrane-associated phosphatidylinositol transfer protein 1	86	SI
Q3TPJ7	Midnolin	89	SI
Q99MT2	MutS protein homolog 4	76	SI
Q80YT7	Myomegalin	78	SI
Q3UIZ8	Myosin light chain kinase 3	138	SI
Q91XS1	Myotubularin-related protein 4	153	SI
Q8R4E4	Myozenin-3	277	SI
Q66X22	NACHT_LRR and PYD domains-containing protein 9B	120	SI
Q99LC3	NADH dehydrogenase [ubiquinone] 1 alpha subcomplex subunit 10_mitochondrial	149	SI
Q91YT0	NADH dehydrogenase [ubiquinone] flavoprotein 1_ mitochondrial	76	SI
Q91WD5	NADH dehydrogenase [ubiquinone] iron-sulfur protein 2_ mitochondrial	89	SI
E9Q7X7	Neurexin II	64	SI
Q6ZQ12	Ninein-like protein	58	SI
Q69ZF3	Non-lysosomal glucosylceramidase	66	SI
Q99ML2	Non-receptor tyrosine-protein kinase TNK1	50	SI
Q9WU42	Nuclear receptor corepressor 2	25	SI
P41593	Parathyroid hormone/parathyroid hormone-related peptide receptor	65	SI
Q8CEE6	PAS domain-containing serine/threonine-protein kinase	63	SI
P15331	Peripherin	83	SI
Q78Y63	Phosducin-like protein 2	95	SI
Q9DBJ1	Phosphoglycerate mutase 1	30	SI
Q3UH93	Plexin-D1	149	SI
Q62083	PRKCA-binding protein	81	SI
P54823	Probable ATP-dependent RNA helicase DDX6	67	SI
Q8CDU6	Probable E3 ubiquitin-protein ligase HECTD2	359	SI
Q8VDC0	Probable leucine--tRNA ligase_ mitochondrial	93	SI
Q9QUM9	Proteasome subunit alpha type-6	86	SI
O70279	Protein DGCR14	68	SI
Q9D4K5	Protein FAM166A	58	SI
Q2VWQ2	Protein kinase C-binding protein NELL1	117	SI
B1AUR6	Protein MMS22-like	162	SI
Q8K2C7	Protein OS-9	76	SI
P97352	Protein S100-A13	135	SI
Q80TF3	Protocadherin-19	48	SI
Q60695	Ral guanine nucleotide dissociation stimulator-like 1	65	SI
Q91YQ1	Ras-related protein Rab-7L1	92	SI
A2AQ19	RNA polymerase-associated protein RTF1 homolog	64	SI
Q60806	Serine/threonine-protein kinase PLK3	77	SI

Q8BKX6	Serine/threonine-protein kinase SMG1	100	SI
Q9Z2E3	Serine/threonine-protein kinase/endoribonuclease IRE2	64	SI
Q9JID9	SH2B adapter protein 2	218	SI
Q8BJA2	Solute carrier family 41 member 1	134	SI
Q3UTJ2	Sorbin and SH3 domain-containing protein 2	136	SI
Q8BI29	Specifically androgen-regulated gene protein	170	SI
Q7TME2	Sperm-associated antigen 5	51	SI
Q5U4C3	Splicing factor_ arginine/serine-rich 19	208	SI
Q9QWI6	SRC kinase signaling inhibitor 1	41	SI
Q91YE8	Synaptopodin-2	152	SI
P70327	T-box transcription factor TBX6	72	SI
A3KMP2	Tetratricopeptide repeat protein 38	69	SI
Q715T0	Thioredoxin domain-containing protein 3	136	SI
Q8K424	Transient receptor potential cation channel subfamily V member 3	59	SI
Q8BGN6	Transmembrane gamma-carboxyglutamic acid protein 4	124	SI
Q922K9	Tyrosine-protein kinase FRK	61	SI
Q9D0L4	Uncharacterized aarF domain-containing protein kinase 1	86	SI
Q3TEI4	Uncharacterized protein C15orf39 homolog	120	SI
Q3TLD5	Unconventional prefoldin RPB5 interactor	81	SI
Q91ZJ5	UTP--glucose-1-phosphate uridylyltransferase	73	SI
Q5KU39	Vacuolar protein sorting-associated protein 41 homolog	49	SI
P29533	Vascular cell adhesion protein 1	84	SI
Q8VDJ3	Vigilin	383	SI
Q60932	Voltage-dependent anion-selective channel protein 1	291	SI
Q3U5F4	YrdC domain-containing protein_ mitochondrial	103	SI
Q5F293	Zinc finger and BTB domain-containing protein 4	71	SI
Q9JJN2	Zinc finger homeobox protein 4	199	SI
Q9JLM4	Zinc finger MYM-type protein 3	76	SI
Q8CJ19	[F-actin]-methionine sulfoxide oxidase MICAL3	80	RI
Q8K4S1	1-phosphatidylinositol 4_5-bisphosphate phosphodiesterase epsilon-1	225	RI
Q9EQC1	3 beta-hydroxysteroid dehydrogenase type 7	491	RI
P97819	85/88 kDa calcium-independent phospholipase A2	373	RI
Q8QZT1	Acetyl-CoA acetyltransferase_ mitochondrial	146	RI
Q80WC9	Acyl-CoA synthetase family member 4	55	RI
P48962	ADP/ATP translocase 1	48	RI

P51881	ADP/ATP translocase 2	48	RI
Q3V132	ADP/ATP translocase 4	50	RI
P07758	Alpha-1-antitrypsin 1-1	132	RI
P22599	Alpha-1-antitrypsin 1-2	132	RI
Q00896	Alpha-1-antitrypsin 1-3	132	RI
Q00897	Alpha-1-antitrypsin 1-4	132	RI
Q9QYC0	Alpha-adducin	130	RI
Q8CFA2	Aminomethyltransferase_ mitochondrial	140	RI
Q80VM7	Ankyrin repeat domain-containing protein 24	250	RI
Q3UMR0	Ankyrin repeat domain-containing protein 27	212	RI
Q8C8R3	Ankyrin-2	131	RI
P14824	Annexin A6	111	RI
Q9JKC8	AP-3 complex subunit mu-1	76	RI
Q80V94	AP-4 complex subunit epsilon-1	38	RI
Q5YD48	APOBEC1 complementation factor	92	RI
Q9Z2A5	Arginyl-tRNA--protein transferase 1	113	RI
Q8R4I1	Ataxin-7	99	RI
Q9CQQ7	ATP synthase F(0) complex subunit B1_ mitochondrial	193	RI
Q8VDW0	ATP-dependent RNA helicase DDX39A	161	RI
Q60936	Atypical kinase COQ8A_ mitochondrial	211	RI
P52963	Band 4.1-like protein 4A	100	RI
P48754	Breast cancer type 1 susceptibility protein homolog	160	RI
Q9WV35	C->U-editing enzyme APOBEC-2	386	RI
Q9WTR5	Cadherin-13	77	RI
Q6Q473	Calcium-activated chloride channel regulator 4A	84	RI
Q9D6P8	Calmodulin-like protein 3	117	RI
Q3UKK2	Carcinoembryonic antigen-related cell adhesion molecule 5	54	RI
Q61301	Catenin alpha-2	67	RI
O54724	Caveolae-associated protein 1	127	RI
Q14B71	Cell division cycle-associated protein 2	464	RI
Q6P8Y0	Cilia- and flagella-associated protein 161	101	RI
Q9CZU6	Citrate synthase_ mitochondrial	121	RI
P49025	Citron Rho-interacting kinase	510	RI
Q68FD5	Clathrin heavy chain 1	91	RI
O35218	Cleavage and polyadenylation specificity factor subunit 2	81	RI
Q640L5	Coiled-coil domain-containing protein 18	63	RI
Q6NS45	Coiled-coil domain-containing protein 66	107	RI
Q504P2	C-type lectin domain family 12 member A	115	RI
Q99KY4	Cyclin-G-associated kinase	199	RI
P12787	Cytochrome c oxidase subunit 5A_ mitochondrial	539	RI
P62897	Cytochrome c_somatic	412	RI

Q570Y9	DEP domain-containing mTOR-interacting protein	133	RI
Q8CDG3	Deubiquitinating protein VCIP135	57	RI
P70175	Disks large homolog 3	122	RI
Q8R4E9	DNA replication factor Cdt1	132	RI
Q99LC5	Electron transfer flavoprotein subunit alpha_ mitochondrial	122	RI
P58252	Elongation factor 2	125	RI
Q8K203	Endonuclease 8-like 3	161	RI
P42567	Epidermal growth factor receptor substrate 15	58	RI
Q8C7X2	ER membrane protein complex subunit 1	77	RI
P47753	F-actin-capping protein subunit alpha-1	90	RI
P47754	F-actin-capping protein subunit alpha-2	289	RI
P50608	Fibromodulin	68	RI
Q80TD3	Folliculin-interacting protein 2	39	RI
Q99JB6	Forkhead box protein P3	70	RI
Q8VDC1	FYVE and coiled-coil domain-containing protein 1	72	RI
Q60928	Gamma-glutamyltranspeptidase 1	219	RI
Q9ESZ8	General transcription factor II-I	141	RI
Q99NI3	General transcription factor II-I repeat domain-containing protein 2	182	RI
Q9CQI3	Glia maturation factor beta	283	RI
Q64467	Glyceraldehyde-3-phosphate dehydrogenase_ testis-specific	108	RI
Q8BKV1	Glypican-2	69	RI
Q60780	Growth arrest-specific protein 7	110	RI
Q60779	Growth arrest-specific protein 8	52	RI
P11499	Heat shock protein HSP 90-beta	105	RI
Q99NG0	Helicase ARIP4	77	RI
A2AJ76	Hemicentin-2	204	RI
Q8BRB7	Histone acetyltransferase KAT6B	193	RI
P97443	Histone-lysine N-methyltransferase Smyd1	79	RI
Q9WUI0	Homeobox protein MIXL1	152	RI
P01586	Interleukin-3	140	RI
P54071	Isocitrate dehydrogenase [NADP]_ mitochondrial O	166	RI
Q497I4	Keratin_ type I cuticular Ha5	139	RI
Q61595	Kinectin	135	RI
Q9QXL1	Kinesin-like protein KIF21B	77	RI
O89112	LanC-like protein 1	101	RI
Q8CGA3	Large neutral amino acids transporter small subunit 4	92	RI
Q8C129	Leucyl-cystinyl aminopeptidase	88	RI
Q9DBN5	Lon protease homolog 2_peroxisomal	80	RI
P34884	Macrophage migration inhibitory factor	163	RI
Q9WV34	MAGUK p55 subfamily member 2	165	RI

Q924M7	Mannose-6-phosphate isomerase	111	RI
Q9JI70	McKusick-Kaufman/Bardet-Biedl syndromes putative chaperonin	99	RI
Q5F2C3	Meiosis-specific kinetochore protein	87	RI
B1AYB6	Methyl-CpG-binding domain protein 5	114	RI
Q9DCS2	Methyltransferase-like 26	319	RI
Q8CAQ8	MICOS complex subunit Mic60	244	RI
Q8C052	Microtubule-associated protein 1S	82	RI
Q9WTX8	Mitotic spindle assembly checkpoint protein MAD1	51	RI
P30306	M-phase inducer phosphatase 2	109	RI
P23949	mRNA decay activator protein ZFP36L2	65	RI
O08539	Myc box-dependent-interacting protein 1	200	RI
Q3UIJ9	Myocardial zonula adherens protein	48	RI
Q8CI43	Myosin light chain 6B	175	RI
P70402	Myosin-binding protein H	207	RI
Q923E4	NAD-dependent protein deacetylase sirtuin-1	170	RI
Q8BMT4	Negative regulator of reactive oxygen species	382	RI
P70232	Neural cell adhesion molecule L1-like protein	174	RI
Q99PJ0	Neurotrimin	122	RI
P70255	Nuclear factor 1 C-type	196	RI
P25799	Nuclear factor NF-kappa-B p105 subunit	172	RI
Q99MH5	Nucleoside diphosphate kinase homolog 5	235	RI
O70209	PDZ and LIM domain protein 3	103	RI
P17742	Peptidyl-prolyl cis-trans isomerase A	501	RI
P30416	Peptidyl-prolyl cis-trans isomerase FKBP4	75	RI
P48725	Pericentrin	138	RI
Q62009	Periostin	90	RI
P16331	Phenylalanine-4-hydroxylase	131	RI
Q69ZK0	Phosphatidylinositol 3_4_5-trisphosphate-dependent Rac exchanger 1 protein	44	RI
Q61194	Phosphatidylinositol 4-phosphate 3-kinase C2 domain-containing subunit alpha	49	RI
P70181	Phosphatidylinositol 4-phosphate 5-kinase type-1 beta	64	RI
Q9Z280	Phospholipase D1	151	RI
B2RPU2	Pleckstrin homology domain-containing family D member 1	87	RI
P01193	Pro-opiomelanocortin	84	RI
Q8C569	Protein FAM118B	197	RI
Q148A4	Protein phosphatase 1 regulatory subunit 32	156	RI
Q9Z1N9	Protein unc-13 homolog B	87	RI
O55134	Protocadherin-12	196	RI
Q7TSK3	Protocadherin-8	68	RI
P06240	Proto-oncogene tyrosine-protein kinase LCK	1024	RI
Q8BRM2	RAB6-interacting golgin	184	RI
P59729	Ras and Rab interactor 3	129	RI

Q8CGE9	Regulator of G-protein signaling 12	59	RI
Q9DC04	Regulator of G-protein signaling 3	91	RI
P00796	Renin-2	110	RI
Q811M1	Rho GTPase-activating protein 15	83	RI
Q9CWR0	Rho guanine nucleotide exchange factor 25	129	RI
O35130	Ribosomal RNA small subunit methyltransferase NEP1	228	RI
Q4VGL6	Roquin-1	143	RI
E9PZQ0	Ryanodine receptor 1	131	RI
Q60988	SCL-interrupting locus protein homolog	104	RI
Q64105	Sepiapterin reductase	148	RI
Q9JIY5	Serine protease HTRA2_ mitochondrial	191	RI
Q7TSI3	Serine/threonine-protein phosphatase 6 regulatory subunit 1	141	RI
Q8BTK5	SET and MYND domain-containing protein 4	64	RI
Q4ACU6	SH3 and multiple ankyrin repeat domains protein 3	163	RI
P98083	SHC-transforming protein 1	71	RI
Q8VDU5	SNF-related serine/threonine-protein kinase	57	RI
Q9D2S4	Sperm acrosome-associated protein 7	218	RI
Q80ZX8	Sperm-associated antigen 1	93	RI
Q9Z1N5	Spliceosome RNA helicase Ddx39b	81	RI
P97496	SWI/SNF complex subunit SMARCC1	96	RI
Q8BWB1	Synaptopodin 2-like protein	170	RI
Q8K1E0	Syntaxin-5	496	RI
P26039	Talin-1	147	RI
Q8CGA2	TBC1 domain family member 14	168	RI
Q6X6Z7	Tektin-3	78	RI
O70548	Telethonin	132	RI
Q9JMH6	Thioredoxin reductase 1_ cytoplasmic	114	RI
Q9JLT4	Thioredoxin reductase 2_ mitochondrial	234	RI
P63058	Thyroid hormone receptor alpha	137	RI
Q60610	T-lymphoma invasion and metastasis-inducing protein 1	57	RI
Q8BHE4	Transmembrane protein 108	70	RI
O70472	Transmembrane protein 131	134	RI
Q64514	Tripeptidyl-peptidase 2	96	RI
Q9WUZ5	Troponin I_ slow skeletal muscle	233	RI
Q9ERD7	Tubulin beta-3 chain	228	RI
Q922F4	Tubulin beta-6 chain	157	RI
A4Q9F4	Tubulin polyglutamylase TTLL11	103	RI
Q8BX43	Tumor necrosis factor receptor superfamily member 19L	147	RI
Q9Z315	U4/U6.U5 tri-snRNP-associated protein 1	79	RI
P56399	Ubiquitin carboxyl-terminal hydrolase 5	119	RI
Q8CB27	Ubiquitin thioesterase OTU1	137	RI
P68037	Ubiquitin-conjugating enzyme E2 L3	79	RI

Q3UTZ3	Uncharacterized protein C7orf43 homolog	87	RI
A9Z1V5	von Willebrand factor A domain-containing protein 5B1	171	RI
Q6PDJ1	VWFA and cache domain-containing protein 1	53	RI
Q80VW5	Whirlin	184	RI
Q6NZF1	Zinc finger CCCH domain-containing protein 11A	107	RI
Q8BYK8	Zinc finger CCCH domain-containing protein 6	114	RI
Q9R0G7	Zinc finger E-box-binding homeobox 2	178	RI
Q8JZL0	Zinc finger protein 467	222	RI
Q8K083	Zinc finger protein 536	412	RI

[a]Identification is based on proteins ID from UniProt protein database, reviewed only (http://www.uniprot.org/).
[b]Proteins with expression significantly altered are organized according to the ratio.
*Indicates unique proteins in alphabetical order.

S5. Proteins with expression significantly altered in the gastrocnemius of SII (A/J, water containing 50 ppm F, no-exercise) and RII (129P3/J, water containing 50 ppm F, no-exercise) mice.

[a]**Acession number**	**Protein name**	**PLGS Score**	[b]***Ratio* SII:RII**
P32848	Parvalbumin alpha	1413	18.36
Q64467	Glyceraldehyde-3-phosphate dehydrogenase testis-specific	204	6.82
Q91VW5	Golgin subfamily A member 4	84	4.06
P21107	Tropomyosin alpha-3 chain	148	3.82
P11404	Fatty acid-binding protein_ heart	393	3.42
Q04690	Neurofibromin	60	2.61
P51881	ADP/ATP translocase 2	217	2.51
O09165	Calsequestrin-1	1611	2.51
P62897	Cytochrome c_ somatic	145	2.46
P48962	ADP/ATP translocase 1	257	2.39
A2AQP0	Myosin-7B	1485	2.34
P13412	Troponin I_ fast skeletal muscle	2483	2.32
Q3V1D3	AMP deaminase 1	175	2.18
P57780	Alpha-actinin-4	172	2.05
P02104	Hemoglobin subunit epsilon-Y2	2086	2.05
Q9QXS1	Plectin	28	1.92
P02089	Hemoglobin subunit beta-2	2086	1.90
P52480	Pyruvate kinase PKM	5611	1.88
O55143	Sarcoplasmic/endoplasmic reticulum calcium ATPase 2	205	1.82
P12382	ATP-dependent 6-phosphofructokinase_liver type	68	1.77
O70250	Phosphoglycerate mutase 2	1811	1.77

P02088	Hemoglobin subunit beta-1	2777	1.73
Q9R0Y5	Adenylate kinase isoenzyme 1	7048	1.68
Q7TQ48	Sarcalumenin	60	1.68
P0DP28	Calmodulin-3	315	1.67
Q9JI91	Alpha-actinin-2	377	1.65
P0DP26	Calmodulin-1	315	1.65
P17751	Triosephosphate isomerase	4428	1.65
Q7TPR4	Alpha-actinin-1	215	1.63
P0DP27	Calmodulin-2	315	1.62
Q3TJD7	PDZ and LIM domain protein 7	950	1.62
P08249	Malate dehydrogenase_ mitochondrial	756	1.60
A2AL36	Centriolin	88	1.57
P16858	Glyceraldehyde-3-phosphate dehydrogenase	19243	1.57
P07310	Creatine kinase M-type	17477	1.52
Q8R429	Sarcoplasmic/endoplasmic reticulum calcium ATPase 1	753	1.52
P05201	Aspartate aminotransferase_ cytoplasmic	393	1.49
P17183	Gamma-enolase	799	1.49
Q9CR68	Cytochrome b-c1 complex subunit Rieske_ mitochondrial	86	1.48
Q5SSE9	ATP-binding cassette sub-family A member 13	128	1.46
P14152	Malate dehydrogenase_ cytoplasmic	150	1.46
Q99LX0	Protein DJ-1	956	1.45
P12787	Cytochrome c oxidase subunit 5A_ mitochondrial	1033	1.43
P10126	Elongation factor 1-alpha 1	82	1.43
P06151	L-lactate dehydrogenase A chain	2878	1.43
P47857	ATP-dependent 6-phosphofructokinase_muscle type	444	1.39
P31001	Desmin	185	1.39
O88990	Alpha-actinin-3	1519	1.38
Q9D0F9	Phosphoglucomutase-1	153	1.38
P07724	Serum albumin	345	1.36
P60710	Actin_ cytoplasmic 1	94968	1.35
P63260	Actin_ cytoplasmic 2	94968	1.35
P04247	Myoglobin	434	1.35
Q01768	Nucleoside diphosphate kinase B	141	1.35
P13542	Myosin-8	10380	1.34
P15532	Nucleoside diphosphate kinase A	141	1.34
P58771	Tropomyosin alpha-1 chain	12103	1.34
Q5SX40	Myosin-1	13724	1.32
Q99KI0	Aconitate hydratase_ mitochondrial	145	1.31
Q5XKE0	Myosin-binding protein C_ fast-type	1808	1.31
P53657	Pyruvate kinase PKLR	698	1.31
P05202	Aspartate aminotransferase_ mitochondrial	117	1.30
P63017	Heat shock cognate 71 kDa protein	117	1.30

Q62234	Myomesin-1	143	1.30
P13541	Myosin-3	4303	1.30
P09411	Phosphoglycerate kinase 1	1372	1.30
P09041	Phosphoglycerate kinase 2	992	1.30
Q03265	ATP synthase subunit alpha_ mitochondrial	549	1.28
P62737	Actin_ aortic smooth muscle	110654	1.26
P63268	Actin_ gamma-enteric smooth muscle	110480	1.26
P56480	ATP synthase subunit beta_ mitochondrial	791	1.26
P16125	L-lactate dehydrogenase B chain	225	1.26
P00342	L-lactate dehydrogenase C chain	1353	1.26
P97457	Myosin regulatory light chain 2_ skeletal muscle isoform	13666	1.26
P68033	Actin_ alpha cardiac muscle 1	117501	1.25
P68134	Actin_ alpha skeletal muscle	121903	1.25
P17156	Heat shock-related 70 kDa protein 2	98	1.25
P05064	Fructose-bisphosphate aldolase A	17992	1.23
Q91Z83	Myosin-7	7181	1.23
P21550	Beta-enolase	6260	1.22
Q02566	Myosin-6	5961	1.22
P16015	Carbonic anhydrase 3	2304	1.21
P09542	Myosin light chain 3	3753	1.21
P20801	Troponin C_ skeletal muscle	677	1.21
P58774	Tropomyosin beta chain	6894	1.20
Q61879	Myosin-10	166	1.17
O08638	Myosin-11	165	1.16
P62631	Elongation factor 1-alpha 2	208	1.15
Q9JKS4	LIM domain-binding protein 3	690	1.15
Q60605	Myosin light polypeptide 6	1250	1.15
Q8VDD5	Myosin-9	165	1.14
P17182	Alpha-enolase	3491	1.13
Q8BFZ3	Beta-actin-like protein 2	19443	1.13
Q6URW6	Myosin-14	279	1.13
Q9QZ47	Troponin T_ fast skeletal muscle	1994	1.12
P05977	Myosin light chain 1/3_ skeletal muscle isoform	24671	1.11
P09541	Myosin light chain 4	4125	1.11
Q5SX39	Myosin-4	19719	1.11
Q9WUB3	Glycogen phosphorylase_ muscle form	5410	1.05
P05063	Fructose-bisphosphate aldolase C	2425	0.87
P42128	Forkhead box protein K1	112	0.61
Q8CHI8	E1A-binding protein p400	77	0.34
Q3UH93	Plexin-D1	206	0.19
Q7TMW6	Cytosolic Fe-S cluster assembly factor NARFL	147	0.15
Q810T2	G2/mitotic-specific cyclin-B3	61	0.12
P70327	T-box transcription factor TBX6	59	0.12
Q4KUS2	Protein unc-13 homolog A	193	0.11

O08810	116 kDa U5 small nuclear ribonucleoprotein component	394	SII*
P62259	14-3-3 protein epsilon	107	SII
Q8VCR2	17-beta-hydroxysteroid dehydrogenase 13	124	SII
P20029	78 kDa glucose-regulated protein	171	SII
P54822	Adenylosuccinate lyase	90	SII
G3X982	Aldehyde oxidase 3	32	SII
P53995	Anaphase-promoting complex subunit 1	68	SII
Q8BZQ7	Anaphase-promoting complex subunit 2	63	SII
Q9D4H4	Angiomotin-like protein 1	50	SII
Q9WVH6	Angiopoietin-4	154	SII
Q99NH0	Ankyrin repeat domain-containing protein 17	94	SII
O88879	Apoptotic protease-activating factor 1	69	SII
A2RTL5	Arginine/serine-rich coiled-coil protein 2	344	SII
Q8BIP0	Aspartate--tRNA ligase_ mitochondrial	41	SII
Q4QY64	ATPase family AAA domain-containing protein 5	30	SII
Q9DC29	ATP-binding cassette sub-family B member 6_ mitochondrial	69	SII
Q9WUA3	ATP-dependent 6-phosphofructokinase_ platelet type	33	SII
O88738	Baculoviral IAP repeat-containing protein 6	80	SII
P21855	B-cell differentiation antigen CD72	68	SII
P41183	B-cell lymphoma 6 protein homolog	80	SII
Q6PAL0	BEN domain-containing protein 3	33	SII
Q8BWG8	Beta-arrestin-1	526	SII
Q9WV35	C->U-editing enzyme APOBEC-2	578	SII
B9EHT4	CAP-Gly domain-containing linker protein 3	265	SII
A2A6Q5	Cell division cycle protein 27 homolog	61	SII
Q6RT24	Centromere-associated protein E	95	SII
D2J0Y4	Centrosomal protein C10orf90 homolog	230	SII
Q80TV8	CLIP-associating protein 1	51	SII
E9Q1U1	Coiled-coil domain-containing protein 171	57	SII
Q6PHN1	Coiled-coil domain-containing protein 57	60	SII
Q6NS45	Coiled-coil domain-containing protein 66	66	SII
Q04447	Creatine kinase B-type	70	SII
P30275	Creatine kinase U-type_ mitochondrial	180	SII
Q9DB77	Cytochrome b-c1 complex subunit 2_ mitochondrial	135	SII
Q91YE9	Cytosolic 5'-nucleotidase 1B	88	SII
Q09M02	Cytosolic carboxypeptidase-like protein 5	142	SII
Q8BIK4	Dedicator of cytokinesis protein 9	51	SII
A6H8H2	DENN domain-containing protein 4C	29	SII
Q7TMD7	Desmoglein-4	58	SII
O08749	Dihydrolipoyl dehydrogenase_ mitochondrial	39	SII
Q8BMF4	Dihydrolipoyllysine-residue acetyltransferase component of pyruvate dehydrogenase complex_ mitochondrial	115	SII
Q9DBT9	Dimethylglycine dehydrogenase_	65	SII

	mitochondrial		
Q811D0	Disks large homolog 1	107	SII
Q91XM9	Disks large homolog 2	50	SII
Q9JMC3	DnaJ homolog subfamily A member 4	166	SII
O70469	Docking protein 2	75	SII
Q4U2R1	E3 ubiquitin-protein ligase HERC2	277	SII
Q8C669	E3 ubiquitin-protein ligase pellino homolog 1	57	SII
A2AN08	E3 ubiquitin-protein ligase UBR4	72	SII
Q9DCW4	Electron transfer flavoprotein subunit beta	151	SII
Q99MI1	ELKS/Rab6-interacting/CAST family member 1	49	SII
P58252	Elongation factor 2	430	SII
Q8C0D5	Elongation factor-like GTPase 1	97	SII
Q9ERK4	Exportin-2	86	SII
Q3TR08	Fibronectin type III domain-containing protein 4	119	SII
Q8VHX6	Filamin-C	40	SII
P58462	Forkhead box protein P1	155	SII
Q99JB6	Forkhead box protein P3	100	SII
Q8VDC1	FYVE and coiled-coil domain-containing protein 1	46	SII
O88741	Ganglioside-induced differentiation-associated protein 1	96	SII
Q9Z1Z0	General vesicular transport factor p115	46	SII
Q5SNZ0	Girdin	86	SII
P19157	Glutathione S-transferase P 1	114	SII
P46425	Glutathione S-transferase P 2	95	SII
P13707	Glycerol-3-phosphate dehydrogenase [NAD(+)]_ cytoplasmic	73	SII
P36916	Guanine nucleotide-binding protein-like 1	78	SII
O54865	Guanylate cyclase soluble subunit beta-1	74	SII
Q5PRF0	HEAT repeat-containing protein 5A	106	SII
P11499	Heat shock protein HSP 90-beta	47	SII
P59438	Hermansky-Pudlak syndrome 5 protein homolog	107	SII
P70696	Histone H2B type 1-A	1016	SII
Q64475	Histone H2B type 1-B	1132	SII
Q6ZWY9	Histone H2B type 1-C/E/G	1132	SII
P10853	Histone H2B type 1-F/J/L	1132	SII
Q64478	Histone H2B type 1-H	1132	SII
Q8CGP1	Histone H2B type 1-K	1132	SII
P10854	Histone H2B type 1-M	1132	SII
Q8CGP2	Histone H2B type 1-P	1132	SII
Q64525	Histone H2B type 2-B	1132	SII
Q64524	Histone H2B type 2-E	1132	SII
Q9D2U9	Histone H2B type 3-A	1132	SII
Q8CGP0	Histone H2B type 3-B	1132	SII
P97443	Histone-lysine N-methyltransferase Smyd1	66	SII
O08934	Homeobox protein unc-4 homolog	120	SII

O35344	Importin subunit alpha-4	58	SII
Q3USB7	Inactive phospholipase C-like protein 1	412	SII
O88351	Inhibitor of nuclear factor kappa-B kinase subunit beta	406	SII
Q9Z1X4	Interleukin enhancer-binding factor 3	110	SII
Q9D6R2	Isocitrate dehydrogenase [NAD] subunit alpha_ mitochondrial	71	SII
O54983	Ketimine reductase mu-crystallin	207	SII
P28738	Kinesin heavy chain isoform 5C	120	SII
O88447	Kinesin light chain 1	74	SII
L0N7N1	Kinesin-like protein KIF14	139	SII
Q60575	Kinesin-like protein KIF1B	29	SII
B1B1A0	Lethal(3)malignant brain tumor-like protein 4	85	SII
P60469	Liprin-alpha-3	44	SII
Q8C8U0	Liprin-beta-1	99	SII
Q61790	Lymphocyte activation gene 3 protein	101	SII
Q924M7	Mannose-6-phosphate isomerase	130	SII
Q3U435	Matrix metalloproteinase-25	89	SII
Q5HZI1	Microtubule-associated tumor suppressor 1 homolog	27	SII
Q9CW42	Mitochondrial amidoxime-reducing component 1	122	SII
Q9CXT8	Mitochondrial-processing peptidase subunit beta	145	SII
Q920G8	Mitoferrin-1	77	SII
P97820	Mitogen-activated protein kinase kinase kinase kinase 4	115	SII
Q8VCM2	NADPH oxidase organizer 1	145	SII
Q61043	Ninein	47	SII
Q6PIJ4	Nuclear factor related to kappa-B-binding protein	72	SII
Q99MH5	Nucleoside diphosphate kinase homolog 5	253	SII
Q9D478	Outer dense fiber protein 2-like	85	SII
P17742	Peptidyl-prolyl cis-trans isomerase A	263	SII
Q62009	Periostin	45	SII
P15331	Peripherin	45	SII
P35700	Peroxiredoxin-1	112	SII
A6H619	PHD and RING finger domain-containing protein 1	63	SII
Q8VEM8	Phosphate carrier protein_ mitochondrial	298	SII
P70296	Phosphatidylethanolamine-binding protein 1	131	SII
O70167	Phosphatidylinositol 4-phosphate 3-kinase C2 domain-containing subunit gamma	180	SII
Q9DBJ1	Phosphoglycerate mutase 1	150	SII
Q08481	Platelet endothelial cell adhesion molecule	143	SII
Q80UG2	Plexin-A4	41	SII
Q64028	Polyhomeotic-like protein 1	68	SII
Q3TVI8	Pre-B-cell leukemia transcription factor-interacting protein 1	89	SII

Q8C8T8	Pre-rRNA-processing protein TSR2 homolog	91	SII
Q62083	PRKCA-binding protein	115	SII
P54823	Probable ATP-dependent RNA helicase DDX6	90	SII
P57774	Pro-neuropeptide Y	135	SII
O70374	Protein CBFA2T2	50	SII
Q9DAF3	Protein DDI1 homolog 1	42	SII
Q9D0F3	Protein ERGIC-53	87	SII
Q80TL7	Protein MON2 homolog	41	SII
O88286	Protein Wiz	177	SII
Q8BQP8	Rab11 family-interacting protein 4	81	SII
Q62172	RalA-binding protein 1	85	SII
Q64487	Receptor-type tyrosine-protein phosphatase delta	140	SII
Q8CGE9	Regulator of G-protein signaling 12	162	SII
Q3UIA2	Rho GTPase-activating protein 17	55	SII
P61588	Rho-related GTP-binding protein RhoE	214	SII
Q64518	Sarcoplasmic/endoplasmic reticulum calcium ATPase 3	52	SII
Q60988	SCL-interrupting locus protein homolog	160	SII
Q3V129	Serine/threonine-protein kinase ULK4	54	SII
Q9EQY0	Serine/threonine-protein kinase/endoribonuclease IRE1	143	SII
Q6PD03	Serine/threonine-protein phosphatase 2A 56 kDa regulatory subunit alpha isoform	161	SII
Q9CQR6	Serine/threonine-protein phosphatase 6 catalytic subunit	73	SII
Q8CIE0	Serpin A11	167	SII
Q923I7	Sodium/glucose cotransporter 2	110	SII
Q9Z0E8	Solute carrier family 22 member 5	69	SII
Q91WM1	Spermatid perinuclear RNA-binding protein	41	SII
Q80TF6	StAR-related lipid transfer protein 9	53	SII
Q8VIM6	Stereocilin	403	SII
P08228	Superoxide dismutase [Cu-Zn]	206	SII
Q8K4L3	Supervillin	159	SII
Q8CHC4	Synaptojanin-1	92	SII
Q91YE8	Synaptopodin-2	97	SII
Q8R1Q0	Syntaxin-19	274	SII
Q9D6E4	Tetratricopeptide repeat protein 9B	385	SII
Q3U0M1	Trafficking protein particle complex subunit 9	68	SII
Q924A0	Transcription factor 7-like 2	80	SII
Q8BRH0	Transmembrane and TPR repeat-containing protein 3	114	SII
Q9ERP3	Tripartite motif-containing protein 54	66	SII
P05214	Tubulin alpha-3 chain	195	SII
P68368	Tubulin alpha-4A chain	195	SII
Q9JJZ2	Tubulin alpha-8 chain	195	SII
Q7TMM9	Tubulin beta-2A chain	548	SII
Q9CWF2	Tubulin beta-2B chain	539	SII
P99024	Tubulin beta-5 chain	542	SII

Q922F4	Tubulin beta-6 chain	57	SII
Q9R1K7	Tubulin delta chain	127	SII
Q61333	Tumor necrosis factor alpha-induced protein 2	188	SII
P48025	Tyrosine-protein kinase SYK	97	SII
Q80WC1	Ubinuclein-2	59	SII
Q9CWU6	Ubiquinol-cytochrome-c reductase complex assembly factor 1	422	SII
Q9ES63	Ubiquitin carboxyl-terminal hydrolase 29	87	SII
Q6P5E4	UDP-glucose:glycoprotein glucosyltransferase 1	292	SII
Q9DAD0	Uncharacterized protein C1orf194 homolog	111	SII
Q99104	Unconventional myosin-Va	66	SII
Q3TLD5	Unconventional prefoldin RPB5 interactor	115	SII
P51163	Uroporphyrinogen-III synthase	161	SII
Q91ZJ5	UTP--glucose-1-phosphate uridylyltransferase	116	SII
P59016	Vacuolar protein sorting-associated protein 33B	119	SII
P29533	Vascular cell adhesion protein 1	62	SII
P20152	Vimentin	119	SII
Q60932	Voltage-dependent anion-selective channel protein 1	155	SII
Q99KC8	von Willebrand factor A domain-containing protein 5A	60	SII
Q5RJ54	Zinc finger and SCAN domain-containing protein 26	104	SII
Q6NS86	Zinc finger protein 366	53	SII
Q69Z99	Zinc finger protein 512	70	SII
Q8BGK2	[Protein ADP-ribosylarginine] hydrolase-like protein 1	280	RII
E9Q9A9	2'-5'-oligoadenylate synthase 2	85	RII
Q8QZS1	3-hydroxyisobutyryl-CoA hydrolase_ mitochondrial	115	RII
Q32Q92	Acyl-coenzyme A thioesterase 6	51	RII
B7ZCC9	Adhesion G-protein coupled receptor G4	84	RII
P61208	ADP-ribosylation factor-like protein 4C	222	RII
Q6P068	ADP-ribosylation factor-like protein 5C	69	RII
Q60604	Adseverin	51	RII
Q9QZQ1	Afadin	111	RII
P29699	Alpha-2-HS-glycoprotein	175	RII
Q8CFA2	Aminomethyltransferase_ mitochondrial	185	RII
Q9DBR4	Amyloid beta A4 precursor protein-binding family B member 2	227	RII
Q5F259	Ankyrin repeat domain-containing protein 13B	62	RII
Q80VM7	Ankyrin repeat domain-containing protein 24	214	RII
Q8BZW2	Ankyrin repeat domain-containing protein SOWAHB	75	RII
Q91YI0	Argininosuccinate lyase	90	RII
Q8K363	ATP-dependent RNA helicase DDX18	84	RII
Q6ZPL9	ATP-dependent RNA helicase DDX55	159	RII

Q80W49	Beta/gamma crystallin domain-containing protein 3	42	RII
O88428	Bifunctional 3'-phosphoadenosine 5'-phosphosulfate synthase 2	80	RII
B2RQC6	CAD protein	70	RII
Q8VHF2	Cadherin-related family member 5	107	RII
Q6Q473	Calcium-activated chloride channel regulator 4A	56	RII
A2AHC3	Calmodulin-regulated spectrin-associated protein 1	64	RII
Q0VEJ0	Centrosomal protein of 76 kDa	65	RII
Q03059	Choline O-acetyltransferase	41	RII
O35218	Cleavage and polyadenylation specificity factor subunit 2	69	RII
Q8CDI7	Coiled-coil domain-containing protein 150	45	RII
Q8CE13	Coiled-coil domain-containing protein 17	55	RII
Q80X19	Collagen alpha-1(XIV) chain	74	RII
P03953	Complement factor D	304	RII
Q9CWX2	Complex I intermediate-associated protein 30_ mitochondrial	59	RII
Q8BLF2	Cyclin-dependent kinase-like 3	360	RII
Q99KY4	Cyclin-G-associated kinase	166	RII
Q9Z1J3	Cysteine desulfurase_ mitochondrial	90	RII
Q9CZ13	Cytochrome b-c1 complex subunit 1_ mitochondrial	95	RII
Q8K3G9	DCC-interacting protein 13-beta	79	RII
Q8CDG3	Deubiquitinating protein VCIP135	77	RII
P97427	Dihydropyrimidinase-related protein 1	136	RII
Q9D8U7	DTW domain-containing protein 1	81	RII
Q3V0Q1	Dynein heavy chain 12_ axonemal	108	RII
Q8C863	E3 ubiquitin-protein ligase Itchy	67	RII
O88196	E3 ubiquitin-protein ligase TTC3	109	RII
P55772	Ectonucleoside triphosphate diphosphohydrolase 1	78	RII
Q6R2P8	Endonuclease 8-like 2	98	RII
Q9CR89	Endoplasmic reticulum-Golgi intermediate compartment protein 2 O	258	RII
Q5D1E7	Endoribonuclease ZC3H12A	80	RII
Q3TLP5	Enoyl-CoA hydratase domain-containing protein 2_ mitochondrial	550	RII
O35393	Ephrin-B3	149	RII
Q924P3	Epididymal-specific lipocalin-8	148	RII
Q80VP1	Epsin-1	107	RII
Q8C7X2	ER membrane protein complex subunit 1	101	RII
P47753	F-actin-capping protein subunit alpha-1	159	RII
P47757	F-actin-capping protein subunit beta	95	RII
P11276	Fibronectin	150	RII
Q91Y97	Fructose-bisphosphate aldolase B	78	RII
Q571F8	Glutaminase liver isoform_ mitochondrial	94	RII

Q8BKV1	Glypican-2	211	RII
Q8VEF1	GRAM domain-containing protein 1A	98	RII
Q80TI0	GRAM domain-containing protein 1B	113	RII
P48722	Heat shock 70 kDa protein 4L	75	RII
A2AJ76	Hemicentin-2	413	RII
P79457	Histone demethylase UTY	42	RII
Q80W88	Homeobox and leucine zipper protein Homez	125	RII
Q08890	Iduronate 2-sulfatase	158	RII
Q91VK4	Integral membrane protein 2C	108	RII
Q9WVP9	Interferon-induced GTP-binding protein Mx2	210	RII
Q80XH2	Interphotoreceptor matrix proteoglycan 2	71	RII
Q6VH22	Intraflagellar transport protein 172 homolog	53	RII
Q8BFQ9	Kelch-like protein 42	137	RII
Q3V300	Kinesin-like protein KIF22	118	RII
Q3TJ91	Lethal(2) giant larvae protein homolog 2	193	RII
P62046	Leucine-rich repeat and calponin homology domain-containing protein 1	56	RII
Q8C0R9	Leucine-rich repeat and death domain-containing protein 1	99	RII
Q6P1C6	Leucine-rich repeats and immunoglobulin-like domains protein 3	88	RII
Q5SUF2	Luc7-like protein 3	135	RII
P27782	Lymphoid enhancer-binding factor 1	156	RII
Q8CAQ8	MICOS complex subunit Mic60	106	RII
P70218	Mitogen-activated protein kinase kinase kinase kinase 1	78	RII
Q61006	Muscle_ skeletal receptor tyrosine-protein kinase	57	RII
Q6NZR2	Myb/SANT-like DNA-binding domain-containing protein 2	59	RII
P11247	Myeloperoxidase	308	RII
Q8CI43	Myosin light chain 6B	74	RII
Q61941	NAD(P) transhydrogenase_ mitochondrial	70	RII
Q91YT0	NADH dehydrogenase [ubiquinone] flavoprotein 1_ mitochondrial	220	RII
P21661	Neuroendocrine convertase 2	111	RII
P49117	Nuclear receptor subfamily 2 group C member 2	71	RII
Q8CH40	Nucleoside diphosphate-linked moiety X motif 6	90	RII
Q80UF9	Otopetrin-3	59	RII
A3KGV1	Outer dense fiber protein 2	101	RII
P41593	Parathyroid hormone/parathyroid hormone-related peptide receptor	66	RII
Q9EPL9	Peroxisomal acyl-coenzyme A oxidase 3	269	RII
Q5SPL2	PHD finger protein 12	375	RII
Q8BLG0	PHD finger protein 20	65	RII
P26262	Plasma kallikrein	50	RII
P70458	Plasma serine protease inhibitor	106	RII

Q8CDU6	Probable E3 ubiquitin-protein ligase HECTD2	339	RII
Q6PAV2	Probable E3 ubiquitin-protein ligase HERC4	53	RII
Q9CR73	Proline-rich nuclear receptor coactivator 2	281	RII
P70403	Protein CASP	109	RII
Q8VE88	Protein FAM114A2	110	RII
Q8C627	Protein FAM221B	113	RII
Q6NZK5	Protein hinderin	107	RII
Q5DTZ0	Protein NYNRIN	48	RII
O35595	Protein patched homolog 2	69	RII
P97352	Protein S100-A13	190	RII
Q91XY4	Protocadherin gamma-A4	92	RII
Q3UNZ8	Quinone oxidoreductase-like protein 2	129	RII
Q60695	Ral guanine nucleotide dissociation stimulator-like 1	83	RII
Q8C2K5	RAS protein activator like-3	90	RII
Q9CX84	Regulator of G-protein signaling 19	131	RII
Q8K4Q0	Regulatory-associated protein of mTOR	120	RII
Q91YE7	RNA-binding protein 5	248	RII
Q8BX22	Sal-like protein 4	131	RII
P42208	Septin-2	255	RII
P98083	SHC-transforming protein 1	117	RII
P42230	Signal transducer and activator of transcription 5A	157	RII
Q8R3P9	SMC5-SMC6 complex localization factor protein 1	77	RII
Q8C0X8	Sperm motility kinase X	71	RII
Q8BWB1	Synaptopodin 2-like protein	100	RII
Q9JKD8	T-box transcription factor TBX21	81	RII
P80318	T-complex protein 1 subunit gamma	90	RII
Q8K1H7	T-complex protein 11-like protein 2	55	RII
Q3URQ0	Testis-expressed protein 10	54	RII
Q61286	Transcription factor 12	235	RII
Q9EPK8	Transient receptor potential cation channel subfamily V member 4	96	RII
Q80W04	Transmembrane and coiled-coil domains protein 2	99	RII
Q6GQT5	Transmembrane protein 151A	125	RII
Q01887	Tyrosine-protein kinase RYK	183	RII
Q99NB8	Ubiquilin-4	102	RII
Q8C2S0	Ubiquitin carboxyl-terminal hydrolase 44	69	RII
O08759	Ubiquitin-protein ligase E3A	118	RII
Q8CE97	Uncharacterized protein C15orf62 homolog_ mitochondrial	194	RII
Q8C456	WD repeat-containing and planar cell polarity effector protein fritz homolog	451	RII
Q8BGF3	WD repeat-containing protein 92	398	RII
Q6NZF1	Zinc finger CCCH domain-containing protein 11A	138	RII
O88532	Zinc finger RNA-binding protein	102	RII

Q60738	Zinc transporter 1	65	RII

[a]Identification is based on proteins ID from UniProt protein database, reviewed only (http://www.uniprot.org/).
[b]Proteins with expression significantly altered are organized according to the ratio.
*Indicates unique proteins in alphabetical order

S6. Proteins with expression significantly altered in the gastrocnemius of of SIII (A/J, water containing 50 ppm F, exercise) and RIII (129P3/J, water containing 50 ppm F, exercise) mice.

[a]Acession number	Protein name	PLGS Score	[b]*Ratio* SIII: RIII
P32848	Parvalbumin alpha	6797	7.10
P97457	Myosin regulatory light chain 2_ skeletal muscle isoform	7435	5.05
P21107	Tropomyosin alpha-3 chain	262	4.53
Q64467	Glyceraldehyde-3-phosphate dehydrogenase_ testis-specific	74	3.53
P02104	Hemoglobin subunit epsilon-Y2	2664	3.49
P16858	Glyceraldehyde-3-phosphate dehydrogenase	14569	3.19
O09165	Calsequestrin-1	1129	2.92
Q3UHK3	Protein GREB1	121	2.89
Q9DBJ1	Phosphoglycerate mutase 1	54	2.86
P02089	Hemoglobin subunit beta-2	2664	2.72
P11404	Fatty acid-binding protein_ heart	178	2.59
Q60611	DNA-binding protein SATB1	218	2.56
Q91VW5	Golgin subfamily A member 4	227	2.53
P02088	Hemoglobin subunit beta-1	3946	2.53
P13412	Troponin I_ fast skeletal muscle	2648	2.53
P07310	Creatine kinase M-type	16395	2.48
P13541	Myosin-3	2675	2.29
Q5SX39	Myosin-4	18478	2.27
A2AQP0	Myosin-7B	428	2.23
P57780	Alpha-actinin-4	80	2.14
P05977	Myosin light chain 1/3_ skeletal muscle isoform	22171	2.10
Q91Z83	Myosin-7	5146	2.05
P70402	Myosin-binding protein H	203	2.01
Q5SX40	Myosin-1	13910	1.99
P17183	Gamma-enolase	806	1.97
Q7TQ48	Sarcalumenin	41	1.95
P52480	Pyruvate kinase PKM	4168	1.92
P17751	Triosephosphate isomerase	3267	1.88
Q9R0Y5	Adenylate kinase isoenzyme 1	2915	1.84
O70250	Phosphoglycerate mutase 2	984	1.80
P08249	Malate dehydrogenase_ mitochondrial	475	1.79
P01942	Hemoglobin subunit alpha	9144	1.77
P53657	Pyruvate kinase PKLR	737	1.77
P17182	Alpha-enolase	2341	1.75

Q8BFZ3	Beta-actin-like protein 2	14800	1.75
Q3TJD7	PDZ and LIM domain protein 7	268	1.73
P60710	Actin_ cytoplasmic 1	49058	1.72
P09041	Phosphoglycerate kinase 2	1520	1.72
P21550	Beta-enolase	4470	1.70
O08638	Myosin-11	255	1.68
P63260	Actin_ cytoplasmic 2	49058	1.67
P47857	ATP-dependent 6-phosphofructokinase_ muscle type	165	1.67
P0DP28	Calmodulin-3	389	1.67
P68033	Actin_ alpha cardiac muscle 1	66606	1.65
P31001	Desmin	273	1.65
P04247	Myoglobin	381	1.65
Q02566	Myosin-6	3955	1.65
P09411	Phosphoglycerate kinase 1	1615	1.65
Q9JI91	Alpha-actinin-2	177	1.63
P0DP27	Calmodulin-2	389	1.63
P58774	Tropomyosin beta chain	6233	1.63
P62737	Actin_ aortic smooth muscle	61441	1.62
P13542	Myosin-8	8481	1.62
Q8VDD5	Myosin-9	255	1.62
P58771	Tropomyosin alpha-1 chain	10393	1.62
P68134	Actin_ alpha skeletal muscle	73343	1.60
P63268	Actin_ gamma-enteric smooth muscle	61339	1.60
P0DP26	Calmodulin-1	389	1.60
P06151	L-lactate dehydrogenase A chain	1760	1.55
O88990	Alpha-actinin-3	989	1.54
Q9D0F9	Phosphoglucomutase-1	80	1.54
Q5XKE0	Myosin-binding protein C_ fast-type	2097	1.52
P16125	L-lactate dehydrogenase B chain	309	1.51
P07724	Serum albumin	636	1.51
P09542	Myosin light chain 3	4350	1.49
Q7TPR4	Alpha-actinin-1	57	1.48
Q60605	Myosin light polypeptide 6	1016	1.48
P05064	Fructose-bisphosphate aldolase A	12552	1.46
P14152	Malate dehydrogenase_ cytoplasmic	202	1.43
P00342	L-lactate dehydrogenase C chain	455	1.42
P09541	Myosin light chain 4	5093	1.34
Q99LX0	Protein DJ-1	503	1.34
Q62234	Myomesin-1	80	1.32
Q6URW6	Myosin-14	258	1.31
Q9QZ47	Troponin T_ fast skeletal muscle	1180	1.30
Q99KI0	Aconitate hydratase_ mitochondrial	100	1.28
Q9JKS4	LIM domain-binding protein 3	618	1.28
Q61879	Myosin-10	256	1.26
O55143	Sarcoplasmic/endoplasmic reticulum calcium ATPase 2	244	1.25
P16015	Carbonic anhydrase 3	1180	1.17

Q6P8J7	Creatine kinase S-type_ mitochondrial	300	1.17
P20801	Troponin C_ skeletal muscle	1693	1.13
P56480	ATP synthase subunit beta_ mitochondrial	1511	1.12
Q9WUB3	Glycogen phosphorylase_ muscle form	4418	1.09
Q8R429	Sarcoplasmic/endoplasmic reticulum calcium ATPase 1	946	1.07
Q5SPL2	PHD finger protein 12	495	0.73
Q3UH93	Plexin-D1	95	0.50
Q80TM9	Nischarin	292	0.35
Q8CJH3	Plexin-B1	169	0.30
Q9CZU6	Citrate synthase_ mitochondrial	51	0.27
Q8R4I1	Ataxin-7	193	0.21
P62259	14-3-3 protein epsilon	81	SIII*
O88986	2-amino-3-ketobutyrate coenzyme A ligase_ mitochondrial	55	SIII
O08756	3-hydroxyacyl-CoA dehydrogenase type-2	73	SIII
Q921H8	3-ketoacyl-CoA thiolase A_ peroxisomal	114	SIII
Q8VCH0	3-ketoacyl-CoA thiolase B_ peroxisomal	114	SIII
P20029	78 kDa glucose-regulated protein	111	SIII
Q6Q2Z6	Acyl-coenzyme A thioesterase 5	71	SIII
Q9ESW4	Acylglycerol kinase_ mitochondrial	50	SIII
Q61315	Adenomatous polyposis coli protein	73	SIII
P45376	Aldose reductase	98	SIII
Q9QYC0	Alpha-adducin	80	SIII
P46660	Alpha-internexin	58	SIII
Q9D4H4	Angiomotin-like protein 1	45	SIII
Q9D0I9	Arginine--tRNA ligase_ cytoplasmic	46	SIII
Q91V24	ATP-binding cassette sub-family A member 7	41	SIII
P12382	ATP-dependent 6-phosphofructokinase_ liver type	71	SIII
P52963	Band 4.1-like protein 4A	50	SIII
P41183	B-cell lymphoma 6 protein homolog	69	SIII
P97929	Breast cancer type 2 susceptibility protein homolog	66	SIII
P97291	Cadherin-8	71	SIII
Q9JKL5	Calcineurin B homologous protein 3	130	SIII
P58660	Caspase recruitment domain-containing protein 10	42	SIII
Q6A065	Centrosomal protein of 170 kDa	73	SIII
Q9ESN9	C-Jun-amino-terminal kinase-interacting protein 3	107	SIII
Q9QXK3	Coatomer subunit gamma-2	47	SIII
Q6NS45	Coiled-coil domain-containing protein 66	51	SIII
Q4QRL3	Coiled-coil domain-containing protein 88B	54	SIII
Q9DBT3	Coiled-coil domain-containing protein 97	97	SIII
P11087	Collagen alpha-1(I) chain	40	SIII
Q01149	Collagen alpha-2(I) chain	36	SIII
Q9CZ13	Cytochrome b-c1 complex subunit 1_ mitochondrial	170	SIII

P12787	Cytochrome c oxidase subunit 5A_ mitochondrial	122	SIII
P62897	Cytochrome c_ somatic	375	SIII
Q91YE9	Cytosolic 5'-nucleotidase 1B	42	SIII
Q91VU6	DDB1- and CUL4-associated factor 11	72	SIII
Q8R1A4	Dedicator of cytokinesis protein 7	28	SIII
Q8VC56	E3 ubiquitin-protein ligase RNF8	49	SIII
Q6P5F9	Exportin-1	86	SIII
P47754	F-actin-capping protein subunit alpha-2	101	SIII
Q61553	Fascin	118	SIII
Q8VHX6	Filamin-C	28	SIII
O08917	Flotillin-1	70	SIII
Q9WTJ4	Flt3-interacting zinc finger protein 1	733	SIII
Q99JB6	Forkhead box protein P3	55	SIII
Q810T2	G2/mitotic-specific cyclin-B3	52	SIII
Q5SNZ0	Girdin	177	SIII
P03995	Glial fibrillary acidic protein	59	SIII
C0HKE1	Histone H2A type 1-B	691	SIII
C0HKE2	Histone H2A type 1-C	691	SIII
C0HKE3	Histone H2A type 1-D	691	SIII
C0HKE4	Histone H2A type 1-E	691	SIII
Q8CGP5	Histone H2A type 1-F	691	SIII
C0HKE5	Histone H2A type 1-G	691	SIII
Q8CGP6	Histone H2A type 1-H	691	SIII
C0HKE6	Histone H2A type 1-I	691	SIII
Q8CGP7	Histone H2A type 1-K	691	SIII
C0HKE7	Histone H2A type 1-N	691	SIII
C0HKE8	Histone H2A type 1-O	691	SIII
C0HKE9	Histone H2A type 1-P	691	SIII
Q6GSS7	Histone H2A type 2-A	691	SIII
Q64522	Histone H2A type 2-B	201	SIII
Q64523	Histone H2A type 2-C	691	SIII
Q8BFU2	Histone H2A type 3	691	SIII
Q8R1M2	Histone H2A.J	691	SIII
Q3THW5	Histone H2A.V	201	SIII
P0C0S6	Histone H2A.Z	201	SIII
P27661	Histone H2AX	201	SIII
P97443	Histone-lysine N-methyltransferase Smyd1	98	SIII
P18533	Ig heavy chain V region 733	108	SIII
Q3USB7	Inactive phospholipase C-like protein 1	353	SIII
Q99PW8	Kinesin-like protein KIF17	36	SIII
Q7TNC6	Kinesin-like protein KIF26B O	38	SIII
Q8CDB0	MAP kinase-interacting serine/threonine- protein kinase 2	56	SIII
P15089	Mast cell carboxypeptidase A	48	SIII
Q9JI70	McKusick-Kaufman/Bardet-Biedl syndromes putative chaperonin	54	SIII
A2AG06	Meiosis-specific coiled-coil domain-	36	SIII

	containing protein MEIOC		
Q8BI84	Melanoma inhibitory activity protein 3	107	SIII
Q9EQ20	Methylmalonate-semialdehyde dehydrogenase [acylating]_ mitochondrial	78	SIII
Q9JIF9	Myotilin	133	SIII
Q3TKR3	NACHT_ LRR and PYD domains-containing protein 4C	31	SIII
P19246	Neurofilament heavy polypeptide	45	SIII
P08551	Neurofilament light polypeptide	45	SIII
P08553	Neurofilament medium polypeptide	45	SIII
Q9WU42	Nuclear receptor corepressor 2	92	SIII
O88708	Origin recognition complex subunit 4	43	SIII
B9EJ86	Oxysterol-binding protein-related protein 8	39	SIII
P48725	Pericentrin	78	SIII
P15331	Peripherin	43	SIII
Q8VD65	Phosphoinositide 3-kinase regulatory subunit 4	42	SIII
Q99KP6	Pre-mRNA-processing factor 19	117	SIII
P54823	Probable ATP-dependent RNA helicase DDX6	88	SIII
Q8CDU6	Probable E3 ubiquitin-protein ligase HECTD2	191	SIII
Q812A5	Proline-rich protein 5	68	SIII
Q9DAU1	Protein canopy homolog 3	167	SIII
Q9DAF3	Protein DDI1 homolog 1	48	SIII
Q8R100	Protein FAM26E	95	SIII
Q8BZ32	Putative Polycomb group protein ASXL2	48	SIII
Q69ZJ7	RAB6A-GEF complex partner protein 1	31	SIII
Q5FWH6	Rho guanine nucleotide exchange factor 15	37	SIII
Q8C2Q3	RNA-binding protein 14	127	SIII
Q9WTM3	Semaphorin-6C	179	SIII
Q9DBP0	Sodium-dependent phosphate transport protein 2B	173	SIII
Q922B9	Sperm-specific antigen 2 homolog	38	SIII
G3X912	SprT-like domain-containing protein Spartan	102	SIII
Q6PE84	Stomatin-like protein 3	133	SIII
P08228	Superoxide dismutase [Cu-Zn]	236	SIII
P70327	T-box transcription factor TBX6	66	SIII
P20108	Thioredoxin-dependent peroxide reductase_ mitochondrial	83	SIII
Q61286	Transcription factor 12	96	SIII
Q9WUZ5	Troponin I_ slow skeletal muscle	116	SIII
Q6QR59	TRPM8 channel-associated factor 3	54	SIII
P68369	Tubulin alpha-1A chain	107	SIII
P05213	Tubulin alpha-1B chain	107	SIII
P68373	Tubulin alpha-1C chain	107	SIII
P05214	Tubulin alpha-3 chain	35	SIII
P68368	Tubulin alpha-4A chain	44	SIII
Q06806	Tyrosine-protein kinase receptor Tie-1	49	SIII
Q01887	Tyrosine-protein kinase RYK	408	SIII
Q91WQ3	Tyrosine--tRNA ligase_ cytoplasmic	71	SIII
Q8C7R4	Ubiquitin-like modifier-activating enzyme 6	43	SIII

O08759	Ubiquitin-protein ligase E3A	100	SIII
Q3TQQ9	Uncharacterized protein C1orf112 homolog	37	SIII
Q8CC96	Uncharacterized protein C6orf222 homolog	48	SIII
Q9D454	Uncharacterized protein CXorf49 homolog	79	SIII
A2AAE1	Uncharacterized protein KIAA1109	24	SIII
Q9QY06	Unconventional myosin-IXb	32	SIII
P20152	Vimentin	71	SIII
Q60932	Voltage-dependent anion-selective channel protein 1	435	SIII
Q3UR50	von Willebrand factor A domain-containing protein 5B2	86	SIII
Q5F293	Zinc finger and BTB domain-containing protein 4	71	SIII
Q61464	Zinc finger protein 638	90	SIII
Q921S7	39S ribosomal protein L37_ mitochondrial	74	RIII
Q9D404	3-oxoacyl-[acyl-carrier-protein] synthase_ mitochondrial	56	RIII
Q9JII1	72 kDa inositol polyphosphate 5-phosphatase	74	RIII
Q9QY83	Actin-like protein 7B	129	RIII
Q8BK64	Activator of 90 kDa heat shock protein ATPase homolog 1	58	RIII
Q9QZQ1	Afadin	101	RIII
Q9DBR4	Amyloid beta A4 precursor protein-binding family B member 2	155	RIII
Q8BZ05	Arf-GAP with Rho-GAP domain_ ANK repeat and PH domain-containing protein 2	91	RIII
Q8R3P0	Aspartoacylase	107	RIII
Q61137	Astrotactin-1	62	RIII
Q9D3D9	ATP synthase subunit delta_ mitochondrial	285	RIII
O88738	Baculoviral IAP repeat-containing protein 6	75	RIII
O88428	Bifunctional 3'-phosphoadenosine 5'-phosphosulfate synthase 2	84	RIII
Q9CWJ9	Bifunctional purine biosynthesis protein PURH	230	RIII
Q6DFY8	BMP/retinoic acid-inducible neural-specific protein 2	97	RIII
Q499E0	BMP/retinoic acid-inducible neural-specific protein 3	158	RIII
Q52KB6	C2 domain-containing protein 3	81	RIII
P08607	C4b-binding protein	84	RIII
Q91ZI0	Cadherin EGF LAG seven-pass G-type receptor 3	76	RIII
Q7TQK5	Coiled-coil domain-containing protein 93	82	RIII
Q8R1U1	Conserved oligomeric Golgi complex subunit 4	86	RIII
Q8BLF2	Cyclin-dependent kinase-like 3	80	RIII
Q7TMW6	Cytosolic Fe-S cluster assembly factor NARFL	89	RIII
Q8K3G9	DCC-interacting protein 13-beta	182	RIII

Q8N7N5	DDB1- and CUL4-associated factor 8	121	RIII
O55111	Desmoglein-2	61	RIII
Q811D0	Disks large homolog 1	41	RIII
P0C6F1	Dynein heavy chain 2_ axonemal	32	RIII
Q4U2R1	E3 ubiquitin-protein ligase HERC2	416	RIII
Q9ERK4	Exportin-2	118	RIII
A2A870	Fas-binding factor 1	359	RIII
P42128	Forkhead box protein K1	75	RIII
Q8K284	General transcription factor 3C polypeptide 1	152	RIII
Q9WUU9	Germinal-center associated nuclear protein	96	RIII
Q9R257	Heme-binding protein 1	83	RIII
Q9JHU9	Inositol-3-phosphate synthase 1	83	RIII
P54071	Isocitrate dehydrogenase [NADP]_ mitochondrial	212	RIII
Q8BIJ6	Isoleucine--tRNA ligase_ mitochondrial	78	RIII
Q69ZK5	Kelch-like protein 14	106	RIII
Q497I4	Keratin_ type I cuticular Ha5	65	RIII
Q99M74	Keratin_ type II cuticular Hb2	88	RIII
Q61097	Kinase suppressor of Ras 1	448	RIII
Q91W40	Kinesin light chain 3	63	RIII
Q8K1S5	Krueppel-like factor 11	365	RIII
A2AHG0	Leucine zipper putative tumor suppressor 3	45	RIII
Q3UZ18	Little elongation complex subunit 2 O	32	RIII
Q99MN1	Lysine--tRNA ligase	57	RIII
Q8CAQ8	MICOS complex subunit Mic60	216	RIII
Q9JM52	Misshapen-like kinase 1	86	RIII
Q9Z2I0	Mitochondrial proton/calcium exchanger protein	72	RIII
Q07174	Mitogen-activated protein kinase kinase kinase 8	121	RIII
Q91YD3	mRNA-decapping enzyme 1A	68	RIII
Q9Z2C4	Myotubularin-related protein 1	86	RIII
Q61578	NADPH:adrenodoxin oxidoreductase_ mitochondrial	56	RIII
E9Q7X7	Neurexin II	61	RIII
B0F2B4	Neuroligin 4-like	101	RIII
Q99K10	Neuroligin-1	107	RIII
Q69ZK9	Neuroligin-2	101	RIII
Q02780	Nuclear factor 1 A-type	123	RIII
P70255	Nuclear factor 1 C-type	123	RIII
Q6ZQH8	Nucleoporin NUP188 homolog	151	RIII
Q9DCM7	Nucleus accumbens-associated protein 2	229	RIII
O70209	PDZ and LIM domain protein 3	169	RIII
Q8CI51	PDZ and LIM domain protein 5	460	RIII
Q3TKY6	Peptidyl-prolyl cis-trans isomerase CWC27 homolog	145	RIII
P70296	Phosphatidylethanolamine-binding protein 1	227	RIII
Q7TQG1	Pleckstrin homology domain-containing family A member 6	424	RIII

Q8JZX3	POC1 centriolar protein homolog A	108	RIII
Q91Z31	Polypyrimidine tract-binding protein 2	65	RIII
Q3URV1	Protein broad-minded	101	RIII
Q8K2Y3	Protein eva-1 homolog B	281	RIII
Q3UY90	Protein FAM198A	78	RIII
Q3HNM7	Protein inscuteable homolog	192	RIII
O35595	Protein patched homolog 2	166	RIII
Q80U72	Protein scribble homolog	284	RIII
Q4KUS2	Protein unc-13 homolog A	116	RIII
Q64455	Receptor-type tyrosine-protein phosphatase eta	103	RIII
Q8CGE9	Regulator of G-protein signaling 12	75	RIII
Q8K4Q0	Regulatory-associated protein of mTOR	111	RIII
Q64518	Sarcoplasmic/endoplasmic reticulum calcium ATPase 3	34	RIII
Q9WUN2	Serine/threonine-protein kinase TBK1	91	RIII
P97470	Serine/threonine-protein phosphatase 4 catalytic subunit	132	RIII
Q921I1	Serotransferrin	419	RIII
Q8BPQ7	Small G protein signaling modulator 1	107	RIII
Q8K4L3	Supervillin	57	RIII
Q9D818	Suppressor APC domain-containing protein 2	74	RIII
Q6A028	Switch-associated protein 70	63	RIII
Q8CHC4	Synaptojanin-1	188	RIII
Q91YE8	Synaptopodin-2	44	RIII
Q62288	Testican-1	92	RIII
Q2TV84	Transient receptor potential cation channel subfamily M member 1	292	RIII
Q9EPK8	Transient receptor potential cation channel subfamily V member 4	79	RIII
Q91VP7	Transmembrane protein 101	78	RIII
Q99PP6	Tripartite motif-containing protein 34A	90	RIII
Q9CWH5	tRNA (guanine(10)-N2)-methyltransferase homolog	185	RIII
Q9D0C4	tRNA (guanine(37)-N1)-methyltransferase	80	RIII
Q9R0M8	UDP-galactose translocator	257	RIII
E9Q035	Uncharacterized protein	122	RIII
F8VQB6	Unconventional myosin-X	136	RIII

[a]Identification is based on proteins ID from UniProt protein database, reviewed only (http://www.uniprot.org/).
[b]Proteins with expression significantly altered are organized according to the ratio.
*Indicates unique proteins in alphabetical order

3 DISCUSSÃO

3 DISCUSSÃO

De acordo com estudos realizados até o momento, muitos fatores podem afetar o metabolismo do F, com potencial para interferir em sua retenção no organismo e alterar a relação entre ingestão de F e risco de fluorose, bem como a homeostase da glicose (BUZALAF; WHITFORD, 2011; BUZALAF, 2018). Um desses fatores é a variabilidade genética, que vem sendo amplamente estudada, (CARVALHO; LEITE ADE; PERES-BUZALAF; SALVATO *et al.*, 2013; CARVALHO; LEITE; YAN; EVERETT *et al.*, 2009; CHARONE; DE LIMA LEITE; PERES-BUZALAF; SILVA FERNANDES *et al.*, 2016; KHAN; SABINO; DE SOUZA MELO; MARTINI *et al.*, 2018; KOBAYASHI; LEITE; PERES-BUZALAF; CARVALHO *et al.*, 2014), bem como fatores epigenéticos, por exemplo o exercício físico (AMARAL; AZEVEDO; BUZALAF; FABRICIO *et al.*, 2018; LOMBARTE; FINA; LUPO; BUZALAF *et al.*, 2013; WHITFORD, 1996). Este é o primeiro estudo que avalia as interações entre os fatores genéticos e epigenéticos no metabolismo do F e também em parâmetros relacionados à homeostase da glicose. Nesse sentido, duas linhagens de camundongos com diferentes suscetibilidades aos efeitos do F foram escolhidas: A/J e 129P3/J (CARVALHO; LEITE; YAN; EVERETT *et al.*, 2009; EVERETT, 2011; EVERETT, E. T.; MCHENRY, M. A. K.; REYNOLDS, N.; EGGERTSSON, H. *et al.*, 2002), que foram expostos ao F com ou sem realização de exercício físico. Os animais 129P3/J (resistentes) tratados com F sem exercicio, tiveram níveis de F no plasma significativamente mais altos do que os animais A/J (susceptíveis). Além disso, os animais A/J apresentaram severa fluorose dentária, o que está em concordância com estudos anteriores (CARVALHO; LEITE; YAN; EVERETT *et al.*, 2009; CHARONE; DE LIMA LEITE; PERES-BUZALAF; SILVA FERNANDES *et al.*, 2016).

Em geral, para as duas linhagens, os resultados mostraram que a capacidade física dos animais diminuiu quando foram expostos ao F e não realizaram exercício físico diariamente. Ao contrário, os animais que realizaram treinamento físico durante todo o período experimental tiveram um aumento da capacidade física (Tabela 2 – Artigo I).

Os animais da linhagem A/J são mais susceptíveis à ocorrência de fluorose dentária, mesmo com os níveis de F no plasma mais baixos do que os camundongos da linhagem 129P3/J, o que vai de encontro com os resultados de outros estudos já realizados (CARVALHO; LEITE; YAN; EVERETT *et al.*, 2009). Em conformidade com a literatura, concentrações mais altas de F no plasma e fêmur dos animais 129P3/J provavelmente são causadas pela alta taxa de retenção de F nesses animais (CARVALHO; LEITE; YAN; EVERETT *et al.*, 2009; KOBAYASHI; LEITE; PERES-BUZALAF; CARVALHO *et al.*, 2014; MOUSNY; BANSE; WISE; EVERETT *et al.*, 2006). Em um estudo anterior, camundongos resistentes, expostos a pequenas doses de F, tiveram concentrações de F no osso mais alta quando comparados aos animais suscetíveis. Os mecanismos envolvidos ainda não são claros, mas acredita-se que estejam relacionados à função renal ou remodelação óssea na linhagem 129P3/J (MOUSNY; BANSE; WISE; EVERETT *et al.*, 2006). Com relação ao exercício físico e a exposição ao F, um estudo prévio de nosso grupo encontrou concentração de F em tecido ósseo significativamente mais alta em animais submetidos a sessões de exercício físico (LOMBARTE; FINA; LUPO; BUZALAF *et al.*, 2013). Comparando os tratamentos, somente para o grupo dos animais resistentes que foram expostos ao F e ao exercício físico, houve um aumento na concentração de F nos rins quando comparados aos grupos controle e somente expostos ao F (Tabela 1 - Artigo I). Em outro estudo realizado com camundongos A/J e 129P3/J, a concentração de F aumentou nos rins dos animais 129P3/J em comparação com os da linhagem A/J (CARVALHO; LEITE ADE; PERES-BUZALAF; SALVATO *et al.*, 2013). Esses resultados sugerem que o exercício crônico não afeta a concentração de F no plasma e no osso de camundongos suscetíveis à fluorose, fornecendo importantes subsídios para o desenvolvimento de estratégias apropriadas para otimizar a saúde geral e oral.

Em relação aos parâmetros relacionados à homeostase da glicose, as únicas diferenças encontradas foram para a concentração de glicose no plasma e %B. Os animais da linhagem A/J, sedentários e tratados com F, tiveram glicemia mais alta, com consequente %B mais baixa quando comparados aos animais da linhagem 129P3/J tratados da mesma forma. Esses dados mostram que a homeostasia da glicose é mais afetada pela genética do que pelos fatores epigenéticos, neste caso o exercício. Isso pode explicar os diferentes resultados encontrados na literatura.

Ratos *Wistar* diabéticos induzidos por estreptozotocina tiveram um aumento da sensibilidade insulínica quando expostos à água contendo 10 ppm F (LOBO; LEITE; PEREIRA; FERNANDES *et al.*, 2015), enquanto camundongos da linhagem *Sprague dawley*, expostos à água contendo 15 ppm F tiveram uma aumento da resistência à insulina (LOMBARTE; FINA; LUPO; BUZALAF *et al.*, 2013). Além disso, camundongos da linhagem NOD (não obesos diabéticos), expostos à água contendo 10 ppm F tiveram glicemia reduzida quando comparados com os camundongos não expostos ao F (MALVEZZI; PEREIRA; DIONIZIO; ARAUJO *et al.*, 2018).

Ressalta-se que, apesar do exercício físico não ter tido um impacto significativo nos parâmetros relacionados à homeostase da glicose após a exposição ao F, os camundongos que foram submetidos ao exercício físico de ambas as linhagens apresentaram níveis plasmáticos de glicose semelhantes, enquanto para os sedentários, os camundongos A/J tiveram glicemia maior em comparação aos da linhagem 129P3/J. Resultado parecido foi encontrado no estudo de Lombarte et al., em que o exercício físico melhorou os efeitos tóxicos do F (LOMBARTE; FINA; LUPO; BUZALAF *et al.*, 2013).

Para a análise proteômica no fígado, os camundongos A/J que não realizaram exercício (grupo controle, principalmente), tiveram um aumento na expressão de proteínas (Tabela 2 – Artigo II), indo de encontro com um estudo prévio em que mostrou um aumento da proteína Formimidoyltransferase-cyclodeaminase (Q91XD4; Tabela S1 – Artigo II) animais da linhagem A/J (KHAN; AHMED; ALI, 2016), que foi encontrada exclusivamente no fígado dos animais susceptíveis do presente estudo. A referida enzima está envolvida na síntese de purinas e pirimidinas, bem como de aminoácidos.

Sabe-se que o aumento do fluxo energético leva ao estresse oxidativo, o que está de acordo com o aumento das enzimas antioxidantes em camundongos susceptíveis não expostos ao F, em comparação com os resistentes. Esses achados também foram observados em um estudo anterior do nosso grupo (KHAN; AHMED; ALI, 2016). Os resultados podem explicar a susceptibilidade dos camundongos A/J aos efeitos do F, uma vez que esse íon é bem conhecido por sua capacidade de induzir estresse oxidativo (BARBIER; ARREOLA-MENDOZA; DEL RAZO, 2010; KHAN; AHMED; ALI, 2016).

Quando expostos ao F, os camundongos A/J ainda apresentaram expressão aumentada de proteínas no fígado (envolvidas no fluxo de energia e no estresse oxidativo), embora em menor extensão quando comparadas com as da linhagem 129P3/J. A categoria com a maior porcentagem de associação de número de genes para esta comparação, foi o Cofactor metabolic process (Fig. 3B). Isso pode estar associado ao fato de o F ser o elemento mais eletronegativo da tabela periódica e possuir alta afinidade por íons metálicos (BUZALAF; WHITFORD, 2011), que atuam como cofatores de diversas enzimas. Destaca-se que a Fructose-1,6-bisphosphatase 1 (Q9QXD6), responsável por catalisar a hidrólise do 1,6-bifosfato de frutose em 6-fosfato de frutose na presença de cátions divalentes, aumentou mais de 2 vezes no grupo SII (Tabela S2 – Artigo II). O F é conhecido como um potente inibidor de enzimas da via glicolítica (enolase, hexocinase, fosfofructoquinase, piruvato quinase), por sua capacidade forte de se ligar a metais (SHERER; SUTTIE, 1970). Portanto, o comprometimento da glicólise pelo F pode ativar o metabolismo de outros combustíveis, o que pode explicar o aumento de Aspartate aminotransferase_mitochondrial, 3-ketoacyl-CoA thiolase, mitochondrial e Fructose-1,6-bisphosphatase 1.

Quando os camundongos foram expostos ao F e submetidos ao exercício, o perfil de expressão proteica mudou. Os animais A/J tiveram uma redução na expressão das proteínas do fígado quando comparados com os da linhagem 129P3/J. Houve redução na expressão de proteínas envolvidas em vias distintas do metabolismo energético, como glicólise aeróbica e anaeróbica, fosforilação oxidativa e metabolismo de aminoácidos. Importantes proteínas envolvidas na detoxificação estavam ausentes nos camundongos A/J, como por exemplo a Protein/nucleic acid deglycase DJ-1, que promovem a deglicação em resíduos de cisteína, arginina e lisina nas proteínas, reativando-as e impedindo a formação de produtos de glicação avançada (AGEs) (UNIPROT), bem como a indolethylamine N-methyltransferase and 2-iminobutanoate/2-iminopropanoate deaminase, que facilita a liberação de amônia a partir de metabólitos reativos potencialmente tóxicos (UNIPROT). Curiosamente, algumas enzimas antioxidantes foram aumentadas nos fígados dos animais é A/J, em comparação com os da linhagem 129P3/J. Apesar disso, a Peroxiredoxin-4 e várias isoformas da Glutathione S-transferase (Mu2, Mu7, Mu5, A1, A2 e A3) diminuíram mais de 2 vezes nos camundongos A/J (Tabela S3).

Em relação ao músculo gastrocnêmio (Tabela 5 – Artigo II), diferentemente do observado no fígado (Tabela 3 - Artigo II), os camundongos A/J não tratados apresentaram uma diminuição na expressão de proteínas quando comparados aos 129P3/J, o que pode ser explicado pela ausência ou menor expressão de algumas proteínas relacionadas à síntese proteica (Tabela 5 - Artigo II). Houve também uma redução e/ou ausência de proteínas envolvidas na contração muscular, para os camundongos da linhagem A/J. Proteínas como a Parvalbumin alpha (P32848), envolvida no relaxamento após a contração, Glyceraldehyde-3-phosphate dehydrogenase (P16858) e Filamin-C (Q8VHX6), essenciais para manter a integridade estrutural das fibras musculares, diminuíram mais de 2 vezes nos camundongos A/J (Tabela S4 - Artigo II). Isso pode indicar diminuição da contração muscular nos camundongos susceptíveis, mesmo na ausência de estressores.

A exposição ao F, associada ou não ao exercício, provocou um aumento na expressão de proteínas nos camundongos A/J em comparação com seus respectivos pares da linhagem 129P3/J, semelhante ao encontrado no fígado (Tabela 2 - Artigo II). Algumas proteínas com expressão alterada interagiram com proteínas envolvidas na regulação do fator nuclear kappa-B (NF-kB). Entre eles estão o inibidor da nuclear factor kappa-B kinase subunit beta (O88351), uma serina quinase que desempenha um papel essencial na ativação da via de sinalização NF-kB por estresses celulares encontrados exclusivamente no grupo do animais A/J expostos ao F não exercitados, bem como a Endoribonuclease ZC3H12A (Q5D1E7) (Fig 9B). Essa enzima, identificada exclusivamente nos camundongos 129P3/J, impede a ativação da via de sinalização de NF-kB, regulando negativamente a resposta inflamatória mediada por macrófagos. O NF-kB, como fator de transcrição, desempenha um papel crucial nas respostas imunes e inflamatórias através da regulação da expressão gênica. Quando não estimulado, o NF-kB está combinado com a proteína inibidora B (IkBs). Quando ativadas por alguns estimuladores, as proteínas IkB tornam-se fosforiladas e desconectam-se do NF-kB, o que desencadeia a translocação de NF-kB para a molécula e a ligação a seus locais de ligação ao DNA para regular a transcrição de seus genes. Alguns dos genes estão relacionados a respostas inflamatórias, como citocinas pró-inflamatórias, quimiocinas, moléculas de adesão e enzimas induzíveis como a ciclooxigenase-2 (COX2) e iNOS (BALDWIN, 2001). Vários estudos relataram que o tratamento com F

aumenta o NF-kB em células distintas, como neurônios (ZHANG; WANG; XIA; HE, 2008), células renais e cardíacas (OYAGBEMI; OMOBOWALE; ASENUGA; ADEJUMOBI *et al.*, 2017). Nossos resultados mostraram aumento da expressão de proteínas relacionadas à ativação da via NF-kB no músculo de animais suscetíveis tratados com F, enquanto os animais resistentes apresentaram aumento de proteínas que impedem a ativação da via de sinalização de NF-kB. Esse pode ser outro mecanismo que ajuda a explicar a resistência dos camundongos 129P3/J aos efeitos de F. As proteínas relacionadas à contração e relaxamento muscular aumentaram mais de duas vezes nos camundongos susceptíveis expostos ao F, como a Parvalbumin alpha (P32848; aumento de mais de 18 vezes), Tropomyosin alpha-3 chain (P21107; aumento de mais de 3 vezes), Myosin-7B (A2AQP0) e Troponin I, fast skeletal muscle (P13412) e Calsequestrin-1 (O09165), proteína que atua como uma reserva interna de cálcio no músculo e regula a liberação de Ca^{2+} luminal através do canal de liberação de cálcio RYR1, desempenhando um papel importante no desencadeamento da contração muscular (Tabela S5 - Artigo II). Além disso, as proteínas relacionadas ao fluxo de energia também aumentaram mais de duas vezes nos camundongos A/J expostos ao F, como a Glyceraldehyde-3-phosphate dehydrogenase testis-specific (Q64467; mais de 6 vezes), Fatty acid-binding protein, heart (P11404; mais de 3 vezes), AMP deaminase 1 (Q3V1D3) and ADP/ATP translocases (isoformas 1 e 2) (Tabela 12 - Artigo II). Interessante observar que algumas dessas proteínas, como Parvalbumin alpha e Glyceraldehyde-3-phosphate dehydrogenase, estavam reduzidas mais de duas vezes nos camundongos susceptíveis não tratados. Além disso, o aumento da Parvalbumina alfa também foi recentemente descrito no músculo de camundongos NOD tratados com 50 ppm de fluoreto (MALVEZZI; PEREIRA; DIONIZIO; ARAUJO *et al.*, 2018). Além disso, a Neurofibromin (Q04690), aumentou mais de 2 vezes nos camundongos A/J expostos ao F (Tabela S5 - Artigo II), o que indica o envolvimento das vias de sinalização MAPK / ERK nos eventos musculares. A exposição simultânea ao F e ao exercício causou um aumento da expressão de proteínas relacionadas ao fluxo de energia em camundongos A/J em comparação com seus equivalentes 129P3/J. Esses resultados indicam um aumento do metabolismo oxidativo nesses camundongos, o que pode induzir hipóxia, consistente com o aumento da carbonic anhydrase 3 (P16015) que também estava aumentada no fígado. Essa enzima aumentou consistentemente mais de duas vezes nos

camundongos susceptíveis em comparação com os 129P3/J, independentemente do tratamento no fígado (Tabelas S1, S2 e S3 - Artigo II) e no músculo gastrocnêmio (Tabelas S4, S5 e S6 - Artigo II). O aumento da síntese de anidrase carbônica (CA) pode ser diretamente induzido por uma menor tensão de oxigênio no nível molecular (MILLION; ZILLNER; BAUMANN, 1991). Níveis elevados de CA em camundongos susceptíveis, independentemente do tratamento, indicam que esses camundongos podem ter sido submetidos à hipóxia, provavelmente causada por metabolismo oxidativo excessivo. A hipóxia pode alterar o metabolismo do F de várias maneiras, dentre elas reduzindo o pH urinário, o que aumenta a retenção de F no organismo (BUZALAF; WHITFORD, 2011). No entanto, os camundongos A/J, apesar de serem mais susceptíveis ao desenvolvimento de fluorose dentária, mostraram níveis mais baixos de F circulante do que os os 129P3/J (CARVALHO; LEITE; YAN; EVERETT *et al.*, 2009). Além disso, a CA é essencial para manter a homeostase do pH no esmalte durante o estágio de maturação, quando o crescimento de cristais de esmalte resulta em quantidades excessivas de íons H^+. Nessa situação, a CA é necessária para evitar que o pH do esmalte em desenvolvimento se torne muito ácido (SMITH; CHONG; BARTLETT; MARGOLIS, 2005). Corroborando com esses achados na literatura, isoformas de CA foram identificadas exclusivamente no esmalte de camundongos A/J tratados com 50 ppm F, mas não em camundongos 129P3/J (CHARONE; DE LIMA LEITE; PERES-BUZALAF; SILVA FERNANDES *et al.*, 2016) indo ao encontro com os resultados do presente estudo, que mostrou níveis aumentados dessa enzima no fígado e músculo de camundongos A/J. Não se sabe quais as implicações disso no desenvolvimento diferencial da fluorose dentária nessas duas linhagens de camundongos, o que deve ser avaliado em estudos posteriores.

Analisando os resultados obtidos através das análises de concentração de F no plasma, rins e fêmur, glicemia e insulinemia, juntamente com os dados proteômicos de fígado e músculo dos animais A/J (susceptíveis) e 129P3/J (resistentes), conclui-se que as interações entre a genética e o exercício no metabolismo do fluoreto são bastante complexas. O exercício parece aumentar o acúmulo de F nos ossos dos animais resistentes, enquanto o estilo de vida sedentário reduz a capacidade física dos camundongos susceptíveis expostos ao F e possivelmente leva a uma alteração renal, relacionada à associação entre

exposição ao F e realização de exercício físico. Os resultados sugerem também um aumento do estresse oxidativo nos camundongos susceptíveis, o que pode ser exacerbado com a exposição ao F, corroborando com outros achados na literatura. (KHAN; AHMED; ALI, 2016; KHAN; SABINO; DE SOUZA MELO; MARTINI *et al.*, 2018). Por fim, nossos resultados sugerem ainda que os indivíduos susceptíveis aos efeitos do F podem se beneficiar mais da ação do exercício físico na homeostase da glicose do que os resistentes, mediante exposição a este íon, o que dá respaldo à utilização do F em saúde pública.

REFERÊNCIAS

REFERÊNCIAS

AMARAL, S. L.; AZEVEDO, L. B.; BUZALAF, M. A. R.; FABRICIO, M. F. *et al.* Effect of chronic exercise on fluoride metabolism in fluorosis-susceptible mice exposed to high fluoride. **Sci Rep**, 8, n. 1, p. 3211, Feb 16 2018.

ARAUJO, T. T.; PEREIRA, H. A. B. S.; DIONIZIO, A.; SANCHEZ, C. C. *et al.* Changes in energy metabolism induced by fluoride: insights from inside the mitochondria. **Chemosphere**, in press, 2019.

BALDWIN, A. S., Jr. Series introduction: the transcription factor NF-kappaB and human disease. **J Clin Invest**, 107, n. 1, p. 3-6, Jan 2001.

BARBIER, O.; ARREOLA-MENDOZA, L.; DEL RAZO, L. M. Molecular mechanisms of fluoride toxicity. **Chem Biol Interact**, 188, n. 2, p. 319-333, Nov 5 2010.

BARRES, R.; ZIERATH, J. R. The role of diet and exercise in the transgenerational epigenetic landscape of T2DM. **Nature Reviews Endocrinology**, 12, n. 8, p. 441-451, Aug 2016.

BARTALUCCI, A.; FERRUCCI, M.; FULCERI, F.; LAZZERI, G. *et al.* High-intensity exercise training produces morphological and biochemical changes in adrenal gland of mice. **Histol Histopathol**, 27, n. 6, p. 753-769, Jun 2012.

BAUER-MEHREN, A. Integration of genomic information with biological networks using Cytoscape. **Methods Mol Biol**, 1021, p. 37-61, 2013.

BOUCHARD, C.; DAW, E. W.; RICE, T.; PERUSSE, L. *et al.* Familial resemblance for VO2max in the sedentary state: the HERITAGE family study. **Med Sci Sports Exerc**, 30, n. 2, p. 252-258, Feb 1998.

BRADFORD, M. M. A rapid and sensitive method for the quantitation of microgram quantities of protein utilizing the principle of protein-dye binding. **Anal Biochem**, 72, p. 248-254, May 7 1976.

BUZALAF, M. A.; WHITFORD, G. M. Fluoride metabolism. **Monogr Oral Sci**, 22, p. 20-36, 2011.

BUZALAF, M. A. R. Review of Fluoride Intake and Appropriateness of Current Guidelines. **Adv Dent Res**, 29, n. 2, p. 157-166, Mar 2018.

CARVALHO, J. G.; LEITE ADE, L.; PERES-BUZALAF, C.; SALVATO, F. *et al.* Renal proteome in mice with different susceptibilities to fluorosis. **PLoS One**, 8, n. 1, p. e53261, 2013.

CARVALHO, J. G.; LEITE, A. L.; YAN, D.; EVERETT, E. T. *et al.* Influence of genetic background on fluoride metabolism in mice. **J Dent Res**, 88, n. 11, p. 1054-1058, Nov 2009.

CHARONE, S.; DE LIMA LEITE, A.; PERES-BUZALAF, C.; SILVA FERNANDES, M. *et al.* Proteomics of Secretory-Stage and Maturation-Stage Enamel of Genetically Distinct Mice. **Caries Res**, 50, n. 1, p. 24-31, 2016.

CHIBA, F. Y.; COLOMBO, N. H.; SHIRAKASHI, D. J.; DA SILVA, V. C. *et al.* NaF treatment increases TNF-alpha and resistin concentrations and reduces insulin signal in rats. **Journal of Fluorine Chemistry**, 136, p. 3-7, Apr 2012.

CHIBA, F. Y.; COLOMBO, N. H.; SHIRAKASHI, D. J.; GOMES, W. D. S. *et al.* Insulin Signal Decrease in Muscle but Not in the Liver of Castrated Male Rats from Chronic Exposure to Fluoride. **Fluoride**, 43, n. 1, p. 25-30, Jan-Mar 2010.

COURTNEY, S. M.; MASSETT, M. P. Identification of exercise capacity QTL using association mapping in inbred mice. **Physiol Genomics**, 44, n. 19, p. 948-955, Oct 02 2012.

DABROWSKA, E.; LETKO, R.; BALUNOWSKA, M. Effect of sodium fluoride on the morphological picture of the rat liver exposed to NaF in drinking water. **Adv Med Sci**, 51 Suppl 1, p. 91-95, 2006.

DEL BALSO, C.; CAFARELLI, E. Adaptations in the activation of human skeletal muscle induced by short-term isometric resistance training. **J Appl Physiol (1985)**, 103, n. 1, p. 402-411, Jul 2007.

DIONIZIO, A. S.; MELO, C. G. S.; SABINO-ARIAS, I. T.; VENTURA, T. M. S. *et al.* Chronic treatment with fluoride affects the jejunum: insights from proteomics and enteric innervation analysis. **Sci Rep**, 8, n. 1, p. 3180, Feb 16 2018.

DJAWDAN, M.; GARLAND, T. Maximal Running Speeds of Bipedal and Quadrupedal Rodents. **Journal of Mammalogy**, 69, n. 4, p. 765-772, Nov 1988.

EVERETT, E. T. Fluoride's Effects on the Formation of Teeth and Bones, and the Influence of Genetics. **Journal of Dental Research**, 90, n. 5, p. 552-560, May 2011.

EVERETT, E. T.; MCHENRY, M. A.; REYNOLDS, N.; EGGERTSSON, H. *et al.* Dental fluorosis: variability among different inbred mouse strains. **J Dent Res**, 81, n. 11, p. 794-798, Nov 2002.

EVERETT, E. T.; MCHENRY, M. A. K.; REYNOLDS, N.; EGGERTSSON, H. *et al.* Dental fluorosis: Variability among different inbred mouse strains. **Journal of Dental Research**, 81, n. 11, p. 794-798, Nov 2002.

EVERETT, E. T.; YAN, D.; WEAVER, M.; LIU, L. *et al.* Detection of dental fluorosis-associated quantitative trait Loci on mouse chromosomes 2 and 11. **Cells Tissues Organs**, 189, n. 1-4, p. 212-218, 2009.

FERREIRA, J. C.; ROLIM, N. P.; BARTHOLOMEU, J. B.; GOBATTO, C. A. *et al.* Maximal lactate steady state in running mice: effect of exercise training. **Clin Exp Pharmacol Physiol**, 34, n. 8, p. 760-765, Aug 2007.

HUANG, H.; BA, Y.; CUI, L.; CHENG, X. *et al.* COL1A2 gene polymorphisms (Pvu II and Rsa I), serum calciotropic hormone levels, and dental fluorosis. **Community Dent Oral Epidemiol**, 36, n. 6, p. 517-522, Dec 2008.

JONES, A. M.; CARTER, H. The effect of endurance training on parameters of aerobic fitness. **Sports Med**, 29, n. 6, p. 373-386, Jun 2000.

JUEL, C.; LUNDBY, C.; SANDER, M.; CALBET, J. A. *et al.* Human skeletal muscle and erythrocyte proteins involved in acid-base homeostasis: adaptations to chronic hypoxia. **J Physiol**, 548, n. Pt 2, p. 639-648, Apr 15 2003.

KASHIWAGI, N.; SHERER, D.; TOWNSEND, C. M.; JACOBS, R. *et al.* Antibody localization in horse, rabbit, and goat antilymphocyte sera. **Surgery**, 67, n. 5, p. 789-798, May 1970.

KHAN, Z. N.; AHMED, S.; ALI, M. Effect of Thermal Budget on the Electrical Characterization of Atomic Layer Deposited HfSiO/TiN Gate Stack MOSCAP Structure. **PLoS One**, 11, n. 8, p. e0161736, 2016.

KHAN, Z. N.; ASSIR, M. Z.; SHAFIQ, M.; CHAUDHARY, A. E. *et al.* High prevalence of preobesity and obesity among medical students of Lahore and its relation with dietary habits and physical activity. **Indian J Endocrinol Metab**, 20, n. 2, p. 206-210, Mar-Apr 2016.

KHAN, Z. N.; LEITE ADE, L.; CHARONE, S.; SABINO, I. T. *et al.* Liver proteome of mice with different genetic susceptibilities to the effects of fluoride. **J Appl Oral Sci**, 24, n. 3, p. 250-257, May-Jun 2016.

KHAN, Z. N.; SABINO, I. T.; DE SOUZA MELO, C. G.; MARTINI, T. *et al.* Liver Proteome of Mice with Distinct Genetic Susceptibilities to Fluorosis Treated with Different Concentrations of F in the Drinking Water. **Biol Trace Elem Res**, Apr 29 2018.

KILIKEVICIUS, A.; VENCKUNAS, T.; ZELNIENE, R.; CARROLL, A. M. *et al.* Divergent physiological characteristics and responses to endurance training among inbred mouse strains. **Scand J Med Sci Sports**, 23, n. 5, p. 657-668, Oct 2013.

KOBAYASHI, C. A.; LEITE, A. L.; PERES-BUZALAF, C.; CARVALHO, J. G. *et al.* Bone response to fluoride exposure is influenced by genetics. **PLoS One**, 9, n. 12, p. e114343, 2014.

KVEDARAS, M.; MINDERIS, P.; FOKIN, A.; RATKEVICIUS, A. *et al.* Forced Running Endurance Is Influenced by Gene(s) on Mouse Chromosome 10. **Front Physiol**, 8, p. 9, 2017.

LAURSEN, P. B. Training for intense exercise performance: high-intensity or high-volume training? **Scand J Med Sci Sports**, 20 Suppl 2, p. 1-10, Oct 2010.

LAURSEN, P. B.; RHODES, E. C. Factors affecting performance in an ultraendurance triathlon. **Sports Med**, 31, n. 3, p. 195-209, 2001.

LEVY, J. C.; MATTHEWS, D. R.; HERMANS, M. P. Correct homeostasis model assessment (HOMA) evaluation uses the computer program. **Diabetes Care**, 21, n. 12, p. 2191-2192, Dec 1998.

LI, G. H.; LIU, H.; MA, C. L.; CHEN, Y. F. *et al.* Exosomes are the novel players involved in the beneficial effects of exercise on type 2 diabetes. **Journal of Cellular Physiology**, 234, n. 9, p. 14896-14905, Sep 2019.

LIMA LEITE, A.; GUALIUME VAZ MADUREIRA LOBO, J.; BARBOSA DA SILVA PEREIRA, H. A.; SILVA FERNANDES, M. *et al.* Proteomic analysis of gastrocnemius muscle in rats with streptozotocin-induced diabetes and chronically exposed to fluoride. **PLoS One**, 9, n. 9, p. e106646, 2014.

LOBO, J. G.; LEITE, A. L.; PEREIRA, H. A.; FERNANDES, M. S. *et al.* Low-Level Fluoride Exposure Increases Insulin Sensitivity in Experimental Diabetes. **J Dent Res**, 94, n. 7, p. 990-997, Jul 2015.

LOMBARTE, M.; FINA, B. L.; LUPO, M.; BUZALAF, M. A. *et al.* Physical exercise ameliorates the toxic effect of fluoride on the insulin-glucose system. **J Endocrinol**, 218, n. 1, p. 99-103, Jul 2013.

MALVEZZI, M.; PEREIRA, H.; DIONIZIO, A.; ARAUJO, T. T. *et al.* Low-level fluoride exposure reduces glycemia in NOD mice. **Ecotoxicol Environ Saf**, 168, p. 198-204, Oct 30 2018.

MILLAN, P. P. Visualization and analysis of biological networks. **Methods Mol Biol**, 1021, p. 63-88, 2013.

MILLION, D.; ZILLNER, P.; BAUMANN, R. Oxygen pressure-dependent control of carbonic anhydrase synthesis in chick embryonic erythrocytes. **Am J Physiol**, 261, n. 5 Pt 2, p. R1188-1196, Nov 1991.

MOUSNY, M.; BANSE, X.; WISE, L.; EVERETT, E. T. *et al.* The genetic influence on bone susceptibility to fluoride. **Bone**, 39, n. 6, p. 1283-1289, Dec 2006.

ORCHARD, S. Molecular interaction databases. **Proteomics**, 12, n. 10, p. 1656-1662, May 2012.

OYAGBEMI, A. A.; OMOBOWALE, T. O.; ASENUGA, E. R.; ADEJUMOBI, A. O. *et al.* Sodium fluoride induces hypertension and cardiac complications through generation of reactive oxygen species and activation of nuclear factor kappa beta. **Environ Toxicol**, 32, n. 4, p. 1089-1101, Apr 2017.

PEREIRA, H.; DIONIZIO, A. S.; ARAUJO, T. T.; FERNANDES, M. D. S. *et al.* Proposed mechanism for understanding the dose- and time-dependency of the effects of fluoride in the liver. **Toxicol Appl Pharmacol**, 358, p. 68-75, Nov 1 2018.

PEREIRA, H. A.; LEITE ADE, L.; CHARONE, S.; LOBO, J. G. *et al.* Proteomic analysis of liver in rats chronically exposed to fluoride. **PLoS One**, 8, n. 9, p. e75343, 2013.

PETROVIC-OGGIANO, G.; DAMJANOV, V.; GURINOVIC, M.; GLIBETIC, M. [Physical activity in prevention and reduction of cardiovascular risk]. **Med Pregl**, 63, n. 3-4, p. 200-207, Mar-Apr 2010.

SHERER, T. R.; SUTTIE, J. W. Effect of fluoride on glycolytic and citric acid cycle metabolites in rat liver. **J Nutr**, 100, n. 7, p. 749-756, Jul 1970.

SMITH, C. E.; CHONG, D. L.; BARTLETT, J. D.; MARGOLIS, H. C. Mineral acquisition rates in developing enamel on maxillary and mandibular incisors of rats and mice: implications to extracellular acid loading as apatite crystals mature. **J Bone Miner Res**, 20, n. 2, p. 240-249, Feb 2005.

TAVES, D. R. Separation of fluoride by rapid diffusion using hexamethyldisiloxane. **Talanta**, 15, n. 9, p. 969-974, Sep 1968.

TOTI, L.; BARTALUCCI, A.; FERRUCCI, M.; FULCERI, F. *et al.* High-intensity exercise training induces morphological and biochemical changes in skeletal muscles. **Biol Sport**, 30, n. 4, p. 301-309, Dec 2013.

WANG, T.; ESKANDARI, D.; ZOU, D.; GROTE, L. *et al.* Increased Carbonic Anhydrase Activity is Associated with Sleep Apnea Severity and Related Hypoxemia. **Sleep**, 38, n. 7, p. 1067-1073, Jul 1 2015.

WHITFORD, G. M. The metabolism and toxicity of fluoride. **Monogr Oral Sci**, 16 Rev 2, p. 1-153, 1996.

ZHANG, M.; WANG, A.; XIA, T.; HE, P. Effects of fluoride on DNA damage, S-phase cell-cycle arrest and the expression of NF-kappaB in primary cultured rat hippocampal neurons. **Toxicol Lett**, 179, n. 1, p. 1-5, Jun 10 2008.

ANEXO

Universidade de São Paulo
Faculdade de Odontologia de Bauru

Comissão de Ética no Ensino e Pesquisa em Animais

CEEPA-Proc. Nº 009/2015

Bauru, 16 de junho de 2015.

Senhora Professora,

Informamos que o projeto de pesquisa intitulado "***Efeito do exercício físico no metabolismo de fluoretos em camundongos com diferentes susceptibilidades à fluorose: análise proteômica***" sob a responsabilidade de Vossa Senhoria, que envolve a utilização de animais (roedores), para fins de pesquisa científica, encontra-se de acordo com os preceitos da Lei nº 11.794, de 8 de outubro de 2008, do Decreto nº 6.899, de 15 de julho de 2009, e com as normas editadas pelo Conselho Nacional de Controle da Experimentação Animal (CONCEA), e foi **aprovado** pela Comissão de Ética no Ensino e Pesquisa em Animais (CEEPA), em reunião realizada no dia **29 de maio de 2015**.

Esta comissão solicita que ao final da pesquisa seja enviado relatório com os resultados obtidos para análise ética e emissão de parecer final, o qual poderá ser utilizado para fins de publicação científica.

Vigência do projeto:	*Agosto/2015 a Agosto/2017*
Espécie/Linhagem:	*A/J e 129P3/J*
Nº de animais:	*n=90 (30 A/J - projeto piloto; 30 A/J - projeto pesquisa, 30 129P3/J - projeto de pesquisa)*
Peso/Idade	*após desmame*
Sexo:	*Macho*
Origem:	*Biotério de criação da FOB-USP*

Cordialmente,

Profª Drª Ana Paula Campanelli

Presidente da Comissão de Ética no Ensino e Pesquisa em Animais

Profª Drª Marília Afonso Rabelo Buzalaf
Docente do Departamento de Ciências Biológicas

Al. Dr. Octávio Pinheiro Brisolla, 9-75 – Bauru-SP – CEP 17012-901 – C.P. 73
e-mail: ceepa@fob.usp.br – Fone/FAX (0xx14) 3235-8356
http://www.fob.usp.br